PHASE EQUILIBRIA IN NON POLAR GAS - LIQUID BINARY SYSTEMS AT HIGH PRESSURE.

Thesis submitted for the Degree of

DOCTOR of PHILOSOPHY

in the

FACULTY of SCIENCE

in the

UNIVERSITY of LONDON

by

ROY GREGORY REYNOLDS, B.Sc.,

Department of Chemical Engineering,
Imperial College of Scienee & Technology,
London, S.W.7.

April 1964.

ABSTRACT

New equipment has been built, incorporating a number of novel features, for measuring binary vapour - liquid equilibrium to an accuracy of ±1%. It was designed for operation at pressures up to 3000 atm, although its use in this investigation was limited to 1500 atm.

Pressure - composition isotherms are reported for the nitrogen - benzene system at 25, 75 and 100°C, and for the argon - heptane and argon - carbon tetrachloride systems, at 30, 50 and 100°C. For the nitrogen - benzene system the measurements are compared with the results of three presvious experimental investigations, and in general the agreement is found to be within the calculated experimental accuracy.

The experimental results are used to test the validity of theoretical equations for predicting vapour - liquid equilibrium. In the case of the liquid composition curve, Henry's Law is found to be applicable only at low concentrations and low pressures, whilst Krichevski's equation accurately reproduces the experimental data at pressures up to near the critical point. For the gas composition curve, the Poynting expression predicts a solubility much less than that observed, but if account is taken of the molecular interaction the agreement is far better.

The phase behaviour is studied by plotting the critical temperatures

of the systems against the critical pressures. The shapes of the curves suggest that a minimum critical temperature exists at high pressures, and that the critical locus curve does not join the critical temperature of the two pure components. This phenomena has not been reported previously for non-polar systems, and represents new experimental evidence regarding the general pattern of phase behaviour for binary systems. The results further suggest that there is a relationship between the shape of the critical locus curve, and the difference between the critical temperature of the pure components.

CONTENTS.

PAGE No.

ACKNOWLEDGEMENTS.

I wish to express my sincere thanks to Dr. K. E. Bett for his patient supervision of all the work presented in this thesis, and especially for his valuable advice in the construction of the high pressure equipment.

I should like to acknowledge the cooperation of Professor J. S. Rowlinson with whom the experimental results were discussed, and the help of Mr A. M. Alger and the workshop staff in the construction of the apparatus. I am also deeply grateful to my wife for her dedication in the typing of this thesis.

Finally I am indebted to the Department of Scientific and Industrial Research for the provision of a maintainance grant.

AUTHOR's NOTE.

Thanks are due to the following Companies for supplying materials gratis:-

Accles & Pollock Ltd., - for the high pressure tubing used in the construction of the gas compressor.

The Distillers Co. Ltd., - for the bursting dics and their accompanying holders.

Shell Petroleum Co. Ltd., - for the oil used in the thermostating bath.

Mullards Ltd., and Murex Co. Ltd., - for all the permanent magnets employed in the apparatus.

CHAPTER I

INTRODUCTION

The increasing use of high pressures in industry during the past decade has shown the need for a better understanding of high pressure phase equilibrium, and for accurate methods of predicting data for those systems which are of industrial importance. Although the effect of pressure on vapour-liquid equilibrium has been of interest to physical chemists and chemical engineers for many years, and in spite of abundant experimental data, especially at pressures below 200 atm. very little consideration has been given to analysing the results with the object of predicting data for other systems.

Although it is ultimately desirable to establish relationships between the macroscopic properties of a binary mixture and the intermolecular forces, at present the forces between unlike molecules are not sufficiently well understood for the methods of statistical thermodynamics to be applied in any but the simplest cases. An alternative approach is to use the equations of classical thermodynamics to relate the solubility data to a number of continuous mathematical functions, which can be expressed analytically with the minimum number of constants. The work of Prausnitz [74], in which the experimental data is expressed in terms of reduced

activity coefficients, is one example of this type of analysis. Unfortunately considerable experimental work is needed to evaluate the partial molal thermodynamic functions, and it is generally necessary to make certain assumptions, which will reduce the accuracy and usefullness of the thermodynamic equations.

Previous experimental investigation of phase behaviour under high pressures have nearly all been concerned with systems which were of immediate technological importance, such as mixtures of hydrocarbons used in the petroleum industries, and the nitrogen - ammonia system. This has meant that very little consideration has been given to the very large range of binary systems, made up of non-polar components, where the molecular energies and sizes differ widely from one another. In such cases one might expect the phase behaviour to be unlike that found for mixture of simple hydrocarbons, since the interaction between unlike molecules, expecially at the very high pressures, will have considerable significance.

The work described in this thesis is concerned solely with three binary mixtures of a permanent non-polar gas, with a non-polar liquid, and one of the objects of this investigation is to show how phase behaviour of these systems might fit into a general pattern embracing the various types of system which have been studied. Although much more work will be needed to establish the general pattern of behaviour in detail, this is a

necessary preliminary step before any attempt is made to collect the large amount of thermodynamic data needed to correlate and interpret binary phase equilibrium.

The thesis divides itself into three section. In the introductory section the general phase behaviour of binary systems is outlined, this is followed in Chapter 3 by a discussion of the theoretical relationships available for predicting vapour - liquid equilibrium, whilst, Chapters 4 and 5, are concerned with describing previous experimental data and methods.

The second section, Chapters 6 to 9, describes the equilibrium apparatus and the experimental procedure, and presents the results obtained in the investigation together with an estimate their accuracy.

In the final section the results are discussed with reference to previous experimental studies, and the theoretical expressions derived in Chapter 3 are applied.

CHAPTER 2

CHARACTERISTIC PHASE BEHAVIOUR OF GAS-LIQUID SYSTEMS

The phase behaviour of a single component system is fully defined by a pressure vs. temperature (P.T.) curve, but in the case of a binary system, curves of pressure vs. composition (P.x.) and temperature vs. composition (T,x), are also required. A typical set of phase curves are shown in Figs. 2.1. 2.2 and 2.3.: these curves are representative of a binary system, where the difference between the critical temperatures of the two components is not very great.

The two phase region bounded by the P, x isotherms in Fig. 2.1. is seen to get smaller as the temperature is increased; it eventually disappears at the critical temperature of the higher boiling component. It may also be observed that at the higher temperature, i.e. T_2 and T_3, two phases do not exist over the whole composition range. In some cases the attainment of a one phase region by increasing the pressure beyond the critical pressure for the mixture is prevented by the formation of a solid phase [12]. Both the (P,x) and (T,x)loops have rounded ends, and as a result it is generally found that the critical point is neither at the maximum temperature, or maximum pressure

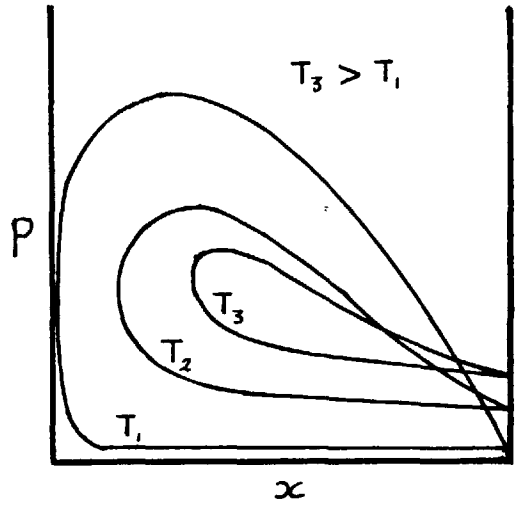

Fig. 2.1 (P - x) curve

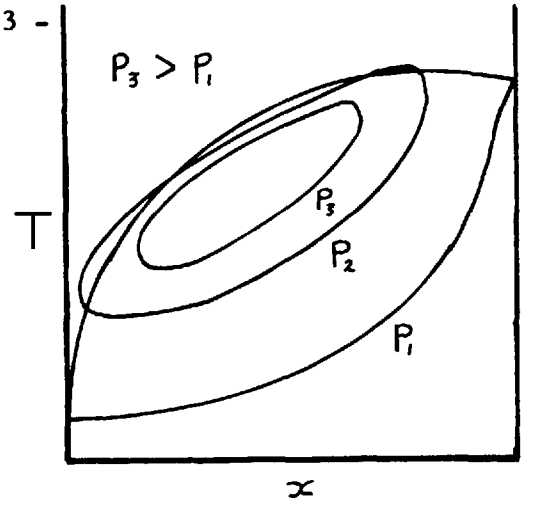

Fig. 2.2 (T - x) curve

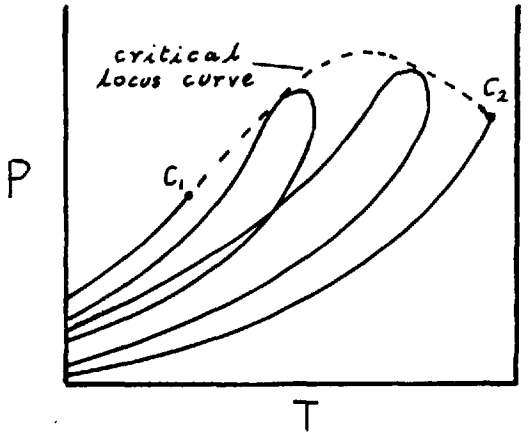

Fig. 2.3 (P -T) curve

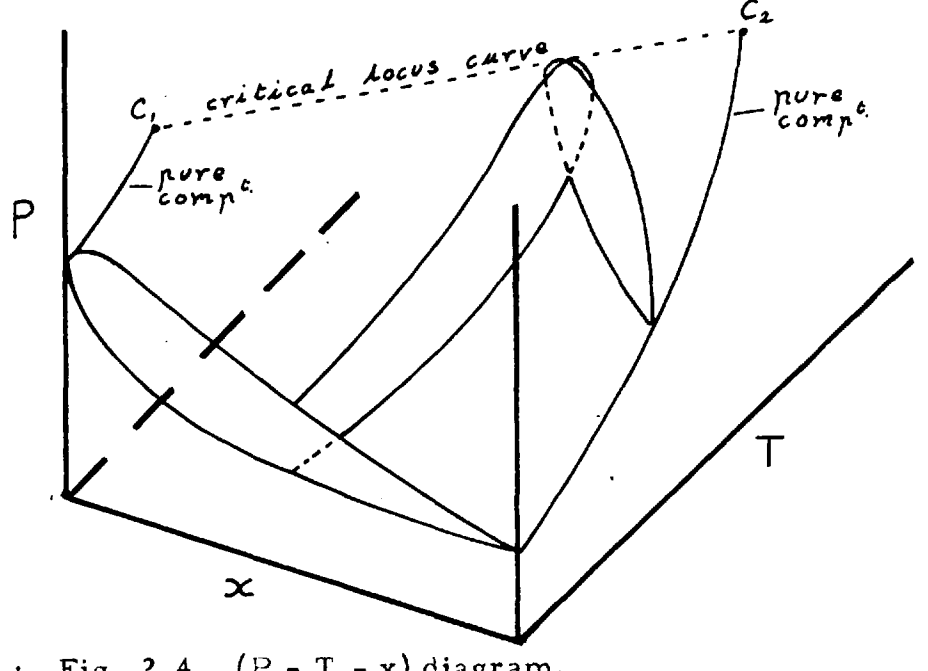

Fig. 2.4 (P - T - x) diagram.

of the (P.T.) loop at constant composition as illustrated in Fig. 2.3 The critical points all lie on the "critical curve" drawn between the critical points of the two pure components, and tangential to the (P.T.) loops.

It is possible to combine Figs. 2.1, 2.2 and 2.3 into one three dimensional diagram, Fig. 2.4, in which the actual shape of the critical locus curve can be seen more easily.

The shape of the (P.T.) (P,x) and (T,x) loops gives rise to an unusual phenomenon first observed by Kuenen [55] and called "Retrograde behaviour". It may be illustrated by considering the head of a (P.T.) loop of constant composition as shown in Fig. 2.5 in which it may be noticed that the critical point C is neither at the maximum pressure A, nor the maximum temperature B.

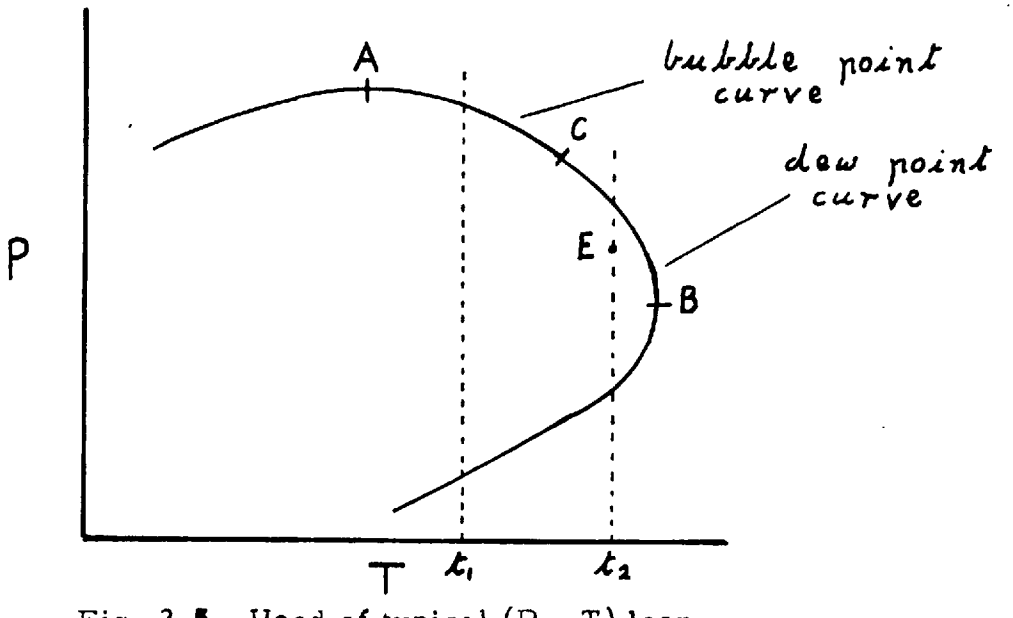

Fig. 2.5 Head of typical (P - T) loop.

If a mixture is compressed at a temperature t_1 below that corresponding to C, then normal condensation occurs, that is, the first drop of liquid appears at the dew point, and the last bubble of gas disappears at the bubble point. However, if the temperature t_2 is between that corresponding to C and B, then the line of increasing pressure at constant temperature, cuts the (P, T_c) curve at two dew points. Hence, on compression, liquid appears at the first dew point, and the amount of liquid present increases to a maximum at E, and then falls again to the second dew point. Since this is the reversal of the expected behaviour, it is termed "retrograde condensation". A similar phenomenon which occurs when an isotherm passes through two bubble points, is called "retrograde vapourization".

The critical solution pressure depends to a large extent upon the difference between the critical temperature of the two components. In the case of the hydrogen - liquid nitrogen system, with critical temperatures of 33.1° K and 125.9°K respectively, it has a maximum of 180 atm.; for the hydrogen - benzene system, critical temperatures 33.1°K and 561.5°K, it is above 3000 atm. even at 150°C. The very high critical solution pressure in the case of hydrogen - benzene is due to the complex phase behaviour that is to be expected with two

molecules of different energies and sizes, and if the critical locus curve were to be completed, it would probably have a different form to that shown in Fig. 2.3.

Krichevski and his colleagues [50,51,52,97] have made a detailed study of the nitrogen - ammonia system, and they obtained a critical curve of the form shown in Fig. 2.6. The critical line starts from the critical point of ammonia, moves first to lower temperatures, but at 87°C and 1100 atm. it becomes vertical and then moves in the direction of higher temperatures, the slope of the curve still being positive at the highest experimental point reached, 180°C and 1500 atm. Lindroos and Dodge [62] have confirmed these results. The shape of the curve suggests that it is possible to separate the fluids even at temperatures above the critical point of pure ammonia.

The results obtained by Krichevski may also be represented on a (P,x) curve - see Fig. 2.7. The point D is the "point of double contact", above which co-existence of the two gas phases takes place. At temperatures below that corresponding to D, the curves have what Rowlinson [88] terms a "waisted" shape, so that with increasing pressure the solubility of the liquid in the gas, and the solubility of the gas in the liquid, both pass through a maximum. Krichevski [49], and Wiebe and Gaddy [109] have shown theoretically that these maximum

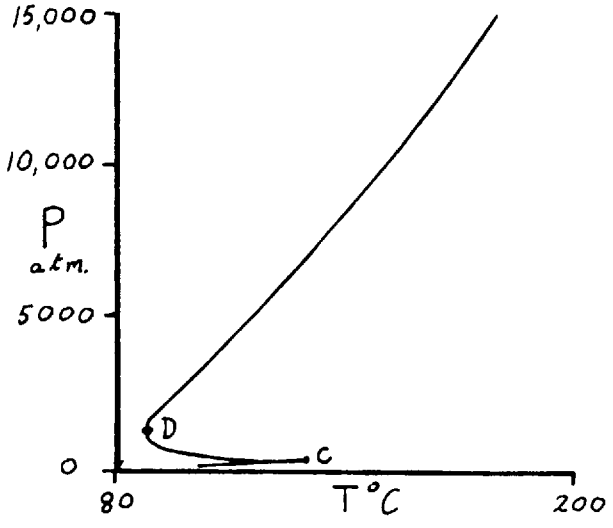

Fig. 2.6 - Critical locus curve for system N_2 — NH_3

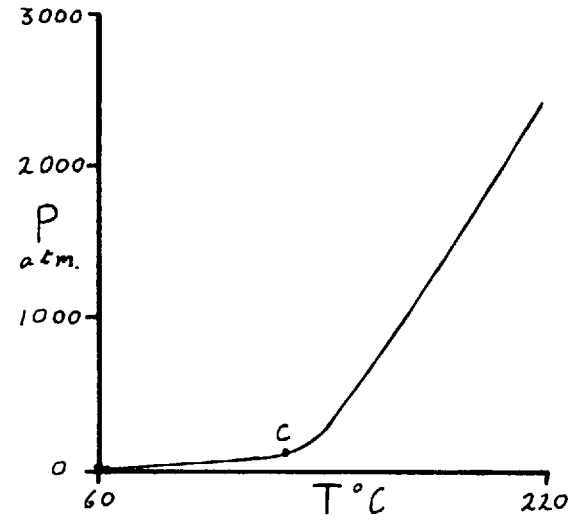

Fig. 2.8 - Critical locus curve for system NH_3 — He

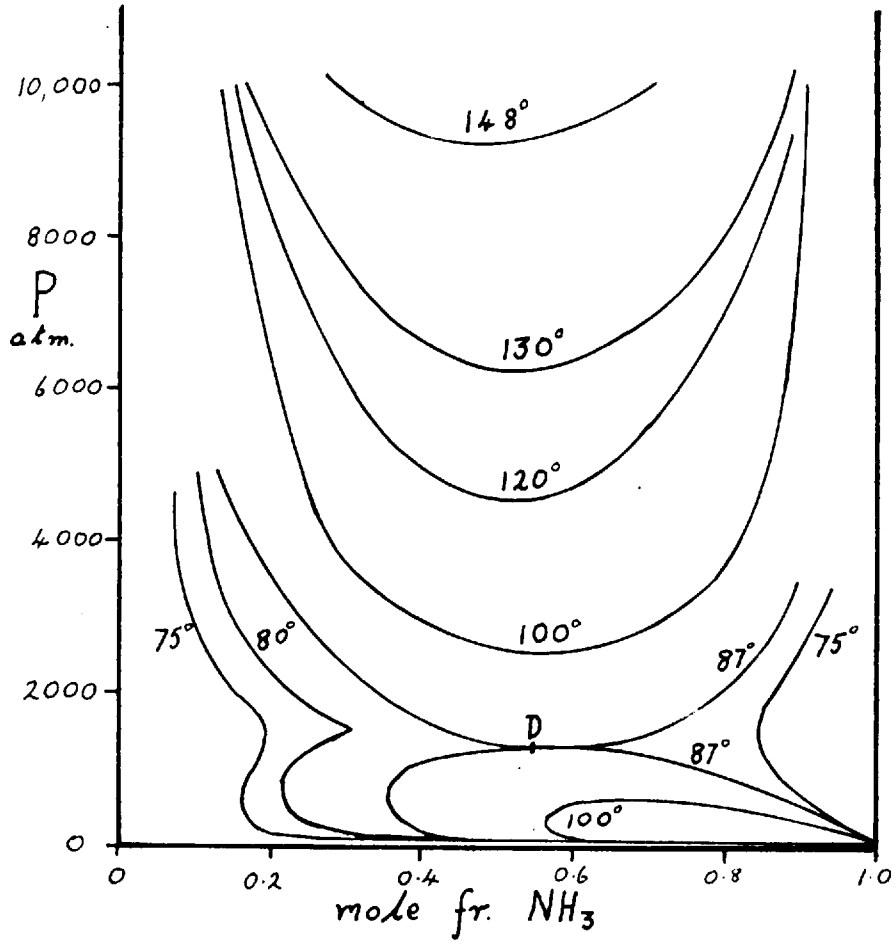

Fig. 2.7 Pressure - composition curve for system N_2 — NH_3

solubilities occur when the partial molal volumes of the liquid and gas become equal in both phases.

During his study of the Nitrogen - Ammonia system, Krichevski also observed a "barometric phenomenon". He found that above 1800 atm. the "gaseous" phase became more dense than the "liquid" phase, and therefore sank to the bottom of the vessel. It is important to note that the consequence of this effect is only to change the relative positions of the phases; it in no way effects the equilibrium of the system.

The type of phase diagram shown in Fig. 2.6 has also been observed for the systems nitrogen - sulphur dioxide [101] , methane - ammonia [44] and carbon dioxide - water [96] . For systems where the disparity between the physical properties of the components is even greater, Tsiklis found that the critical locus curve has a slope of the type shown in Fig. 2.8, the slope of the line always being positive from the critical point of the less volatile component. Systems which exhibit such behaviour are mixtures of Helium with carbon dioxide [100] ethylene [99] propane [98] and ammonia [100] . As in the case of the nitrogen - ammonia system, it is again possible to separate the phases even at temperatures above the critical point of both components. This extra ordinary behaviour is termed "immiscibility of two gases", or more commonly, "gas - gas equilibrium". It is interesting to note that this type of equilibrium was originally predicted many years ago by Van der

Waals [103] in 1894, and discussed in some detail from a theoretical point of view by Onnes & Keesom [70] in 1907. More recently Rott [84] has predicted the criterion of gas - gas equilibrium from a statistical theory based on nominal probabilities.

Because of the very high pressures involved it has not yet been established whether the critical locus curve eventually returns to the critical point of the most volatile component; Rowlinson [88] has suggested that this is most probably not the case, but that the (P,x) loops are open at the top at all temperatures.

CHAPTER 3

THEORETICAL APPROACHES TO GAS - LIQUID EQUILIBRIUM

If one considers a (P - x) diagram - Fig. 2.1, then for theoretical purposes the loops may be thought of as consisting of two curves one either side of the critical point, one representing the composition of the liquid phase, and the other, the composition of the gas phase. This chapter reviews the theories which are available for the prediction of these curves.

3.1 Composition of the liquid phase

3.1.1 Solubilities at atmospheric pressure

At the present time solution theory has not yet reached a stage where it is possible to predict the thermodynamic properties of a solution from the nature of its pure components. The most successful theory from a practical standpoint is the "theory of regular solutions", first formulated by Hildebrand [29] . This theory provides a simple method for estimating solubility, and partial pressure relationships for solutions of non polar liquids, but its applicability to gas solution is very limited as will be discussed later.

It is possible to obtain a rough estimate of the solubility of a gas at a partial pressure of one atmosphere, by calculating its ideal solubility from Raoult's Law.

$$x_1 = \frac{p_2}{p_2^\circ} \qquad \ldots\ldots (3.1)$$

x_1 = mole fraction of gaseous solute in liquid

p_2 = partial pressure of the gas over the solution

p_1° = vapour pressure of the gas

For a gas above its critical temperature p_2° no longer has any physical meaning and its value can therefore only be obtained by extrapolation; the extrapolation usually employed is to assume a linear relationship between p_1° and $1/T$ as shown in Fig. 3.1. The use of equation 3.1 to

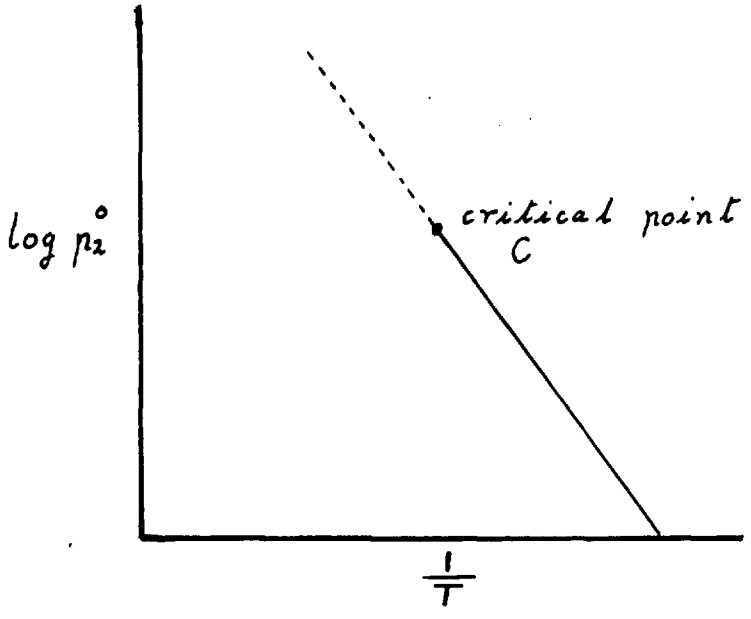

Fig. 3.1 Log. Vapour pressure vs. 1/temperature.

estimate gas solubilities has two serious limitations. Firstly, it implies that the ideal solubility of a given gas is the same in all solvents. Secondly, if a linear relationship between μ_2° and $1/T$ is assumed, then the solubility of all gases must always decrease with rising temperature. Both these implications are contrary to experimental findings.

For an ideal solution, the internal energies of the solute and solvent must be similar. This is not so for many solutions, and therefore Hildebrand [31] developed a general solubility equation based on his theory of regular solutions, which took into account the internal energy. The equation may be written for component 2 in a two component system. as follows;-

$$\ln \frac{\bar{f}_2}{f_2^\circ} = \frac{\bar{v}_2 \Phi_1^2 (\delta_1 - \delta_2)^2}{RT} + \ln x_2 \quad \ldots\ldots (3.2)$$

$\bar{f}_2$ = fugacity of component 2 in the solution

f_1° = fugacity of pure component as a liquid at the temperature and pressure of the solution.

Φ = volume fraction

δ = solubility parameter, this is given by $\left(\frac{\Delta E^v}{v}\right)^{1/2}$ where ΔE^v is the molal energy of vapourization of a liquid in going to the gas at zero pressure

V = molal volume

$\bar{V}_2$ = partial molal volume

In the derivation of this equation, Hildebrand made the following assumptions:-

(1) The energy between two molecules depends only upon the distance between them, and not at all on the nature of the other molecules.

(2) The distribution of the molecules is random, and also, the entropy of solution at constant volume is equal to that of an ideal solution.

(3) The energy of interaction between two molecules of unlike species, is given by the geometric mean of the energies of interaction for the two species of like molecules.

(4) The change of volume on mixing at constant temperature and pressure is zero.

In the case of a gas - liquid solution, Hildebrand's fourth assumption is no longer valid, since there is always a great change of gas volume on mixing. A further difficulty in applying equation 3.2 to gases dissolved in liquids, is that δ_2 and f_2° cannot be deduced easily for a component above its critical temperature.

Gjaldbach and Hildebrand [24], have however, used equation 3.2 with a reasonable measure of success, as a basis for a semi - emperical method of correlating solubilities. The procedure used

was to let $\Phi = 1$, since only a small number of gas molecules were dissolved in the liquid, and then, using an experimentally determined value of δ_1, find values of δ_2, f_2° and $\bar{v}_2$ which gave a good correlation of the gas solubilities.

In cases where the difference between the molal volumes of the gas and solvent are very large (greater than 2), Gjaldbach and Hildebrand [24] found that the entropy of solution was greater than that for an ideal solution, that is $-R \ln. x_2$, and they introduced a correction term of the Flory - Huggins type [30]. Equation 3.2 then becomes:-

$$\ln. \frac{\bar{f}_2}{f_2^\circ} = \ln. x_2 + \frac{\bar{v}_2 (\delta_1 - \delta_2)^2}{RT} + \log. \left(\frac{\bar{v}_2}{v_1} \right) + 0.434 \left(1 - \frac{\bar{v}_2}{v_1} \right) \quad \ldots\ldots (3.3)$$

Prausnitz and Shair [75], have overcome some of the difficulties in applying the regular solution equations to gas - liquid systems, by considering the isothermal dissolution of the gas in two separate steps. The first step takes into account the free energy change accompanying the condensation of the gas to a hypothetical state having a liquid - like volume, whilst the second, that of the dissolution of the hypothetical liquid - like fluid into the solvent. The free energy change for the first step is;-

$$\Delta G_1 = RT \ln. \frac{f_2^L}{f_2^G} \quad \ldots\ldots (3.4)$$

and for the second

$$\Delta G_{II} = \bar{v}_2 \Phi_1^2 (\delta_1 - \delta_2)^2 + RT \ln x_2 \quad \ldots\ldots (3.5)$$

this expression is obtained from the regular solution equation

where G = Gibbs free energy.

f_2^L = fugacity of gas as a hypothetical liquid at 1 atm.

and f_2^G = fugacity of pure gas at initial conditions.

Now since the solute in the liquid solution is in equilibrium with the gas at unit fugacity.

$$\Delta G = \Delta G_I + \Delta G_{II} \quad \ldots\ldots (3.6)$$

Combining equations 3.4, 3.5, 3.6 & rearranging;

$$\frac{1}{x_2} = \frac{f_2^L}{f_2^G} \exp. \frac{\bar{v}_2 \Phi (\delta_1 - \delta_2)}{RT} \quad \ldots\ldots (3.7)$$

Prausnitz and Shair show how f_2^L may be determined from a correlation based on the theory of corresponding states, and they also give methods for estimating the parameters $\bar{v}_2$ and δ_2. For non polar systems to which equation 3.7 has been applied [75,60] differences between the calculated and the observed values of solubility, are of the order of 13%.

A more basic approach to the problem of gas solubility is that used by Uhlig [102]. He considered the introduction of a gas solute molecule into the solvent, as the sum of the two energy changes that take place when: firstly a cavity is created in the solvent of a suitable

size to accomodate the solute molecule; and secondly when the solute molecule is introduced into the cavity, and interacts with the solvent. Using this model, Uhlig derived the equation:-

$$\ln L = -\frac{4\pi r^2 \theta}{kT} + \frac{\epsilon}{kT} \quad \ldots\ldots (3.8)$$

where L = Ostwald coefft. = $\frac{\text{conc.}^n \text{ of solute in sol}^n}{\text{conc}^n \text{ of solute in gas}^n}$.

θ = solvent surface tension

ϵ = interaction energy

and k = attraction constant

As equation 3.8 predicts, a linear relationship is found to exist between $\ln L$ and θ, if the interactions energy is constant for the various solvents considered.

Very recently Pierotti [72], using a similar approach to Uhlig, has developed a more exact equation for gas solubility, which in its general form may be expressed:-

$$\ln K = \frac{\bar{G}_i}{RT} + \frac{\bar{G}_c}{RT} + \ln\left(\frac{RT}{V_1}\right) \quad \ldots\ldots (3.9)$$

where K = Henry's Law constant

$\bar{G}_c$ = Partial molar Gibbs free energy of creating a cavity

$\bar{G}_i$ = Partial molar Gibbs free energy for the interaction with the solvent

and V_1 = Molar volume of solvent

In order to test his theory, Pierotti further deduced the temperature dependency of solubility by calculating the heat of mixing, and he found good agreement between calculated and observed values.

The effect of temperature on the solubility of a gas is directly related to the entropy of mixing as shown in equation:-

$$\frac{d \ln . x_2}{dT} = \frac{\Delta \bar{S}_2}{R \left(d \ln . a_2 / d \ln . x_2 \right)_T} \quad \ldots\ldots (3.10)$$

$\Delta \bar{S}_2$ = partial molal entropy change of solute

a = activity

In all cases $\left(d \ln . a_2 / d \ln x_2 \right)_T$ is positive and, therefore, it is evident from equation 3.10 that the solubility increases with temperature if the partial entropy change is positive, and decreases with temperature if it is negative. Hildebrand [32] has shown this to be the case, by plotting Log. x_2 vs. Log. T, and $- R \ln x_2$ vs. $\Delta \bar{S}_2$, for a large number of non polar solutions.

3.1.2 Gas solubilities at elevated pressures.

In the previous section 3.1.1, consideration was given to the development of a general solution equation which could be used to predict the composition of the liquid phase, from the thermodynamic properties of the pure components. Such an equation may be applied

with reasonable success at atmospheric pressure, but its extension to higher pressures is restricted, since all the variables in the equation are pressure dependent, and can only be estimated from data at 1 atm. A further complication arises from the fact that, as the mole fraction of the gas in the liquid x_2 increases with increasing pressure, the volume fraction or its equivalent may no longer be assumed to be one, and hence the equation is not explicit in x_2. For these reasons it is customery to compute the composition of the liquid phase at elevated pressures from a direct relationship between pressure and solubility, using the known solubility of the gas at one atmosphere.

The simplest and best known expression relating pressures to the solubility of a gas is Henry's Law, according to which; the mass of gas dissolved by a given volume of solvent at constant temperature is proportional to the pressure of the gas with which it is at equilibrium.

i.e. $$m = K p \qquad \ldots\ldots(3.11)$$

where m = mass of gas dissolved by unit mass of solvent.

and K = a constant

In equation 3.11 it is important to realise that p is the partial pressure of the gas, and not the total pressure, for the difference can be ignored only for solvents with low vapour pressures.

Henry's Law may be expressed mathematically in a number of other ways:-

$$m = K' f_2 \qquad \ldots\ldots(3.12)$$

$$x_2 = K'' p_2 \qquad \ldots\ldots(3.13)$$

$$\frac{x_2}{x_1} = K p_2 \qquad \ldots\ldots(3.14)$$

x_1 & x_2 = mole fraction of the solvent and gas respectively.

At low pressures and with dilute solutions these expressions become equivalent, but at higher concentrations only expressions 3.12 and 3.24 are equivalent.

It is possible to derive Henry's Law for an ideal solution by integrating the following form of the Gibbs - Duhem equation.

$$x_1 \, d\ln f_1 + x_2 \, d\ln f_2 = 0 \qquad \ldots\ldots(3.15)$$

However, for the system nitrogen - water, it is found that even if an ideal solution is assumed, Henry's Law does not give a good fit with experimental data at pressures above 100 atm. [107]. The inaccuracy of Henry's Law under such circumstances, is due to the eroneous application of the Gibbs - Duhem equation, in which it is wrongly assumed that the pressure remains constant throughout the integration. For solubilities at low pressure the change in pressure is small and may be neglected, but at high pressures there can be no question of disregarding its influence, and a correction must be made to Henry's

Law. The following equation 3.16 developed independantly by Krichevski [48] and by Michels [65], corrects for the change in pressure, and hence may be applied to slightly soluble gases at high pressure.

$$\ln \frac{f_2}{x_2} = K + \frac{\bar{v}_2 P}{2.3 RT} \qquad \ldots\ldots (3.16)$$

Equation 3.16 is known as the "Krichevski equation".

The success of the Krichevski equation is shown in Fig. 3.2 where agreement with the experimental data for nitrogen dissolved in water, is obtainedfor pressures as high as 1000 atm., compared with 100 atm. for Henry's Law.

In theory equation 3.16 only applies to slightly soluble gases and if the concentration of the gas is too great it becomes inaccurate. This is shown very well for the system nitrogen - ammonia in Fig. 3.3. At $0^{\circ}C$ and 1000 atm. the mole fraction of nitrogen is only 0.0221 and the Krichevski equation is obeyed; if the temperature is now increased to $70^{\circ}C$, the mole fraction of nitrogen at 1000 atm. rises to 0.129, and the solution can no longer be assumed to be dilute, hence significant deviations occur.

Henry's Law and the Krichevski equation, may be applied successfully under certain circumstances [45, 4], but they are in fact,

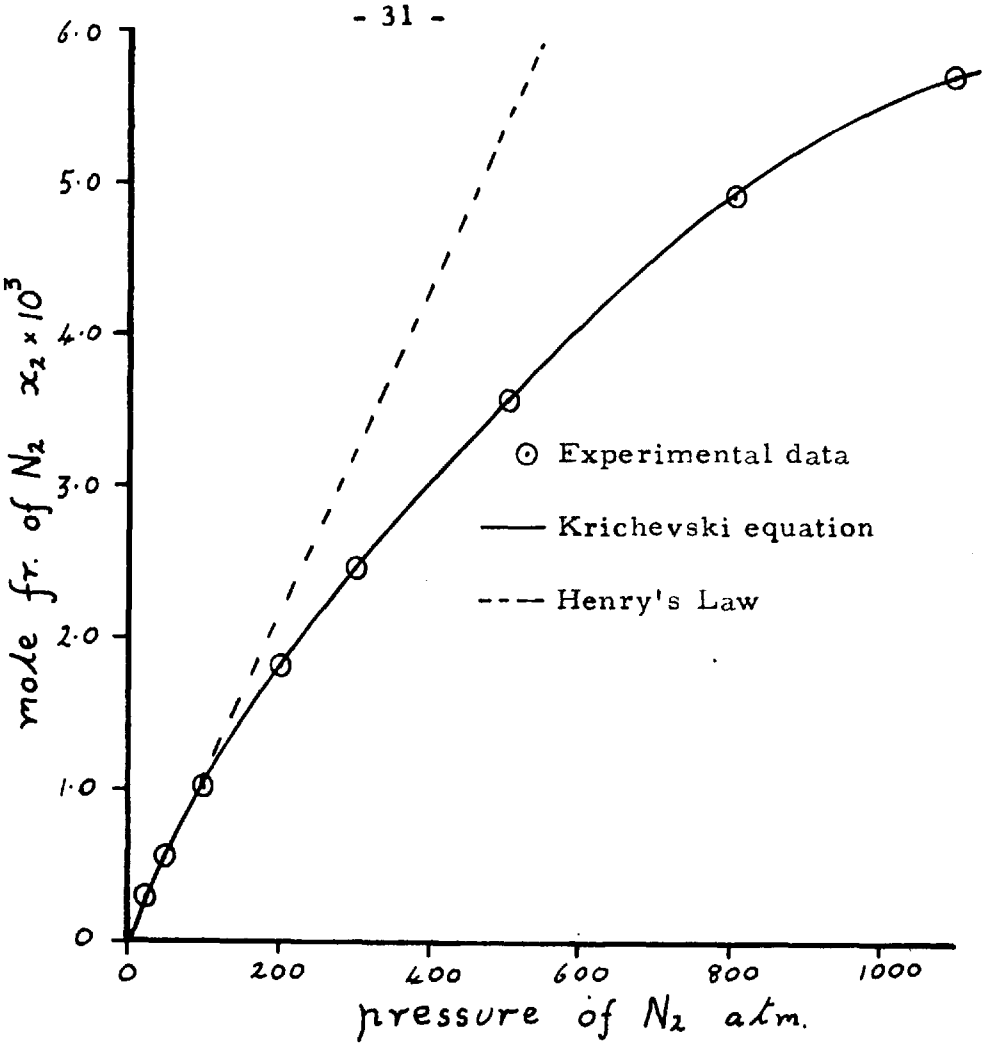

Fig. 3.2 Equilibrium data for system N_2 - H_2O at 25°C.

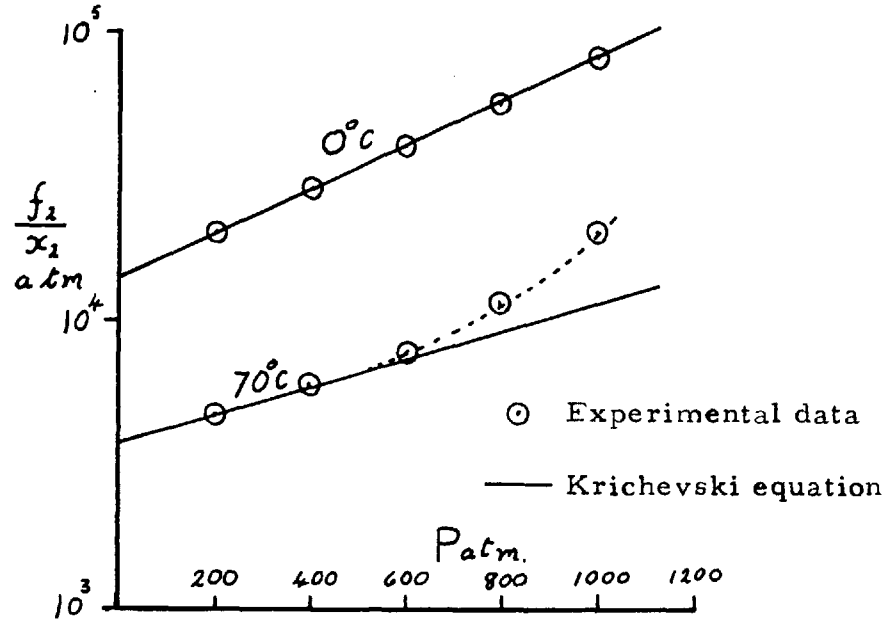

Fig. 3.3 The Krichevski equation applied to the N_2 - NH_3 system.

only approximations. It is therefore worth while to consider an exact thermodynamic expression, relating the composition of the liquid phase, to the pressure acting on the system.

Consider a binary gas - liquid system of components 1 & 2. Let x_1^G and x_2^G donate the mole fraction of 1 & 2 in the gas phase, and x_1^L and x_2^L the mole fraction in the liquid phase. The corresponding chemical potentials may then be written, μ_1^G, μ_2^G and μ_1^L, μ_2^L

When the system is at equilibrium.

$$\mu_1^G = \mu_1^L \qquad \ldots\ldots(3.17)$$

$$\mu_2^G = \mu_2^L \qquad \ldots\ldots(3.18)$$

Chemical potentials are function of pressure, temperature and composition and therefore from equations 3.17 and 3.18 we may write:-

$$\frac{\partial \mu_1^G}{\partial T} dT + \frac{\partial \mu_1^G}{\partial P} dP + \frac{\partial \mu_1^G}{\partial x_1^G} dx_1^G = \frac{\partial \mu_1^L}{\partial T} dT + \frac{\partial \mu_1^L}{\partial P} dP + \frac{\partial \mu_1^L}{\partial x_1^L} dx_1^L \qquad \ldots\ldots(3.19)$$

$$\frac{\partial \mu_2^G}{\partial T} dT \quad \frac{\partial \mu_2^G}{\partial T} dT \quad \frac{\partial \mu_2^G}{\partial x_1^G} dx_1^G = \frac{\partial \mu_2^L}{\partial T} dT \quad \frac{\partial \mu_2^L}{\partial P} dP \quad \frac{\partial \mu_2^L}{\partial x_1^L} dx_2^L \qquad \ldots\ldots(3.20)$$

where x_1 is the mole fraction of the solute gas.

If G is the free energy per mole of any phase and N denotes the number of moles, then for a particular component i we have,

$$G = \int_{P^\circ}^{P} v\,dP + \sum N_i G_i^\circ + RT \sum N_i \ln \frac{N_i}{N} \quad \ldots\ldots (3.21)$$

where G_i° is the free energy of the pure component in the standard state at a pressure P°.

But by definition:-

$$\mu_i = \frac{\partial G}{\partial N_i} \quad \ldots\ldots (3.22)$$

Hence equation 3.21 becomes:-

$$\mu_i = \int_{P^\circ}^{P} \frac{\partial v}{\partial N_i} . dP + G_i^\circ + RT \ln x_i \quad \ldots\ldots (3.23)$$

and

$$\frac{\partial \mu_i}{\partial P} = \frac{\partial v}{\partial N_i} = \bar{v}_i \quad \ldots\ldots (3.24)$$

Substituting equation 3.24 into 3.19 and 3.20 at constant temperature:-

$$\bar{v}_1^G . dP + \frac{\partial \mu_1^G}{\partial x_2^G} . dx_2^G = \bar{v}_1^L . dP + \frac{\partial \mu_1^L}{\partial x_2^L} . dx_2^L \quad \ldots\ldots (3.25)$$

$$\bar{v}_2^G . dP + \frac{\partial \mu_2^G}{\partial x_1^G} . dx_1^G = \bar{v}_2^L . dP + \frac{\partial \mu_2^L}{\partial x_1^L} . dx_1^L \quad \ldots\ldots (3.26)$$

Combining equations 3.25 and 3.26

$$\frac{1}{\frac{\delta \mu_1^{\alpha}}{\delta x_2^{\alpha}}} \left[\left(\bar{V}_1^{\beta} - \bar{V}_1^{\alpha} \right) dP + \frac{\delta \mu_1^{\beta}}{\delta x_2^{\beta}} \cdot dx_2^{\beta} \right]$$

$$= \frac{1}{\frac{\delta \mu_2^{\alpha}}{\delta x_2^{\alpha}}} \left[\left(\bar{V}_2^{\beta} - \bar{V}_2^{\alpha} \right) dP \quad \frac{\delta \mu_2^{\beta}}{\delta x_2^{\beta}} \cdot dx_2^{\beta} \right] \qquad \ldots\ldots (3.27)$$

Since chemical potential is a partial molal quantity then we may write [17];

$$\mu_1 = G - x_2 \frac{\delta G}{\delta x_2} \qquad \ldots\ldots (3.28)$$

$$\mu_2 = G + (1 - x_2) \frac{\delta G}{\delta x_2} \qquad \ldots\ldots (3.29)$$

Since for a binary system at equilibrium

$$x_1 \delta \mu_1 + x_2 \delta \mu_2 = 0 \quad \text{(Gibbs - Duhem equation)}$$

$$\delta x_2 = - \delta x_1$$

Then

$$\frac{\delta \mu_1}{\delta x_2} = - x_2 \frac{\delta^2 G}{\delta x_2^2} \qquad \ldots\ldots (3.30)$$

$$\frac{\delta \mu_2}{\delta x_2} = (1 - x_2) \frac{\delta^2 G}{\delta x_2^2} \qquad \ldots\ldots (3.31)$$

Substituting 3.30 and 3.31 in 3.27 and rearranging,

$$\frac{\delta x_2^{L}}{\delta P} = \frac{(x_2^{G}-1)(\bar{v}_1^{L}-\bar{v}_1^{G}) - x_2^{G}(\bar{v}_2^{L}-\bar{v}_2^{G})}{\frac{\delta^2 G}{\delta x_2^{L\,2}}\left(x_2^{G}-x_2^{L}\right)} \qquad \ldots\ldots (3.32)$$

Rewriting equation 3.21. for a two component system

$$G = \int_{P^0}^{P} v\,dP + x_1 G_1^{\circ} + x_2 G_2^{\circ} + RT(x_1 \ln x_1 + x_2 \ln x_2) \qquad \ldots\ldots (3.33)$$

$$\frac{d^2 G}{d x_2^2} = \int_{P^0}^{P} \frac{d^2 v}{d x_2^2}\, dP + \frac{RT}{x_2(1-x_2)} \qquad \ldots\ldots (3.34)$$

Combining 3.32 and 3.34 for the liquid phase

$$\frac{\delta x_2^{L}}{dP} = \frac{(x_2^{G}-1)(\bar{v}_1^{L}-\bar{v}_1^{G}) - x_2^{G}(\bar{v}_2^{L}-\bar{v}_2^{G})}{(x_2^{G}-x_2^{L})\left[\int_{P^0}^{P} \frac{\delta^2 v}{\delta x_2^{L\,2}}\, dP + \frac{RT}{x_2^{L}(1-x_2^{L})}\right]} \qquad \ldots (3.35)$$

Equation 3.35 is a general expression relating the mole fraction of soluble gas in the liquid phase of a binary two phase system, to the pressure at constant temperature. An analogous expression for the concentration of solvent vapour in the gas phase may also be derived.

In its present form it is not possible to evaluate equation 3.35 for real systems, nevertheless, under certain conditions simplifying assumptions may be made so that a more tractable expression is

obtained.

In the case where the gas is only slightly soluble and the liquid is non volatile the following assumptions may be made:-

(1) The mole fraction of gas in the gas phase is equal to unity

$$x_2^G = 1$$

(2) The partial molar volume of gas in the gas phase, is equal to the molar volume of the pure gas under the same conditions of temperature and pressure.

$$\bar{V}_2^G = V_2$$

(3) At constant temperature and pressure, the molar volume of the liquid phase can be assumed to increase linearly with concentration of gas up to the saturation value.

$$V^L = c x_2^L \quad V_0^L$$

$$\therefore \frac{d^2 V^L}{d x_2^{L^2}} = 0$$

This assumption has been verified experimentally by Krichevski and Efremova [45] for hydrogen and nitrogen dissolved in benzene at 25°C for values of x_2^L up to 0.6.

If the above assumptions are made equations 3.35 reduces to:-

$$\frac{d x_2^L}{dP} = \frac{-1\left(\bar{V}_2^L - V_2\right)}{(1 - x_2^L)\cdot\frac{RT}{x_2^L(1 - x_2^L)}} = \frac{x_2^L\left(V_2 - \bar{V}_2^L\right)}{RT} \quad \ldots(3.36)$$

Omitting the superscript $_L$ and integrating between the limits P_o and P.

$$RT \ln \frac{x_{2(P)}}{x_{2(P_o)}} = \int_{P_o}^{P} V_2 \, dP - \int_{P_o}^{P} \bar{V}_2 \, dP \quad \ldots\ldots (3.37)$$

Now $$\int_{P_o}^{P} V_2 \, dP = RT \ln \frac{f_{(P)}}{f_{(P_o)}} \quad \ldots\ldots (3.38)$$

where $f_{(P_o)}$ and $f_{(P)}$ = fugacity of gas at pressure P_o and P. If P_o is assumed to be 1 atm. that is $f_{(P_o)} = 1$, and $\bar{V}_2$ is independant of pressure then equation 3.37 becomes:-

$$\ln x_{2(P)} = \ln x_{2(P_o)} + \ln f_2 - \frac{\bar{V}_2}{RT}(P-1) \ldots (3.39)$$

or using Henry's Law i.e. $\ln x_{2(P_o)} = \ln K$ and rearranging

$$\log \frac{f_2}{x_2} = \log K + \frac{\bar{V}_2}{2.3RT}(P-1) \ldots\ldots (3.40)$$

Equation 3.40 is identical with the "Krichevski equation". 3.16.

In the derivation of equation 3.40 it is assumed that the partial molar volume of the gas in the solution $\bar{V}_2$, does not change with pressure. However, it has been found experimentally [45, 106] that this assumption is inaccurate, and Krichevski [48] has put forward the following simple relationship:-

$$\bar{V}_2 = V_2^{\circ}(1 - \beta P) \quad \ldots\ldots (3.41)$$

$\bar{V}_1^{\circ}$ = Partial molar volume of gas in solution when P approaches zero.

β = a constant identified with the average compressibility gas in solution.

Substitution of equation 3.41 into 3.36 and integrating as before now gives the expression:-

$$RT \ln \frac{f_2}{K x_2} = \bar{v}_2^{\circ} (\rho - 1) - c (\rho - 1) \qquad \ldots\ldots (3.42)$$

where

$$c = \frac{\bar{v}_2^{\circ} \beta}{2}$$

Equation 3.42 is the "Krichevski - Kasarnovski equation". For low solute concentrations it expresses extremly well the variation of gas solubilities with pressure, but it has been shown to be only an empirical equation because of the method used in calculating $\bar{v}_2$.

It was first pointed out by Krichevski and Il'inskaya [43], that there was a large difference between the partial molar volume determined experimentally at low pressure, and the value calculated from the Krichevski - Kasarnovski equation. In order to allow for this difference they developed the following expression for solubility:-

$$RT \ln \frac{f_2}{x_2} = RT \ln K - \int_1^{\rho} \bar{v}_2 \, d\rho - A (1 - x_1^2) \qquad \ldots\ldots (3.43)$$

where A is an emoirical constant independent of pressure. However, it is inconvenient to use equation 3.43 since A has to be determined experimentally at each temperature, as does the change of $\bar{v}_2$ with pressure.

3.2 Composition of the gas phase

The solubility of a liquid in a gas at low pressure may be computed by Raoult's Law.

$$y_1 = \frac{(1 - x_2)\, p_1^{\circ}}{P} \qquad \ldots\ldots (3.44)$$

Here y refers to the gaseous phase, x the liquid phase, and the subscripts 1 & 2 are the liquid and gas components respectively.

At low pressures x_2 is negligible compared with unity, and hence the solubility of the liquid in the gas becomes equal to the ratio of the vapour pressure to the total pressure. If the pressure is now increased, two additional factors must be taken into account:-

(1) The increase in the vapour pressure of the liquid due to its compression; this is called the Poynting effect [74] and is independent of the nature of the gas.

(2) The interaction between the gas and liquid molecules.

At high pressures it is the second effect which has the largest influence, and the solubility of the liquid in the gas tends to increase until the critical pressure is reached.

The Poynting effect can be estimated by integrating the relation;

$$\left(\frac{\delta \ln f}{\delta P}\right)_T = \frac{V_1}{RT} \qquad \ldots\ldots (3.45)$$

If V_l is assumed to be constant within the pressure range of integration.

then $$\ln \frac{f_P}{f_{p_1^\circ}} = \frac{V_l (P - p_1^\circ)}{RT} \quad \ldots\ldots (3.46)$$

where f_P = Fugacity of vapour at total pressure P.

and $f_{p_1^\circ}$ = Fugacity of vapour at normal vapour pressure

For low pressures the fugacity f_P will be approximately equal to the vapour pressure of the solvent and also $f_{p_1^\circ} = p_1^\circ$. Therefore when V_l the molar volume of the liquid, and p_1° are known, the values of the vapour pressure at high pressures p_1^{OH} can be obtained from the relation,

$$\ln p_1^{OH} = \ln p_1^\circ + \frac{V_l (P - p_1^\circ)}{RT} \quad \ldots\ldots (3.47)$$

The actual values of the liquid phase vapour pressure will always be greater than those calculated by the Poynting relationship, because of the greater molecular interaction which takes place with increasing gas density.

For very dilute solutions Robin & Vodar [81] assumed the interaction between molecules of types A and B to obey the Lennard - Jones Potential,

$$\epsilon_{12} = 4 \epsilon_{12}^* \left[\left(\frac{\sigma_{12}}{r} \right)^{12} - \left(\frac{\sigma_{12}}{r} \right)^{6} \right] \quad \ldots\ldots (3.48)$$

in which σ_{12} is the low - velocity collision diameter and ϵ_{12}^* is the depth of the potential well [34] . If it is now assumed as a first and very crude approximation that the gas phase mixture follows an equation of

state limited to the 2nd. virial coefficient, then the following equation may be derived by statistical thermodynamics [82, 83] .

$$\ln \frac{m}{m_o} = \frac{v_1 \rho}{22.4} - \frac{2 B_{12} N \rho}{22.4} \quad \ldots\ldots (3.49)$$

where

$$B_{12} = \int_0^{\infty} \left[1 - \exp. \left(- \frac{\epsilon_{12}}{kT} \right) \right] 4\pi r^2 dr \ldots (3.50)$$

m = mass of solute per cm of gaseous solution.

m_o = mass of solute per cm in absence of foreign gas.

ρ = density of the gaseous solution in amagat units.

N = Avogadro's number .

k = Boltzmann's constant.

The first term in equation 3.49 can be shown [83] to represent the Poynting effect, and is therefore independent of the nature of the gas. The second term depends on the gas, and accounts for the different solubilities of a given liquid dissolved in various gases.

With a few approximations [81, 82] equation 3.49 may be reduced to a more usable form; the reduced form of B_{12} is :-

$$B_{12} = \pi/6 \left[\sigma_{12}^3 . B_r.(T_r) \right] \quad \ldots\ldots (3.51)$$

with

$$\frac{1}{T_r} = \frac{\epsilon_{12}^*}{kT} \quad \ldots\ldots (3.52)$$

$B_r(T_r)$ is a universal function [33] and for $B_r < 0$ and small changes in $(1/T_r)$ it may be expressed,

$$B_r = a - \left(\frac{b}{T_r}\right) \qquad \ldots\ldots(3.53)$$

Equation 3.49 may now be written:-

$$\log_{10}\frac{m}{m_0} = 0{\cdot}43\frac{v_1\rho}{22{\cdot}4} \quad 0{\cdot}86\frac{\pi}{6}\sigma_{12}^{3}\frac{N\rho}{22{\cdot}4}\left(a - \frac{b\epsilon^*}{kT}\right) \ldots(3.54)$$

Equation 3.54 will be called the "Robin - Vodar equation".

The force constants for the mixture σ_{12} and ϵ_{12}^* may be calculated from the force constants of the pure components using the relationships,

$$\sigma_{12} = \frac{1}{2}(\sigma_{11} + \sigma_{22}) \qquad \ldots\ldots(3.55)$$

and $$\epsilon_{12}^* = (\epsilon_{11}^* . \epsilon_{22}^*)^{1/2} \qquad \ldots\ldots(3.56)$$

Constants 'a' and 'b' are determined graphically from a plot of B_r against T_r.

Robin and Vodar [79] found that in a great many cases the experimental data could be represented in the form:-

$$\log m = A + B\rho \qquad \ldots\ldots(3.57)$$

where A and B as a first approximation are independent of ρ. Therefore since equation 3.54 also becomes linear in ρ at constant temperature, Robin & Vodar considered their equation qualitatively satisfactory.

Fig. 3.4 shows the degree of success afforded by the Poynting relationship and equation 3.54, in expressing the solubility of carbon disulphide in nitrogen, hydrogen, and carbon dioxide.

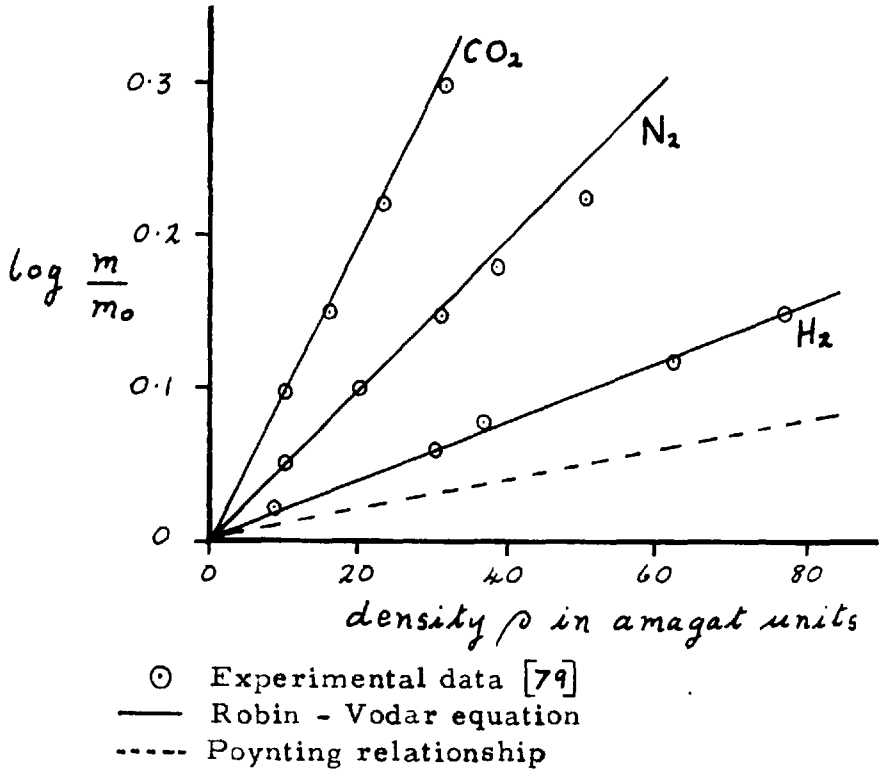

Fig. 3.4 Solubility of CS_2 in H_2 , N_2 and CO_2

At high pressures the Robin - Vodar equation becomes increasingly inaccurate since it is based on an equation of state limited to the 2nd virial coefficient. Rowlinson et al [86] have therefore developed a relation which in addition to the first approximation term of equation 3.49, also contains higher order terms, in particular the 3rd virial coefficient, which allows for the interaction between one solute and two solvent molecules.

$$\ln \frac{y_1}{y_1^{\circ}} = \frac{V_1 - 2B_{12}}{V} + \frac{V_1 B_{11} - \frac{3}{2} C_{12}}{V^2} + \frac{V_1 C_{111} - \frac{4}{3} D_{1112}}{V^3} + \ldots \quad \ldots\ldots (3.58)$$

V = molar volume of the mixture.

y_1° = mole fraction of solvent in saturated vapour at atmospheric pressure.

3.3. Prediction of the complete pressure-composition loop.

In a recent paper Prausnitz [74] has outlined a method for estimating the complete pressure-composition loop for a binary system. Therefore, in order to give a complete picture of the present day theory, a brief resume of this method will be presented.

It is assumed that data is available for, the solubility of the gas in the liquid at low pressures (i.e. Henry's Law constant), and also the composition, and pressure at the critical point. From this information the adjusted activity coefficients $\gamma_1^{(P,t)_c}$ & $\gamma_2^{*(P,t)_c}$ [5] of components 1 & 2 at the critical point can be calculated from the equations:-

$$\gamma_1^{(P,t)_c} = \frac{\phi_1^c P^c}{f_1^{(P,t)_0}} \exp. - \int_{P_1^s}^{P^c} \frac{\bar{V}_1^c \, dP}{RT} \quad \ldots\ldots (3.59)$$

$$\gamma_2^{*(P,t)_c} = \frac{\phi_2^c P^c}{K^{(P,t)}} \exp. - \int_{P_1^s}^{P^c} \frac{\bar{V}_2^c \, dP}{RT} \quad \ldots\ldots (3.60)$$

where ϕ = fugacity coefficient, p_i^s = saturation vapour pressure of the liquid, and superscript c refers to the critical point. The fugacity coefficients, and the partial molar volumes for both components, are computed from an equation of state for the vapour phase.

Knowing the values of $\gamma_1^{(p_i^s)_c}$ & $\gamma_2^{*(p_i^s)_c}$ at the critical point, it is now possible to compute the constants in some analytical solution of the Gibbs - Duhem equation, such as those by Van Laar. For example, the Van Laar constants A & B may be found by the simultaneous solution of the two equations:-

$$\ln \gamma_1^{(p_i^s)_c} = \frac{A}{\left[1 + \frac{A/B}{x_2^c/x_1^c}\right]} \quad \ldots\ldots (3.61)$$

$$\ln \gamma_2^{*(p_i^s)_c} = B\left[\frac{1}{\left[1 + \frac{B/A}{x_2^c/x_1^c}\right]} - 1\right] \ldots\ldots (3.62)$$

Using the values of A & B determined from equations 3.61, 3.62, the adjusted activity coefficients for the components are calculated over the entire range of composition at constant temperature.

In the calculations so far it may be assumed that the partial molar volumes are functions of composition but not of pressure. In order to calculate the effect of the liquid composition on the partial molar volumes, Prausnitz has suggested a simple empirical relationship [74].

The isothermal P - y - x diagram is now constructed as follows.

At some arbitrary liquid composition x, the adjusted activity coefficients and the partial molar volumes for both components are calculated.

The equilibrium vapour composition y is found from the expressions:-

$$y_1 = \frac{\gamma_1^{(P,S)} x_1 f^{(P,S),o}}{P \phi_1} \exp. \int_{P_i^S}^{P} \frac{\bar{v}_1 dP}{RT} \quad \ldots\ldots (3.63)$$

$$y_2 = \frac{\gamma_2^{*(P,S)} x_2 K^{(P,S)}}{P \phi_2} \exp. \int_{P_i^S}^{P} \frac{\bar{v}_2 dP}{RT} \quad \ldots\ldots (3.64)$$

The total pressure P is obtained by summing equations 3.63 & 3.64 to give,

$$P = \frac{\gamma_1^{(P,S)} x_1 f_1^{(P,S),o}}{\phi_1} \exp. \int_{P_i^S}^{P} \frac{\bar{v}_1 dP}{RT} + \frac{\gamma_2^{*(P,S)} x_2 K^{(P,S)}}{\phi_2} \exp. \int_{P_i^S}^{P} \frac{\bar{v}_2 dP}{RT} \quad \ldots (3.65)$$

Any two of the last two equations are used to determine the two unknown y_1 (or y_2) and P. The solution of these equations must be done by trial and error, since the fugacity coefficients ϕ_1 & ϕ_2 depend on y and on P as given by an equation of state for the vapour phase.

The measure of success of this technique is shown in Fig. 3.5 where the experimental results for the system nitrogen - methane 5 are compared with the calculated results of Prausnitz.

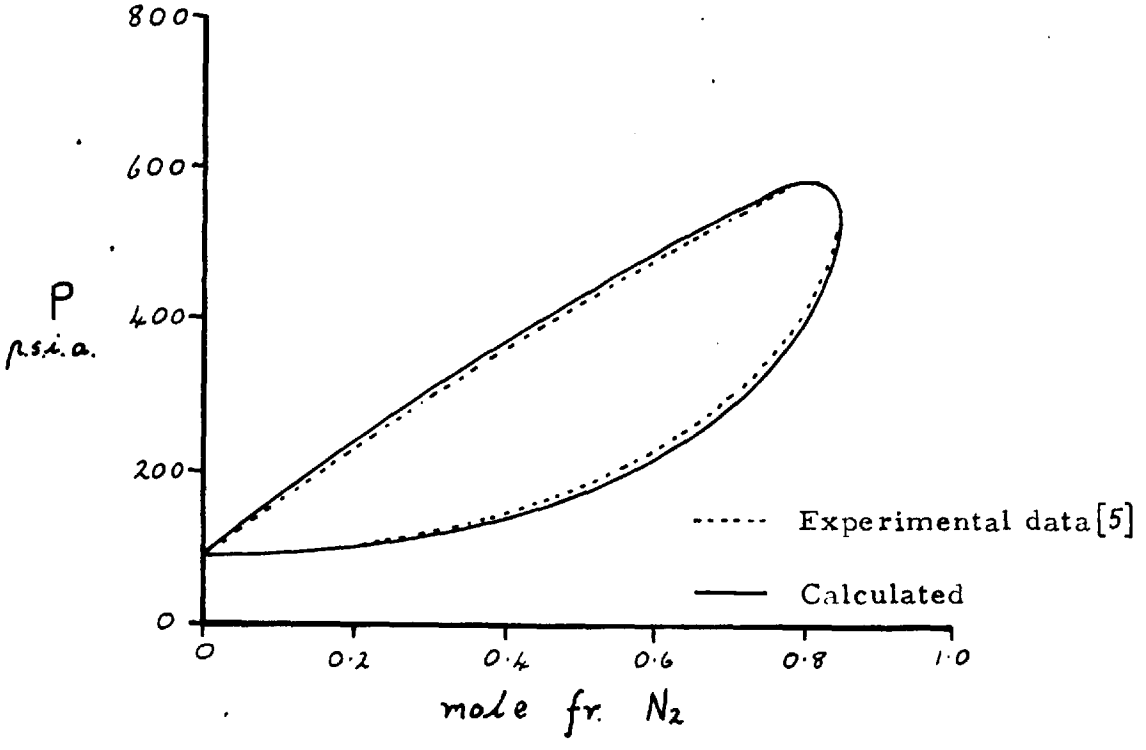

Fig. 3.5. Vapour - liquid equilibrium data for nitrogen - methane system at -210^0F.

CHAPTER 4

REVIEW OF EXISTING DATA

4.1 Gas solubilities at 1 atmosphere pressure.

The last few years have seen a great increase in the amount of accurate experimental data available for the solubility of gases at atmospheric pressure. Hildebrand [32], in a recent publication, has correlated all the data by plotting log solubility, in terms of mole fractions x_2, first against the solubility parameter of the solvent δ_1, and then against the force constant of the gases ϵ/k. An important feature of these curves, is that they make it possible to estimate accurately the solubility of any gas in a wide range of non polar liquids. In addition curves of log x_2 vs log T, also given in reference [32], are useful for predicting the change in solubility with temperature.

4.2 Vapour - liquid equilibrium data.

In the past, binary vapour - liquid equilibrium data has in general, only been determined for those systems of industrial importance. The result of this has been to restrict investigations, primarily to mixtures of hydrocarbons used in the petroleum industry [93], and to a few isolated polar systems such as Nitrogen - Ammonia [62,97], and Nitrogen - Water [3,107].

There is comparatively little work on permanent gas - non polar liquid systems with which this investigation is concerned, and of the data that is available, much of it refers to hydrogen - aliphatic hydrocarbon solvents. This is apparent in Tables I, II & III of Appendix I., where a summary is presented of all the published binary vapour - liquid equilibrium data in this field.

A comprehensive assessment of the data quoted in Appendix I. is difficult, since separate sets of results have very often been obtained at different temperatures. However, in the following discussion a brief comparison of results will be made wherever possible.

4.2.1. Systems containing hydrogen (Table 1 Appendix 1)

A system investigated by a number of workers is hydrogen - benzene. Ipatiev [36 & 37], Sattler [94] and Krichevski and Efremara [45] have all shown that the solubility of hydrogen in benzene increases with temperature, and that Henry's Law is only followed up to a pressure of 500 atm. Ipatiev [37], by going to higher pressures succeeded in freezing the liquid phase at 1900 atm. and 25°C, and reached the critical solution pressure at 150°C between 2000 and 3000 atm.

The gas phase composition as measured by Ipatiev [37] is well reproduced by the Robin - Vodar equation up to a pressure of 500 atm.

and at a temperature of 150°C, however, at lower temperatures the agreement is poor.

Katz & Williams [40], have measured the vapour - liquid equilibrium data for hydrogen in each of the hydrocarbons ethylene, ethene, propylene and propane at temperatures between + 70 and - 200°C. They plotted their results using the equilibrium constant K_E, which is equivalent to the ratio, composition of the gas phase over the composition of the liquid phase. A typical curve is that of the hydrogen - propane system shown in Figure 4.1. For the systems studied, they obtained a correlation for the hydrogen equilibrium constant K_E, involving the reduced temperature of the hydrogen in the binary system. However, there was no relation between the critical temperatures, the boiling points and the variations in .

The maximum pressure that could be obtained with the apparatus was 550 atm, and it is interesting to note that the lowest temperature at which the critical solution pressure could be attained, decreased from + 37.5°C for propane, to - 45.5°C for ethylene, the respective critical temperatures being 368.6°K and 282.7°K.

The data for the hydrogen - propane system is in good agreement with that of Sage et al. [91].

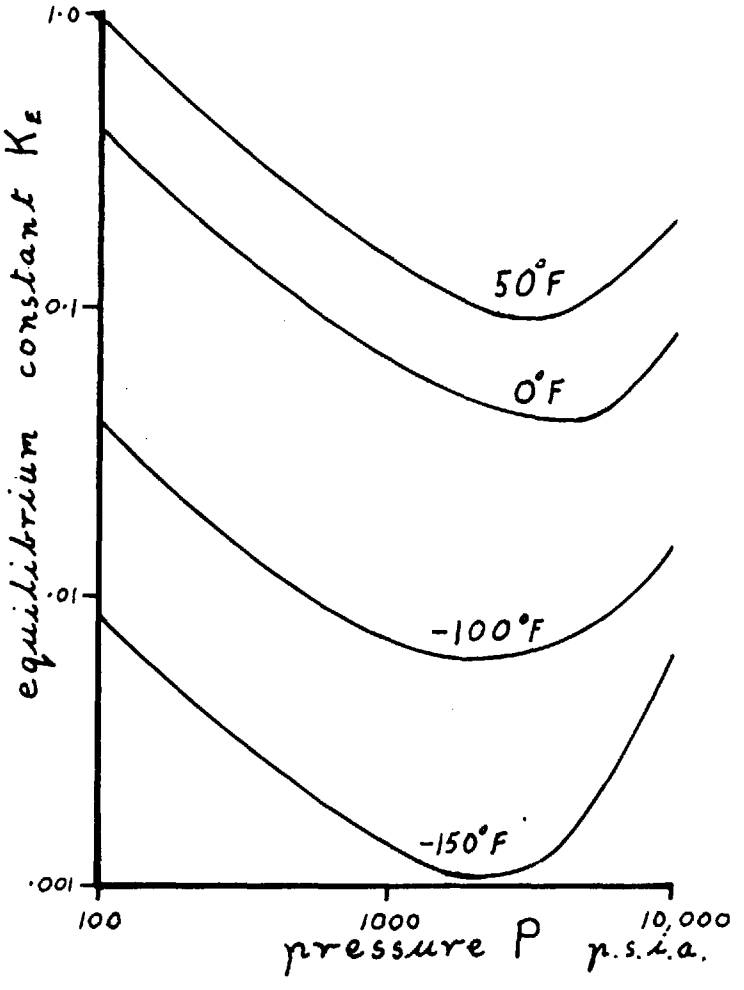

Fig. 4.1 Equilibrium constant K_E vs. pressure for H_2 - C_3H_8

The system hydrogen - liquid methane has been studied by Freeth & Verschoyle [20] , and by Gonikberg & Fastovski [25] . Their results at - 182.5°C agree well, but the experimental points of Freeth & Verschoyle show a rather greater scatter.

Nichols, Reamer & Sage [69] have completed the pressure - composition loop for the mixture hydrogen - hexane at a temperature of 171°C. At all temperatures below this they found that the critical solution pressure exceeded 680 atm., the maximum pressure range of their apparatus.

Dean & Tooke [13] have measured the solubility of hydrogen in isobutane, iso octane, and the isomeric dodecanes at pressures below 320 atm., and at temperatures between 37.5 and 150°C. In all cases the solubility increased with temperatures and pressure, but it was noticeable that it decreased for solvents of higher molecular weight. Only in isobutane below 65.5°C did the solubility of hydrogen follow Henry's Law, in the other two hydrocarbons the solubility increased more rapidly with pressure at lower pressures than at higher pressures.

The results for iso octane at 150°C have been confirmed by the more recent work of Peter & Reinhartz, [71] .

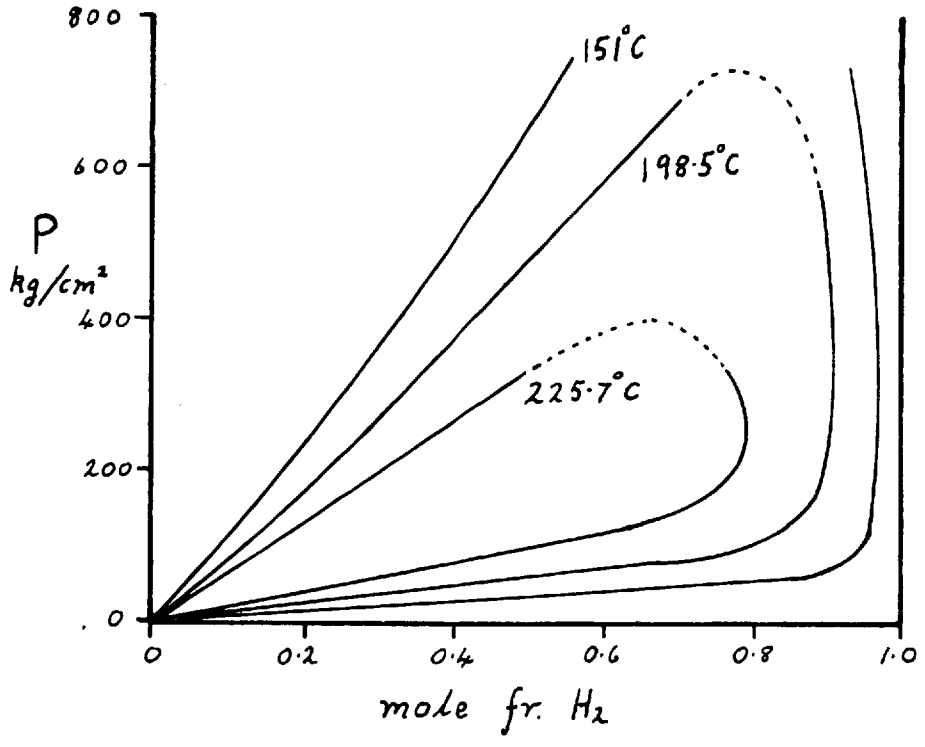

Fig. 4.2 Vapour - liquid equilibrium for system H_2 - nC_7H_{16}

Peter & Reinhartz [71] have also studied the system hydrogen - n. heptane, and hydrogen - methylcyclohexane. The critical solution pressure was found to increase quite sharply with decrease in temperature as shown in Fig. 4.2. For both n.- heptane and iso-octane the critical solution pressure was reached at about 400 atm., and 730 atm., at temperatures of 225.7 and 198.5°C, respectively, however, in the case of methylcyclohexane, the extrapolated critical solution pressure

was 980 atm at 225.5°C. They suggested that the smaller solubility of hydrogen in methylcyclohexane, is probably due to the closer packing of its molecular structure.

In an interesting series of experiments Lachowicz & Weale [57] measured the solubilities of hydrogen, and deuterium, in n. heptane and n.- octane for pressures between 100 and 300 atm., in an attempt to separate the two isotopes. Within the limits of experimental error, there was no difference in the solubilities of the two gases, and Henry's Law was obeyed over the whole pressure range.

4.2.2. Systems containing nitrogen & argon (Tables II & III Appendix I)

Miller & Dodge [6], and Krichevski & Efremova [45], have both measured the solubility of nitrogen in benzene. Their results agree within the experimental accuracy of 1 to 3%, and are well reproduced at 25°C by the Krichevski - Kasarnovski equation (see equation 3.42) up to the maximum solute concentration recorded of 0.20.

Miller & Dodge have also recorded the composition of the gas phase, and they found that the mole fraction of benzene always goes

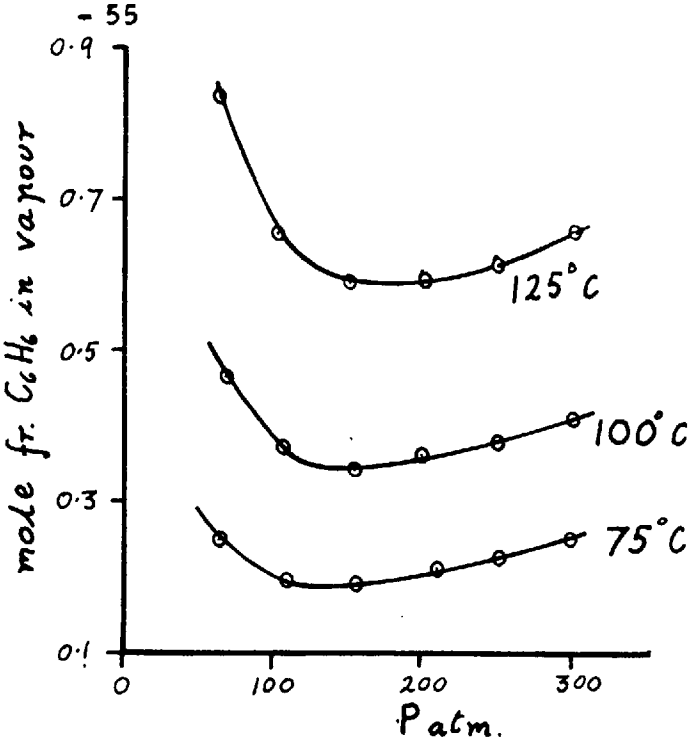

Fig. 4.3 Solubility of C_6H_6 in N_2

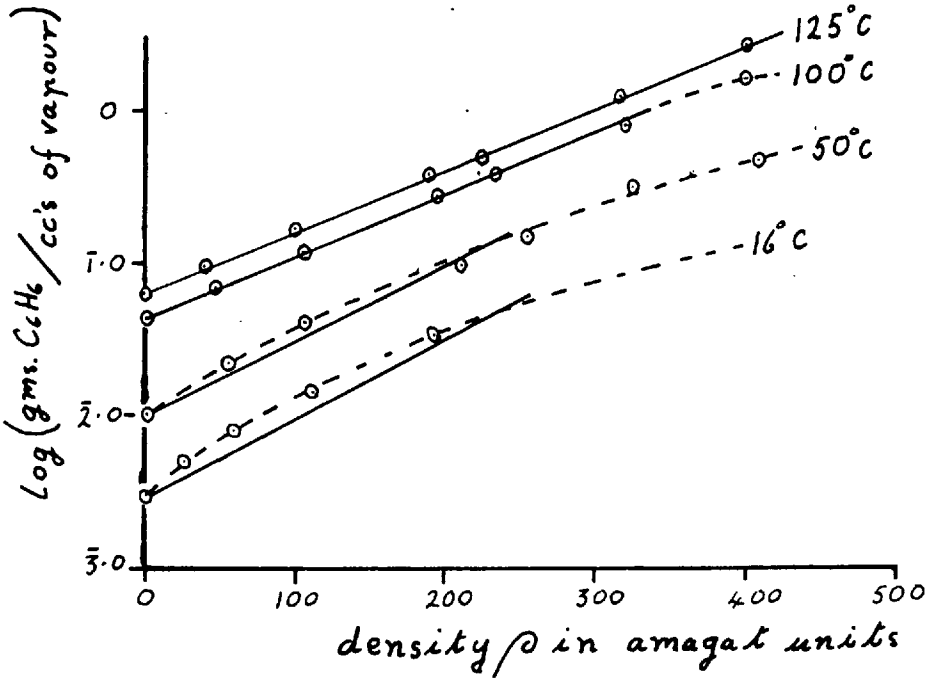

Fig. 4.4 Shows the fit of experimental data for solubility of C_6H_6 in N_2 with Robin Vodar equation.

through a minimum with increasing pressure; (see Fig. 4.3) the pressure at which the minimum occurs increasing from 140 ats. at 75°C, to 180 ats. at 125°C. The existence of this minimum has been confirmed by Krichevski & Gamburg [53] in their measurements up to 1000 atm, and in the temperature range 16 to 100°C. Above 30°C the Robin - Vodar equation fits these experimental results reasonably well, (see Figure 4.4), but beyond this pressure the experimental values tend to curve towards the pressure axis. At temperatures of 100 & 125°C agreement was obtained up to pressures of 1000 atm.

Both Miller & Dodge and Krichevski & Gamburg reported solubilities approximately 15% greater than the values given in an earlier work by Lewis & Luke [61].

The vapour - liquid equilibrium curves for the system nitrogen n. butane were measured by Roberts & McKetta [78]. Their results show that the critical solution pressure decreased from 210 to 75 atm., as the temperature changed from 71°C to 137.5°C. Above 37.5°C these results are not in agreement with the earlier work of Akers and his co - workers [1], probably because the gas density balance used for the analysis was not sufficiently accurate.

Graham [27, 111] measured the solubilities of nitrogen and argon in iso - octane and n-octane, and argon in carbon tetrachloride, at temperatures of 50, 75 and 100°C, and at pressures between 50 & 300 atm. The solubility of argon in perfluoromethylcyclohexane at 50°C in the same pressure range was also reported. It was found that Henry's Law would be applied to the system nitrogen - n-octane up to a solute concentration of 0.3., but that in all other systems deviations of as much as 15 and 56% occured. The Krichevski - Kasarnovski equation gave a better fit with the data than Henry's Law, but due to the uncertainty in the value of tha partial molar volume of the gas in the solution it was not used to predict the solubilities in other systems.

Over a considerable pressure range Graham found that the solubility isotherms could be expressed by a purely empirical equation of the form:-

$$s = aP + bP^2$$

where a and b are constants and s is the liquid phase composition.

The results for the system argon - carbon tetrachloride are interesting in that, contrary to the general behaviour the solubility of argon decreases with increasing temperature even at pressures as high as 300 atm. (see Fig. 4.5). This is to be expected at low pressures, since the solubility of argon in carbon tetrachloride at atmospheric pressure is greater at lower temperatures [77]. However, as the

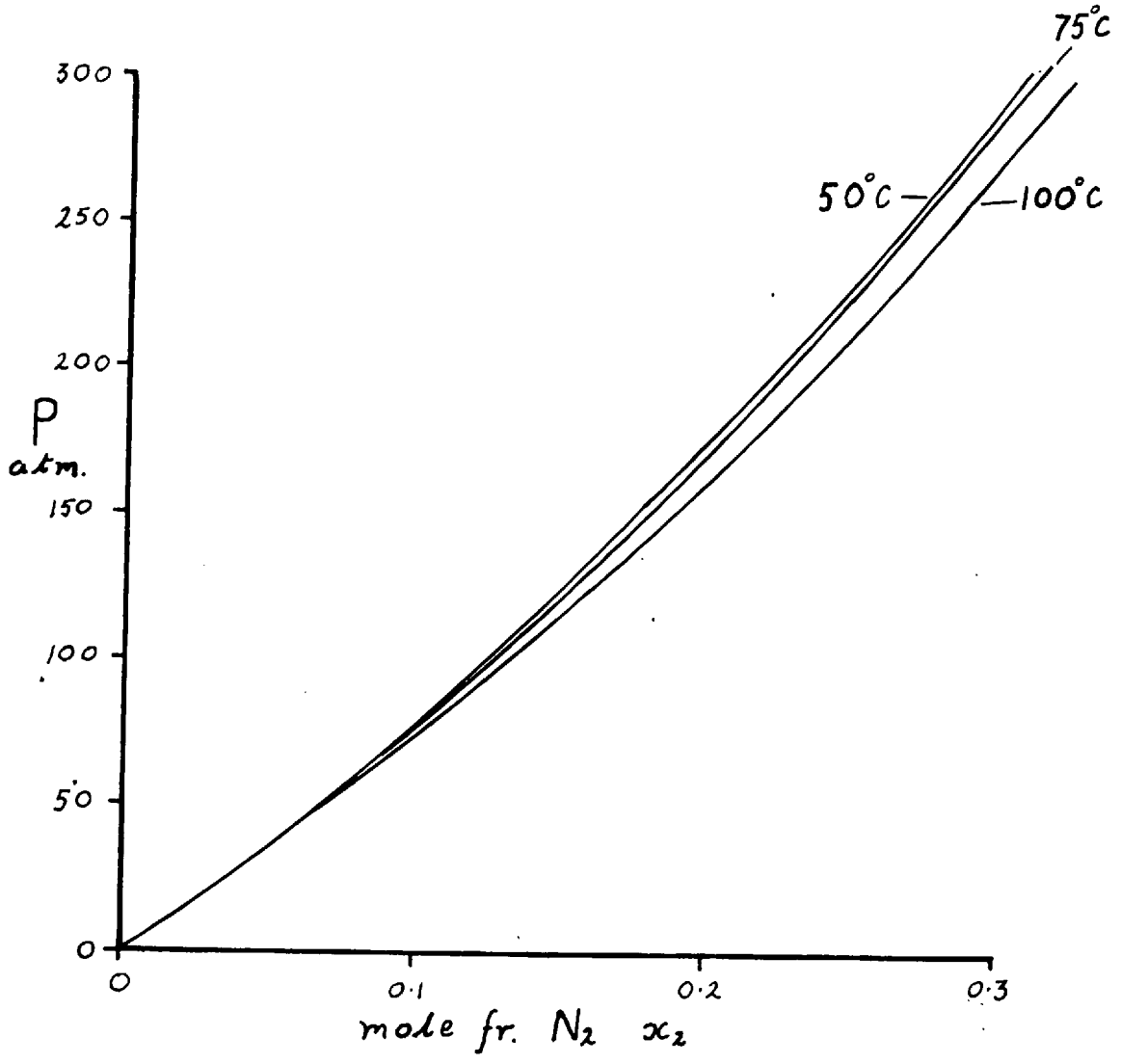

Fig. 4.5 Graham's results for solubility of N_2 in CCl_4

pressure is increased the solubility isotherms must cross at some point due to the trend of the critical pressure to lower values at higher temperatures.

A major limitation of Graham's apparatus was that the composition of the gas phase could only be measured to an accuracy of 10%. Nevertheless, the Robin - Vodar equation gave a disagreement with the experimental values of well over 10%, and for argon - perfluoromethylcyclohexane the disagreement was 60% at 300 atm.

4.2.3 Summary.

Although a large amount of binary vapour - liquid equilibrium data is available, there is very little concerning simple systems composed of a permanent gas and a non polar liquid. Where measurements have been reported, only in a few cases has any consideration been given to the thermodynamics of the system or to the theoretical equations presented in Chapter 3. Nevertheless, it is possible to make the following generalizations.

(1) The relationship between the solubility of a gas and the pressure obeys Henry's Law over a limited pressure range. This pressure range depends upon the concentration of the gas in the solution, the general rule being that the higher the solubility, the smaller the pressure range over which the relationship holds.

(2) Deviations from Henry's Law are in the direction of increased solubility, and this is accompanied by an increase in the amount of liquid in the gas as the pressure approaches the critical pressure.

(3) At low concentrations of solute, the Krichevski & Kasarnovski equation gives a better fit with experimental results than does Henry's Law.

(4) For most solvents at elevated pressures, the solubility increases with temperature, and the critical solution pressure tends to lower values at higher temperatures. This means that the heat of solution is positive.

(5) From (4) it follows that, for systems having a negative temperature coefficient of solubility at atmospheric pressure the solubility isotherms must cross at some pressure below the critical solution pressure.

(6) The gas phase composition may be represented by the Robin - Vodar equation in a limited pressure range. The pressure range tends to increase as the temperature is increased.

(7) The gas phase composition goes through a minimum with increasing pressure.

CHAPTER 5

SURVEY OF EXPERIMENTAL METHODS USED IN PREVIOUS INVESTIGATIONS

Since for binary systems pressure, temperature and composition are all variables, vapour - liquid equilibrium data can be measured in the following three ways:-

(1) with temperature constant and measuring the variations of phase compositions with pressure — in which case the results provide the (P - x) loop.

(2) with pressure constant and measuring the variation of phase compositions with temperature — in which case the results provide the (T - x) loop.

(3) with the composition constant and measuring the variation of pressure with temperature -in which case the results provide the (P - T) loop.

The actual procedure which is used is generally dependant on the form in which the data is required,and also to some extent on the temperature and pressure ranges of the measurements.

However, when discussing the experimental methods that have been used in previous investigation, it is more convenient to consider the procedures as consisting of two operations. Firstly, the attainment

of equilibrium in the system by some method of mixing, and secondly, the determination of the composition of each phase at equilibrium, or, as in the case of method (3), the detection of the bubble and dew points of the mixture.

5.1 Methods of achieving equilibrium

In order to obtain equilibrium throughout the whole system, some method of mixing or agitation of the two phases must be employed. The methods most commonly used are, mechanical stirring or shaking of the equilibrium vessel, or a flow method in which the gas is bubbled through the liquid at constant pressure. These three techniques will now be briefly discussed with special regard to their advantages and disadvantages.

5.1.1 Mechanical stirring

When the stirrer is driven from outside the high pressure vessel, the principle difficulty is to obtain a pressure seal at the point where the moving shaft passes into the vessel. To avoid this difficulty, Tsiklis [97] used a stirrer actuated by a solenoid placed inside the pressure vessel, this restricts the possibility of leakage to the static pressure seals around the insulated leads conducting the current. There are two drawbacks to this arrangement, firstly, the heat generated by the solenoid disturbs the isothermal conditions in the system, and secondly, the additional space taken up by the solenoid increases the dimensions

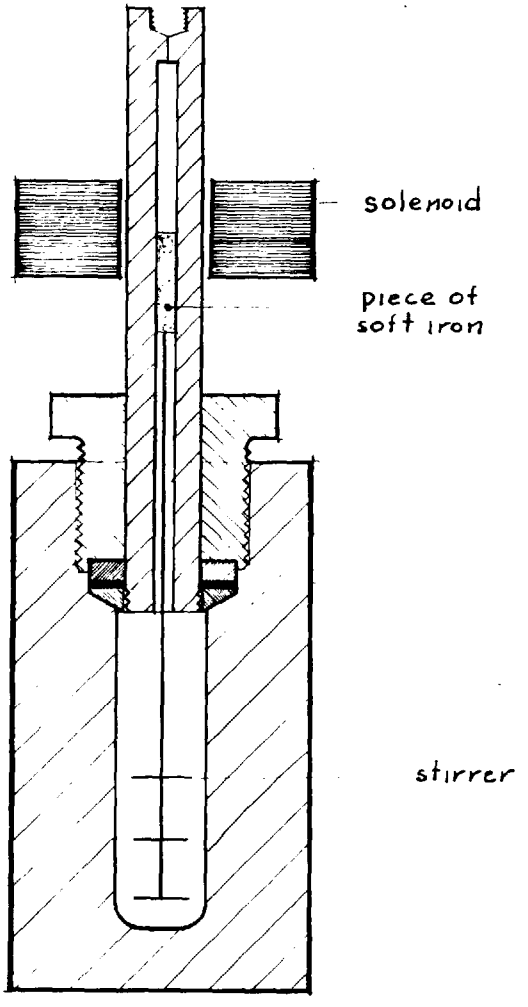

FIG. 5.1. SKETCH SHOWING MAGNETIC STIRRER USED BY LINDROOS & DODGE [62]

of the pressure vessel.

A better design is that used by Krichevski & Efremova [45] , and Lindroos & Dodge [62] ; in both investigations the top of the stirrer shaft was encased in a head of a non-magnetic material, so that the solenoid could be located externally, as shown in Fig. 5.1 When the solenoid was switched on and off, the piece of soft iron attached to the stirrer shaft moved up and down inside the pressure vessel, so that the ensuing oscillating motion mixed the two phases. A similar idea was employed by Shanbag [95] and Graham [27] , but instead of a solenoid they used a large permanent magnet which they rotated around the outside of a non-magnetic head, so that the magnetic flux rotated a smaller magnet placed inside the head, and to which was attached the stirrer shaft.

Although a magnetically driven stirrer overcomes the difficulty of a moving pressure seal, it cannot be employed for very viscous fluids, such as liquid paraffin at 3000 atm, since the magnetic torque required to drive the stirrer would be impractically large. Therefore, this method is limited to the less viscous fluids, such as pentane, and even in this case care must be taken to allow for the increase of viscosity with pressure.

A further design factor associated with mechanical stirring is the optimum diameter of the equilibrium vessel. In high pressure

vessel design, it is generally more convenient to arrange for the diameter to be small relative to the length. However, the smaller the diameter, the smaller the area of contact between the phases, and hence the longer it takes for the system to reach equilibrium .

5.1.2 Shaking of the equilibrium vessel

This procedure has been used by a number of workers [13,21,58, 65,94,105] . The usual arrangement is to have the equilibrium vessel in a cradle pivoted at it's centre, the rocking motion being produced by a crank arm attached to an electric motor. Dean & Tooke [13] rocked the vessel through an angle of 60° at 30 revolutions per minute, and found that below 300 atm. equilibrium could be attained for the system hydrogen-iso-octane in ten minutes; other workers [58,65] have found the time taken under similar conditions is much longer; of the order of several hours.

The great disadvantage of this method, is that it is necessary to disconnect the equilibrium vessel from that section of apparatus which it is expedient not to shake (e.g. the pressure gauge). This disadvantage may be overcome if a flexible connecting pipe line is used, but then the possibility of fatigue failure arises due to the continual flexing of the pipe.

5.1.3 Bubbling the gas through the liquid at constant pressure (The dynamic or flow method)

This is the procedure employed by Wiebe & Gaddy [107,108] , Krichevski [42] , Saddington & Krase [89] , Miller & Dodge [66] , Michels

et al [64] and Dodge & Dunbar [18].

It is a more efficient method than mechanical stirring or shaking, since the bubbles of gas passing through the liquid make for a very large area of contact between the phases. However, if the gas is passed through the liquid once only, the contacting time is very short and the gas phase may not reach equilibrium. Michels et al [64] overcame the difficulty by employing a porous plug soaked with liquid, this ensured a slow passage of the gas bubbles in intimate contact with the solvent. Another approach used by Miller & Dodge [66], was to supersaturate the gas in pre-saturaters before passing it into the equilibrium vessel.

The chief advantage of the dynamic method, is that it is particularly suitable for gas - liquid systems in which the concentration of liquid vapour in the gas phase is small. On the other hand it has two practical drawbacks. Firstly, the pressure must be kept constant during saturation, and it is generally necessary to do this manually. Secondly, it is difficult and expensive to maintain a continuous supply of pure gas at a constant high pressure- this is especially true at pressures above 200 atm.

It is possible to avoid a number of the troubles inherent in the dynamic method, if the gas is continually recirculated through the liquid. This idea was used by Roberts & McKetta [78] in their work in the nitrogen - n-butane system at pressures up to 213 atm.

In the three methods discussed, the saturation of the two phases may be approached either by increasing the pressure to the desired value, or reducing it from some higher pressure. In this way errors caused by failure to reach equilibrium may be detected, since which ever technique is used the resulting data should be the same.

5.2 Methods of determining the phase composition

5.2.1 Sampling Technique

This is by far the most common method of determining phase composition. It involves taking small samples of the gas phase and the liquid phase from the system at equilibrium, and then analysing these samples at atmospheric pressure. In most of the experiments, errors were introduced by not making an allowance for the drop in pressure that occured during sampling. Only in a few cases [45, 106, 110] were the samples isolated at the equilibrium pressure, before expansion and subsequent analysis. In Graham's apparatus, [27] the sampling vessel was made part of a pressure loop by connecting it to the top and bottom of the main equilibrium cell. Samples of the two phases could then be isolated without altering the pressure in the system. This technique was applied successfully to the liquid phase, but Graham found that without circulating the gas in the high pressure loop, he could not obtain a sample of the gas phase at true equilibrium.

The simplest method of analysis is to freeze out the heavier

component in the system, and to measure the volume of the remaining gas in a burette. This procedure has been employed by a large number of experimenters [45,58,66,94,105]. It is successful when there is a large difference between the freezing points of the two components, but it is not applicable for a system of the type carbon dioxide — carbon - disulphide, where the freezing points are relatively close. In such cases it is often preferable to absorb one of the components in a suitable chemical reagent.

Although very rarely applied in this field, probably one of the most effective analytical procedures would be to measure the composition of the phases by vapour phase chromatography.

5.2.2 Direct measurement

When applied to the liquid phase, this method involves measuring directly the volume of gas required to saturate a given volume of liquid. The technique of Michels, Gever & Bijl [65] was to have two pressure vessels of known volume connected by a valve, one vessel contained the liquid, and the other the high pressure gas. When the connecting valve was opened and the contents of the two vessels mixed, a drop in pressure occured, which was indicative of the solubility. In spite of measuring the pressure to an accuracy of 0.004%, the estimated overall error of the determination was in the order of 5%.

Using a similar approach Gamburg [22] studied the nitrogen - benzene system at pressures up to 1100 atm. He measured, by piston displacement, the increase of volume caused by the introduction of known amounts of liquid into the compressed gas chamber.

5.2.3 Radioactive tracers

If radioactive tracers are added to one of the components, then at equilibrium the composition of the phases can be deduced from the quantity of radioactivity they emit. At first sight this is an attractive method, since the determinations can be carried out without disturbing the equilibrium, but very often it is found difficult to apply. It has been used by Rowlinson et al [38] to measure the solubility of mercury in propane and n-butane at pressures up to 30 atm. and in the temperature range 184 to 256°C.

5.2.4 Absorption spectrography

Although this method is capable of high accuracy it is limited to dilute solutions in the gaseous phase. It is based on the fact that dissolved substances often possess band spectra in a region in which the gas is "transparent". Robin & Vodar [80] used this phenomenon to determine the solubility of phenanthrene in compressed nitrogen, hydrogen, and argon at pressures up to 1200 atm.

5.3 Detection of Dew and Bubble Points

Briefly, this procedure entails increasing the pressure in a gaseous mixture of a known fixed composition, until the first drop of liquid appears (this is the dew point), and then increasing the pressure still further, until all the liquid disappears (this is the bubble point). Bloomer & Parent [5] observed the phase change through a visual cell, but Sage & Lacey [92] preferred to induce condensation on a thermocouple junction, so that the phase change was indicated by the deflection of the galvanometer needle.

These methods are not very accurate, and can only be applied at low pressures in the region of a few hundred atmospheres and to systems of high solubility such as mixtures of hydrocarbons.

5.4 Conclusions

This investigation is concerned with systems of permanent gases and non polar liquids which are known to have low solubilities even at 200 or 300 atm. Therefore, since the pressures are likely to be high if measurements are taken up to the critical point, the best experimental procedure is to determine the effect of pressure on the phase composition, at a number of constant temperatures i.e. the $(P - x)$ loop.

Hence the apparatus for this work must be developed with two

problems in mind, firstly, a reliable method of attaining equilibrium, and secondly, an accurate technique for measuring the composition of the gas and liquid phases.

At the pressures envisaged, the dynamic method of attaining equilibrium is not possible, due to the difficulty and cost of obtaining a steady flow of high pressure gas. Of the other two methods, shaking the equilibrium vessel is unattractive due to the necessity of disconnecting the pressure gauge for each run, and therefore mechanical stirring is the most desireable.

Although a number of refined techniques have been used by previous investigaters to measure the composition of the two phases at equilibrium, these methods are limited in their applicability, and furthermore their accuracy is very often difficult to predict. Hence, for the type of system being investigated it is best to use the sampling technique, which is both accurate and simple to apply.

CHAPTER 6

DESCRIPTION OF APPARATUS

It was required to design an apparatus to measure vapour - liquid equilibrium over a pressure range of 50 to 300 atm. , at temperatures between 0 and 100°C, with an accuracy of approximately 1%. With these limits in mind, it was decided that the best procedure would be to employ a constant volume apparatus similar to that used by Graham [27], but in addition to have the gas continually circulating through the liquid. Such an apparatus has the advantages of using a minimum quantity of high pressure gas, and yet producing complete saturation of the gas phase, which Graham [27] failed to achieve. An outline of the apparatus used in the investigations is shown in the schematic diagram Fig. 6. 1.

The two phases are brought to equilibrium by, (i) circulating the high pressure gas around the system using a small pump and, (ii) by mechanical stirring of the equilibrium vessel E; the stirring in E is essential in order to prevent supersaturation of the liquid phase. A small flowmeter in the form of a hot wire anemometer is inserted in the apparatus, and this gives an indication of whether the circulating pump is operating successfully.

At equilibrium, the liquid sample is isolated in the sampling

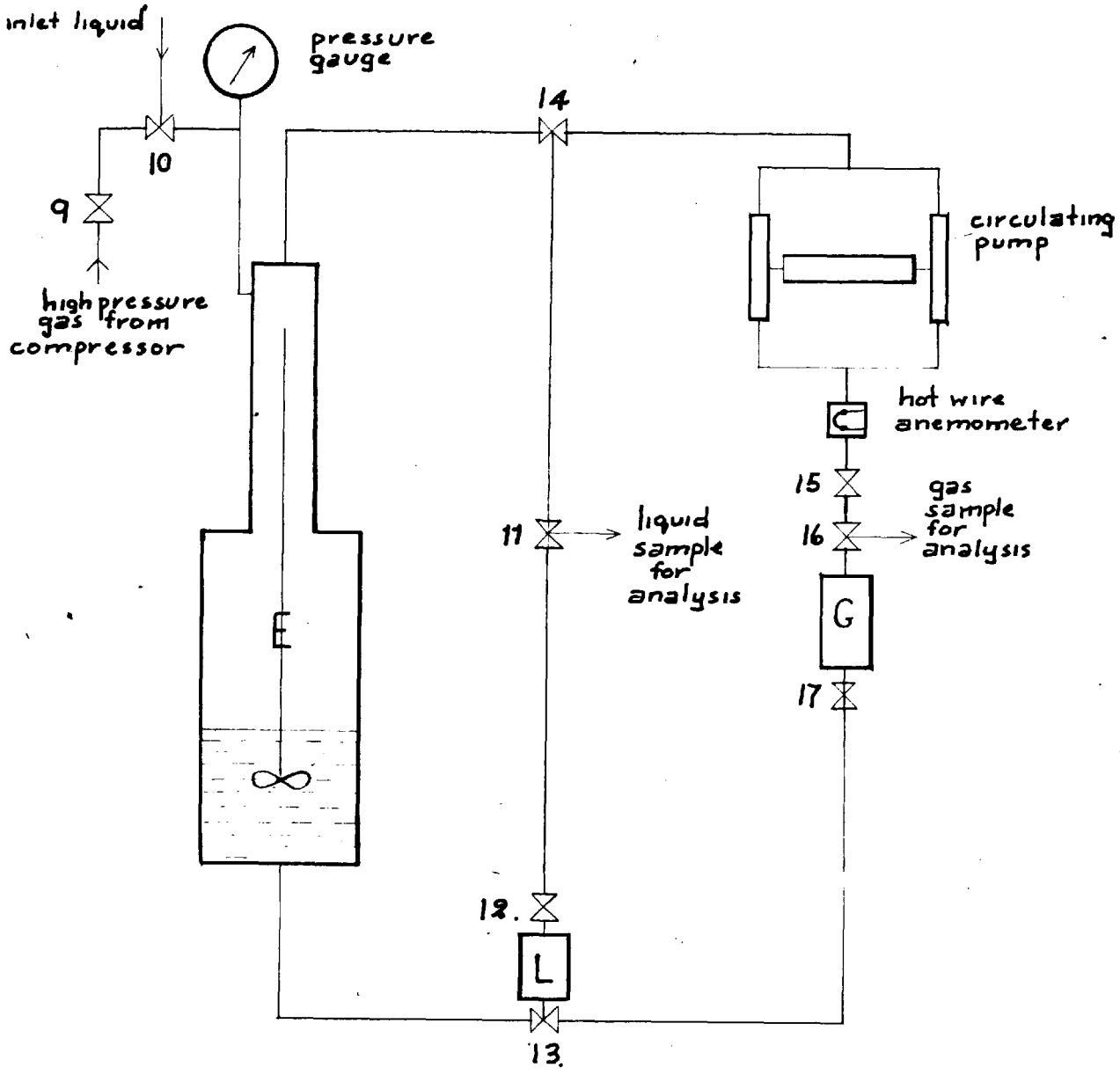

FIG. 6.1. SCHEMATIC DIAGRAM OF EQUILIBRIUM APPARATUS

vessel L by opening valve 13, and allowing the liquid phase to drain into the vessel by gravity. An interesting feature of this design, is that it avoids any change of pressure in the system during sampling, due to vessel L being connected to the remainder of the high pressure apparatus via valve 14. The gas phase sample is isolated in vessel G by closing valves 15 and 17. The relative positions of the two sampling vessels are important, since L must be below the liquid level in E, to avoid the possibility of some of the gas phase being trapped in the sample, and similarly G must be above the liquid level, to prevent any of the liquid phase being trapped in the gas sample.

Finally, the pressure of the system is measured by a bourdon tube pressure gauge, the range of which depends upon the maximum pressure being measured.

Both the liquid and gas phase samples are analysed by freezing out the liquid component, and measuring the volume of the remaining gas at room temperature and pressure. As concluded in Chapter 5 this is the simplest procedure, and for the type of system being investigated is undoubtedly the most suitable. A flow diagram of the all glass apparatus used, is given in Fig. 6.2,

The samples leave the equilibrium apparatus via tap 1 and tap 2, and the solvent is frozen out in the trap T. Liquid nitrogen is used as

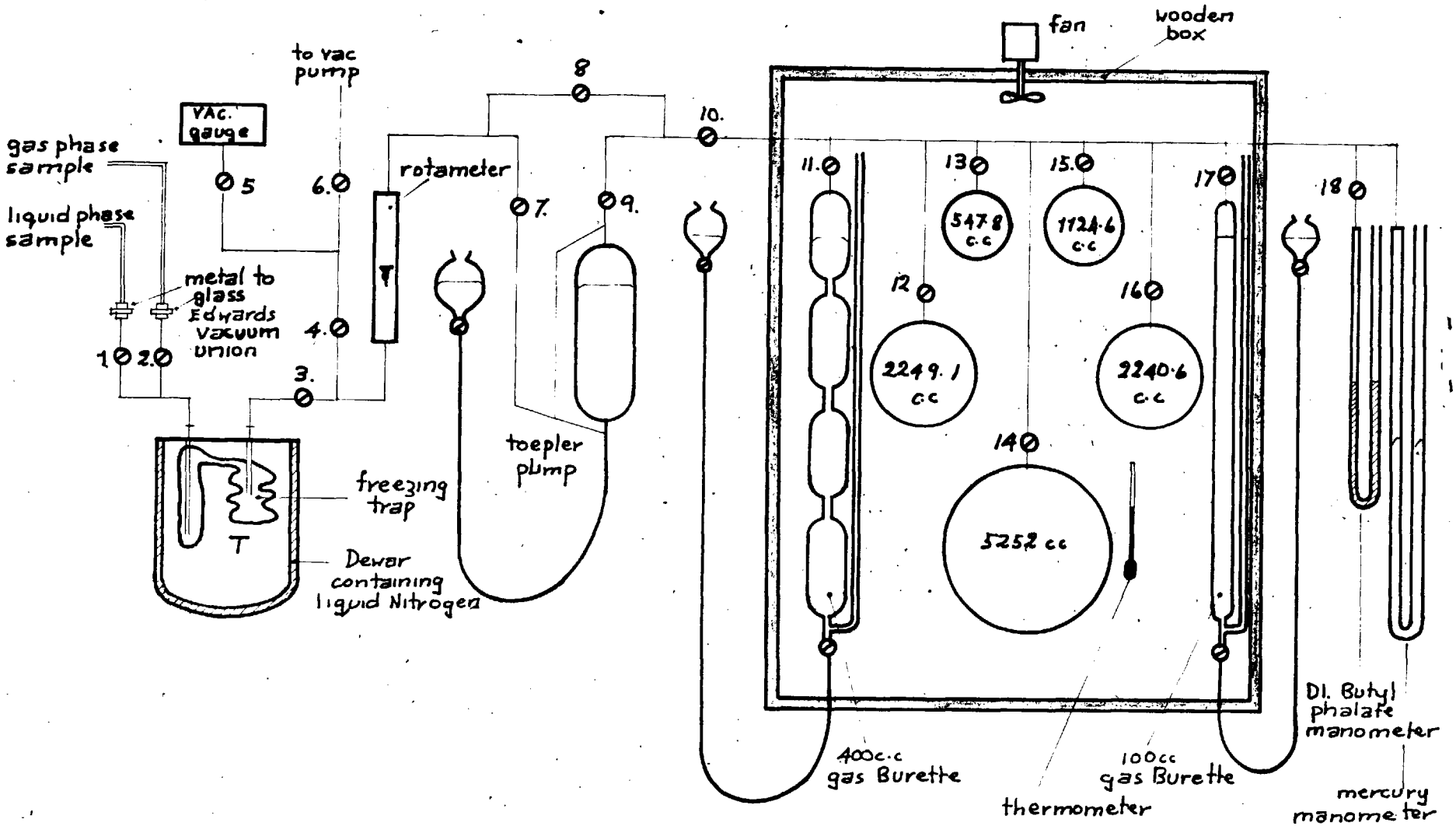

FIG. 6.2. SCHEMATIC DIAGRAM OF ANALYSIS APPARATUS

the freezing liquid, and since its boiling point is -210°C the vapour pressure of the solvent will be very small, even compared with the vacuum of 10^{-1} m. m. of mercury developed in the line. After passing through the solvent trap the remaining gas is pulled via a rotameter and Toepler pump into the mercury gas burettes and calibrated flasks, where its volume is measured. Two manometers, one filled with mercury and the other with di-butyl phalate, enables the system to be adjusted to atmospheric pressure before each reading is taken. Also attached to the line after the solvent trap is a two stage vacuum pump, which evacuates the apparatus to a vacuum of 10^{-2}m. m. of mercury as read on the vacustat.

Gas volumes up to 500 c. c are measured in the two mercury gas burettes (one has four calibrated bulbs of approximately 100c. c each, and the other has a capacity of 100c. c. calibrated in 0.2c. c.); for larger volumes the mercury burettes are used in conjunction with the calibrated flasks (these have approximate volumes of 500, 1000, 2000 and 5000c. c's). The 500 and 1000c. c flasks and the burettes are calibrated to 0.1°C, and the 2000 and 5000c. c flasks to better than 1c. c. using the technique recommended by the National Physical Laboratory [6]. In order to avoid an uneven temperature the gas measuring vessels are surrounded by a wooden box in which the air is circulated. The box

has a perspex front with small doors in it, through which the taps can be operated.

In addition to the equilibrium and analysis apparatus, it is necessary to have some means of developing gas pressures up to 3000 atm. Since a continuous flow of high pressure gas is not required, the best method is to use a simple Mercury Lute Compressor [63], where the moving mercury piston compresses the gas. This type of machine was first used by Amagat and Cailletet, and later adapted by Imperial Chemical Industries Ltd., for their polyethylene process [2].

The Mercury Lute Compressor designed for this work has two stages and is shown diagramatically in Fig. 6.3. The first stage compresses the gas from cylinder pressure to 1000 atm., and consists of two cylinders A and B connected at their base by a steel capillary U tube. Cylinder C acts as the second stage and serves to boost the pressure up to the required 3000 atm. Inside C there are two containers which hold the mercury, the upper one is termed C_1 and the lower one C_2.

Operation of the compressor is extremly simple and may be briefly explained as follows:-

Gas at cylinder pressure is allowed into B and C_1, and then compressed with the mercury piston by pumping oil into cylinder A. When the pressure is in the region of 1000 atm., the first stage is isolated and

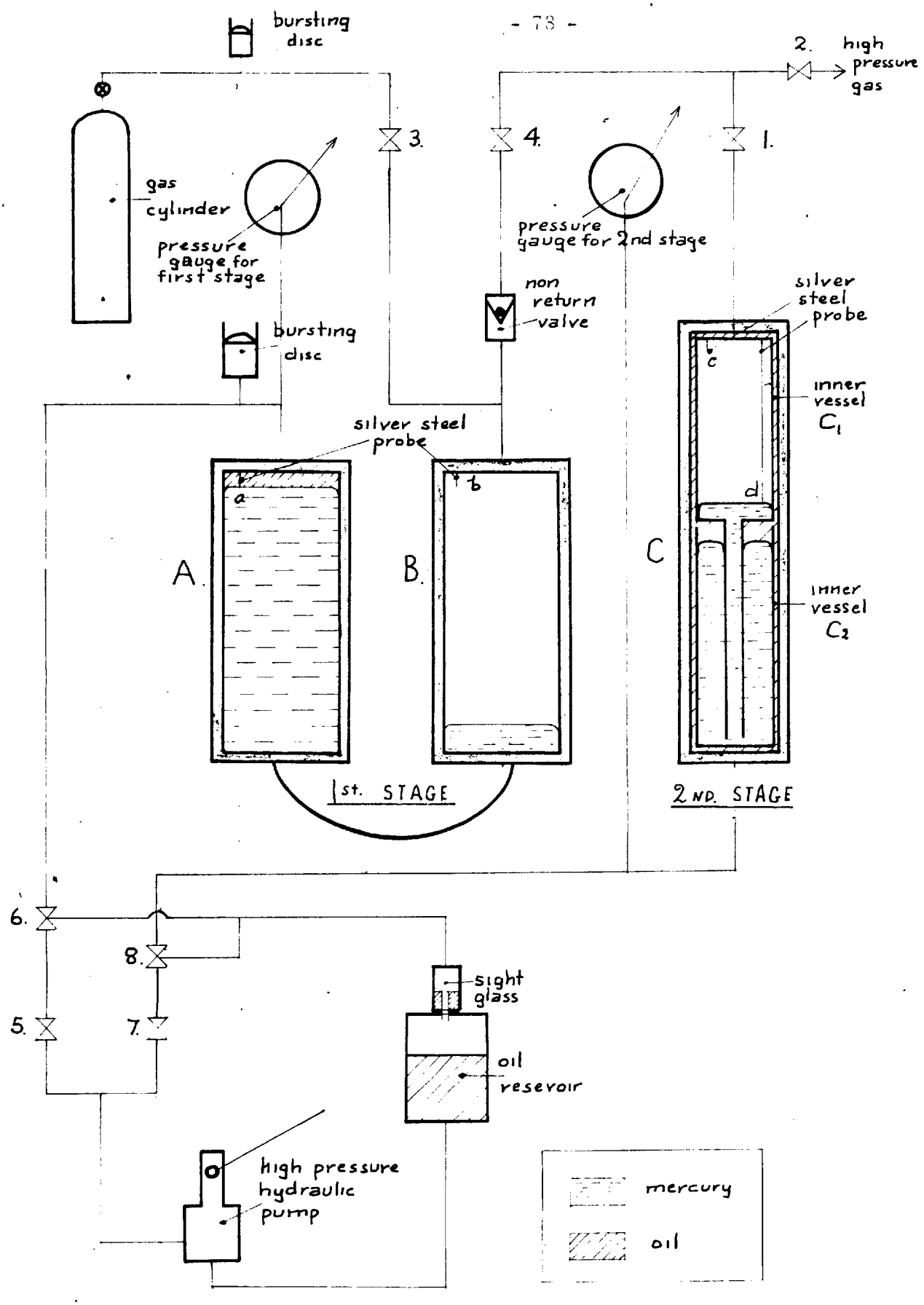

FIG. 6.3. SCHEMATIC DIAGRAM OF GAS COMPRESSOR

oil is pumped only into C_2 , until the gas is compressed to 3000atm. in the upper vessel C_1 . Using this procedure it is possible to obtain for each compression 185c.c of nitrogen at 3000 atm. from gas at 100 atm. Before carrying out a second compression the mercury level in B and C, must be lowered, and this is done by opening valves 6 and 8, and allowing the oil to flow back into the oil reservoir.

To keep the stroke of the mercury piston within certain limits the upper and lower extremities of the mercury level are detected with the silver steel probes "a", "b","c", and "d". When the mercury makes, or in the case of "d", breaks contact with the probes, a low voltage electrical circuit is completed which actuates a relay and turns on an indicator light.

To illustrate the appearance of the apparatus a photograph of the entire equipment is reproduced in Plate I. From left to right the three sections of the equipment are, the gas compressor, the high pressure equilibrium apparatus, and the analysis section. A more detailed description of the design and construction of the compression and the equilibrium section is given in Chapter 7.

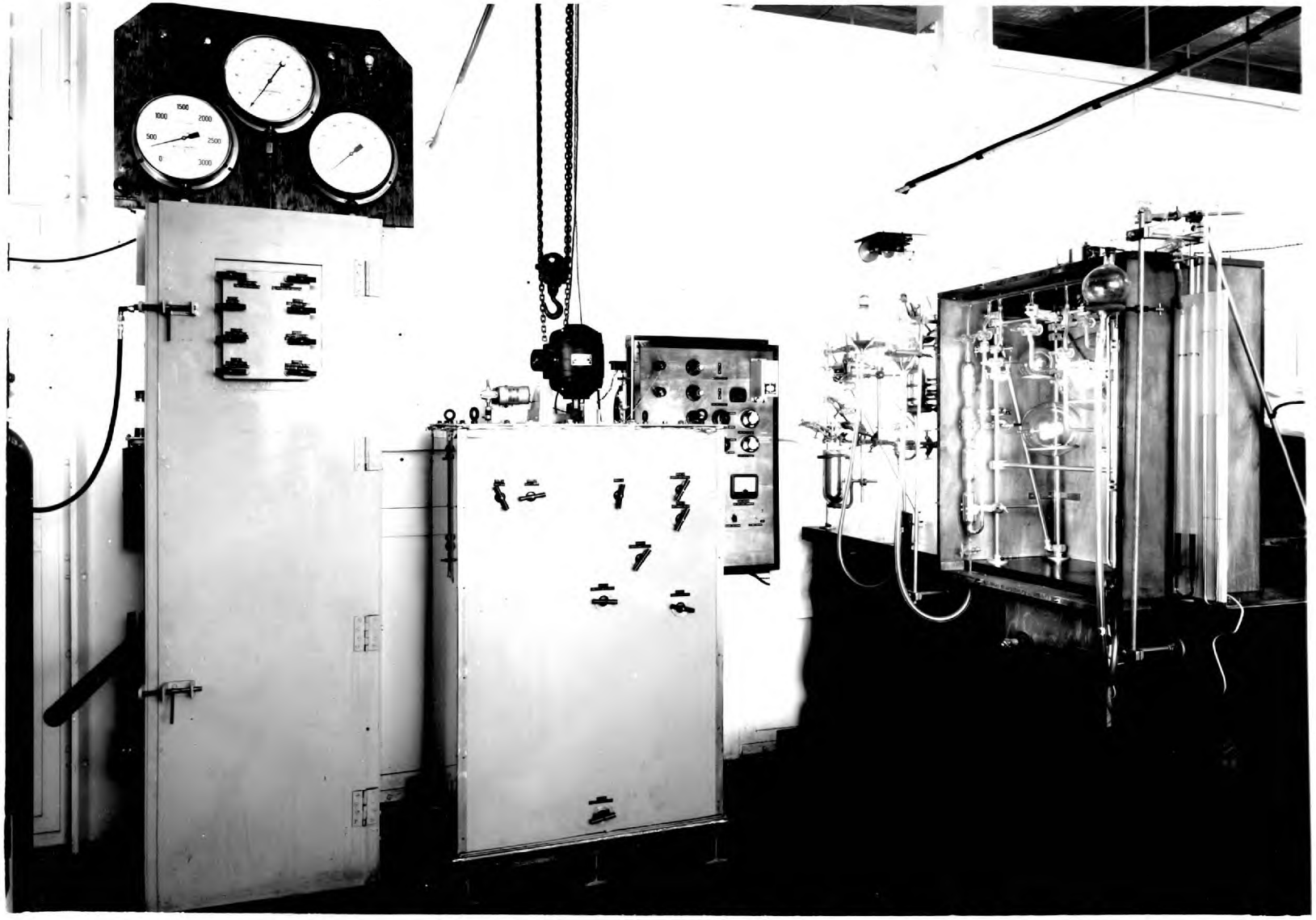

PLATE I General View of the Apparatus

CHAPTER 7

DETAILED DESIGN AND CONSTRUCTION OF THE EQUILIBRIUM AND COMPRESSOR SECTIONS

7.1 High pressure auxilliary equipment

Wherever possible standard high pressure equipment such as valves, elbows, tees, and tubing have been obtained from the American Instrument Co. Inc.,

The valves, suitable for a maximum working pressure of 4000atm, have a port opening of 1/16" and are fabricated from 316 stainless steel. An important feature in their design is that both spindle and seating are removable, so that they may be easily replaced or refurbished whenever necessary.

All the elbows, tees, and tubing have a maximum working pressure of 6,500 atm. The tubing is made from chrome molybdenum steel and has a bore of 1/16", the outside diameter being 1/4".

A total of three pressure gauges are used in the apparatus, two for the compressor and one for the equilibrium section. Each gauge is of the bourdon tube type, and for reasons of safety is fitted with special safety glass and a loose fitting back.

7.2 Detailed design of equilibrium section

7.2.1 General design features

Except for those components where non magnetic steels are required, all the pressure vessels are fabricated from B. S. 970 (En 25). This steel used in its fully annealed condition, is easy to machine, has an ultimate tensile strength of 60 tons per square inch, and an elongation of 20%. For a pressure vessel constructed with En 25 a radius ratio (ratio of outside diameter to inside diameter) of 3 is required to give a working pressure of 3000 atm. This figure is calculated on the basis of the bursting pressure P_B using the relationship:-

P_B = 3 × maximum working pressure = $2\sigma\left(\frac{k-1}{k+1}\right)$

and σ = ultimate tensile strength

k = radius ratio

It may be noticed in the later more detailed description of the equipment, that cone ring closures have been widely employed throughout the apparatus. A detailed drawing of a typical cone ring joint is shown in Fig. 7.1.

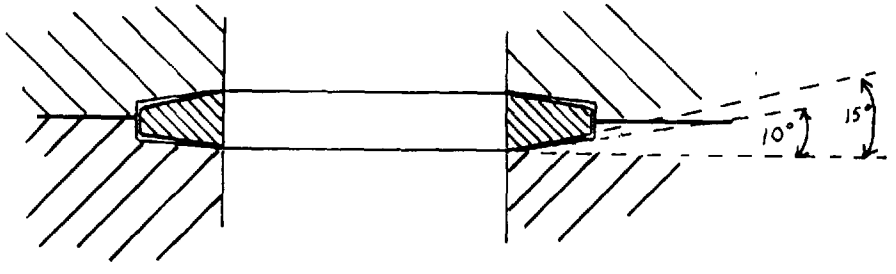

Fig. 7.1

The chief advantage of the cone ring is that it is a relatively simple self sealing joint, which may be taken apart and reassembled without difficulty.

Great care is taken in all the vessels to avoid any design feature which might give rise to high concentrations of intrinsic stress. To this end the following design principles have been observed wherever possible; (i) the avoidance of holes through the side of a vessel, (ii) the under - cutting of all threads, (iii) the removal of all sharpe corners, (iv) the provision of a smooth bore in the vessels.

7.2.2 Equilibrium vessel

The design of this vessel is dependent to a large extent upon the type of stirring device that is employed. As explained in Chapter 5 the best technique is to use a magnetic stirrer, with the driving force being produced either by a solenoid, or a permanent magnet. In either case this involves fabricating some part of the equilibrium vessel from a non magnetic material.

The vessel has therefore been constructed in three parts as shown in Fig. 7.2; the top and bottom sections are fabricated from En 25, and the middle section from a precipitation hardening non - magnetic steel specially cast for this work by Hadfields L.d., Sheffield. This steel carries the trademark "Resista P.H." and is basically of the 8% Nickel, 8% Manganese, 4% Chromium type, a typical analysis being:-

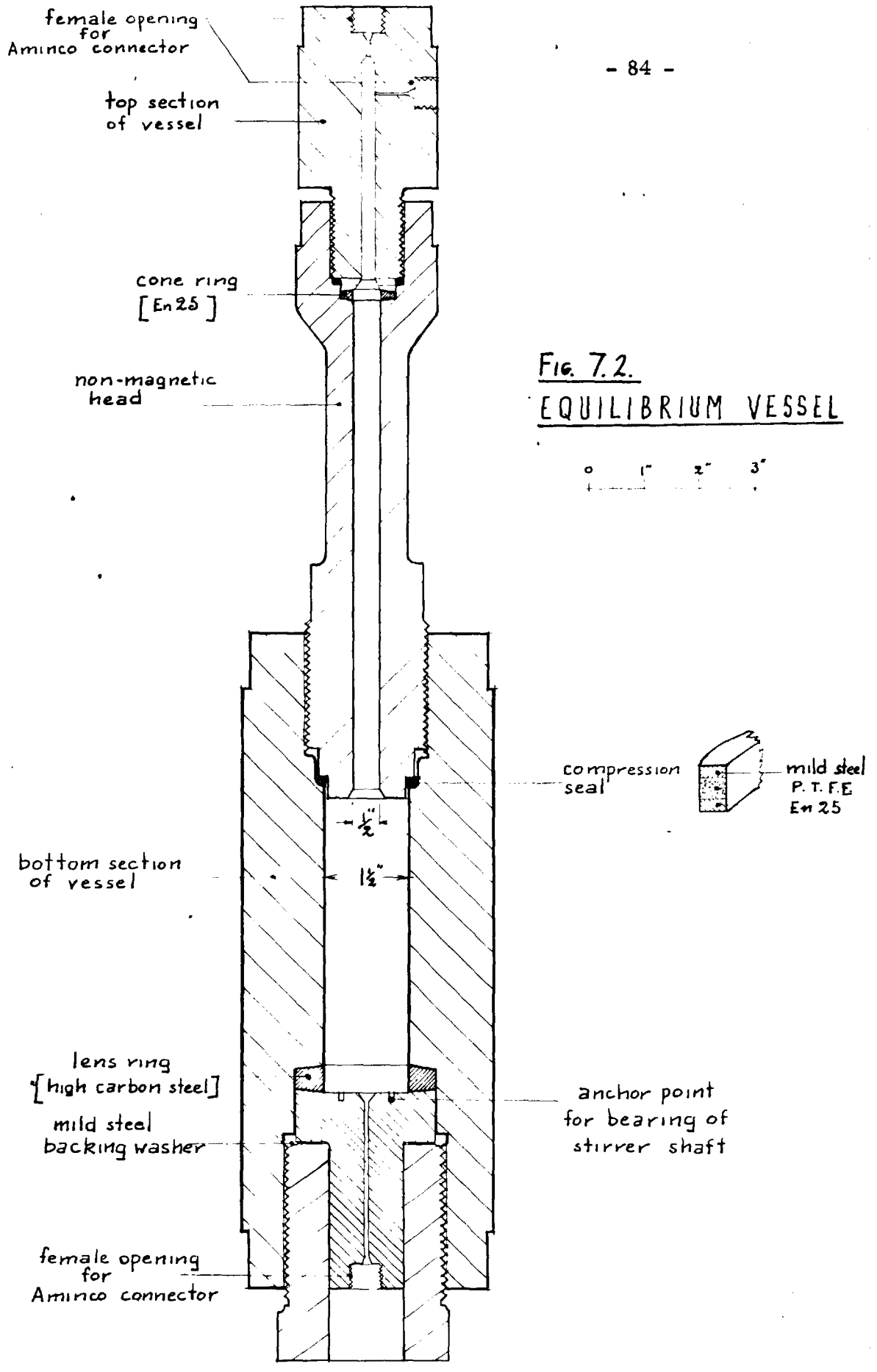

FIG. 7.2.

EQUILIBRIUM VESSEL

C.	Si.	Mn	Cr.	Ni.	V.
0.60	0.80	8.0	4.0	8.50	1.60

Mechanical tests carried out by Hadfields showed that the steel has an ultimate tensile strength of 61.5 tons per square inch, an elongation of 25%, and a reduction of area of 25%. A radius of 3 is therefore sufficient to withstand the maximum working pressure of 3000 atm.

Since Fig. 7.2 is drawn approximately to scale it is possible to judge the relative sizes of each section. The bottom section is by far the largest and has an internal volume of 160c.c, whilst the total capacity of the vessel is 200c.c.

In order to determine whether the stirrer should be driven by a solenoid or permanent magnet a few preliminary experiments were carried out. It was found that a solenoid big enough to operate the stirrer was extremly large, and also that local heating of the soft iron core occured due to eddy effects when using A.C. On the other hand an arrangement similar to that employed by Graham [27], with a large permanent magnet rotating around the non magnetic head, produced a torque sufficient to operate the stirrer under all conditions of temperature and pressure envisaged, with no heating effects. It was therefore decided to actuate the stirrer with a permanent magnet, and details of the type of construction used is given in Fig. 7.3.

Inside the non magnetic head a small shaped magnet, is clamped

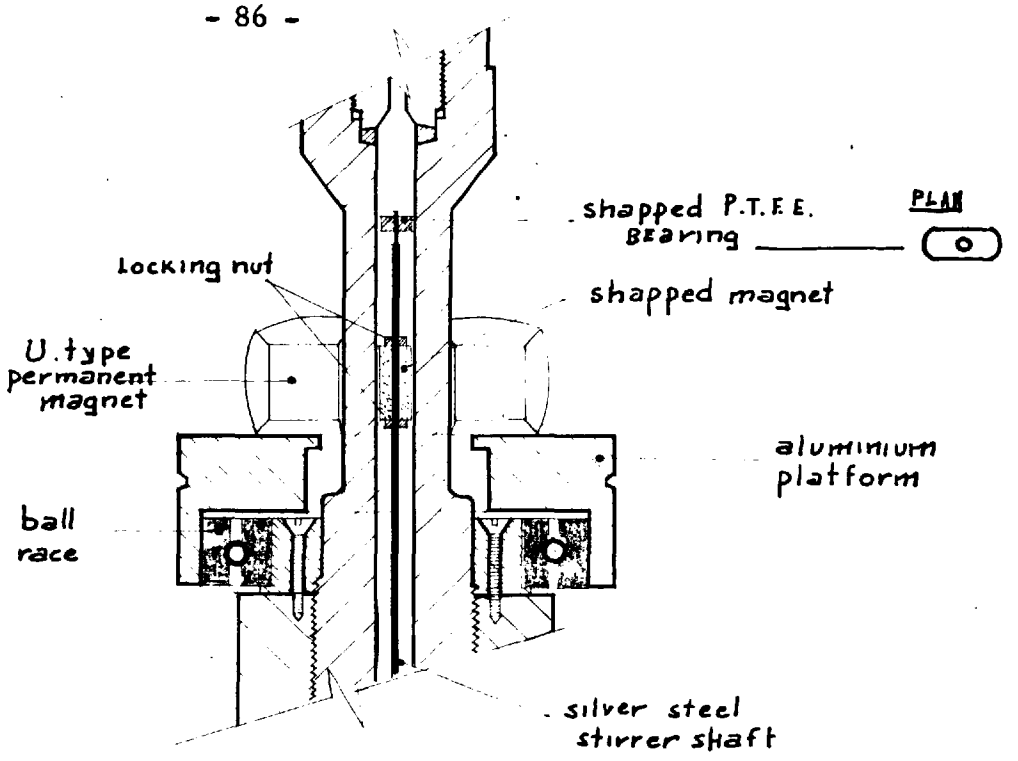

FIG 7.3. DETAILS OF DRIVE FOR STIRRER

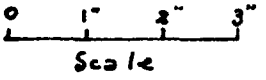

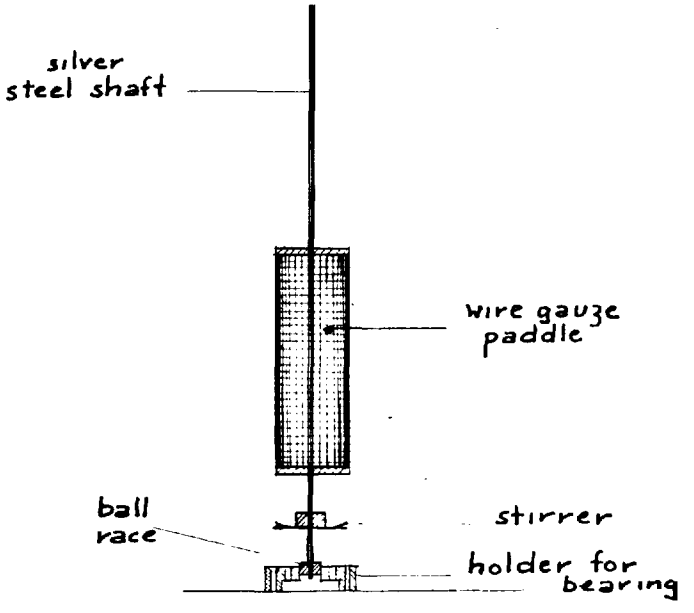

FIG. 7.4. TYPE OF AGITATOR EMPLOYED

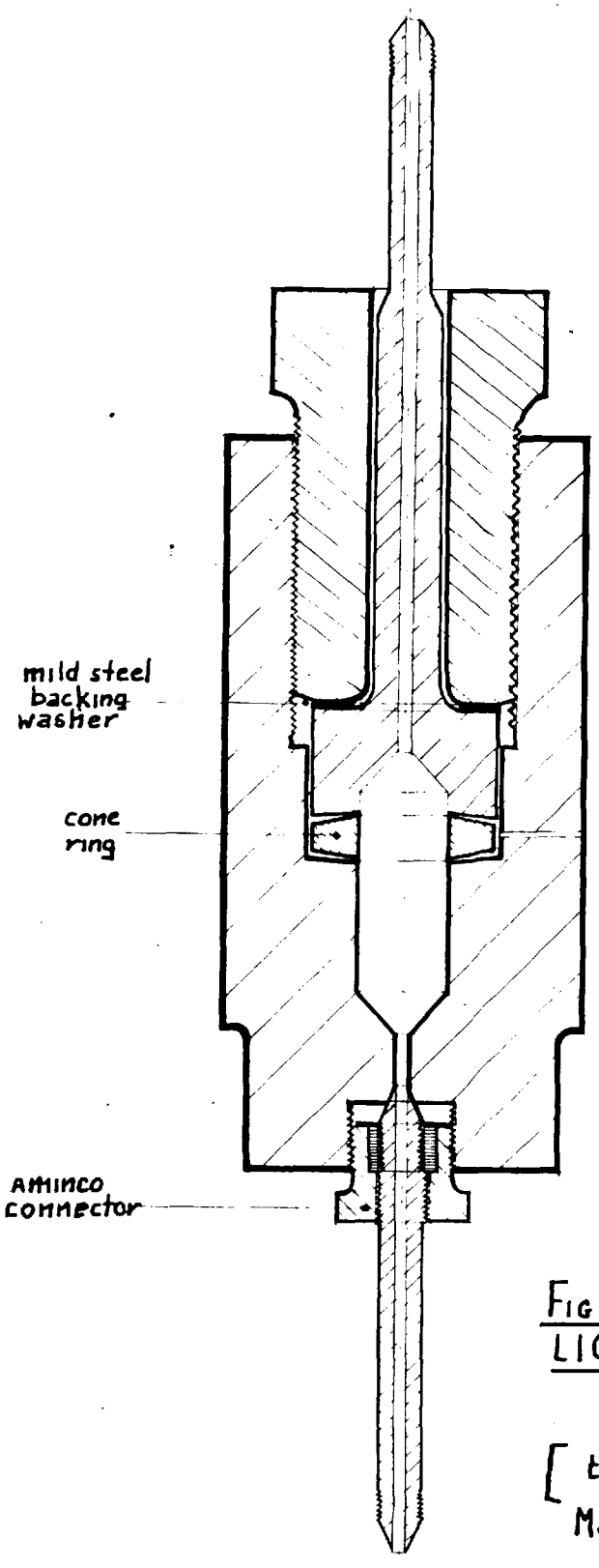

Fig 7.5.
LIQUID PHASE SAMPLING
VESSEL
[to scale - full size]
Material - En 25

to a silver steel rod which acts as the stirrer driving shaft. The shaft is held in place by a shaped P.T.F.E. bearing just above the magnet, and a ball race fixed to the bottom plug of the vessel. Attached to the shaft (see Fig. 7.4) is a small propeller and a wire mesh paddle; this arrangement is designed to mix both the gas and the liquid phases. The shape of the inner magnet is such that it allows easy passage of the gas phase through the vessel, and yet also helps to remove any entrained liquid. The large outer U - shaped magnet is clamped to an aluminium platform, with the pole pieces directly across the diameter of the non magnetic head. In this way a flux density of 4000 oersteds is maintained across the polepieces, and tests showed that this was more than sufficient to drive the stirrer in liquidparaffin, which has a viscosity several times, that of carbon tetrachloride at 3000 atm. and 30°C. The speed of rotation is 150 revs. per minute.

7.2.3 Gas and liquid sampling vessels

A detailed drawing of the liquid phase sampling vessel is given in Fig. 7.5. Great care is taken to have the cone rings seating flush with the bore, so that when the liquid phase enters the vessel no gas bubbles are trapped. Similarly, valves 11 and 13 are placed immediately before and after the vessel in such a way that no blind holes are left in the sampling section.

The gas phase sampling vessel is constructed in the same way as shown in Fig 7.5, but the length of the bore is increased so that its capacity becomes 10c.c, whereas the liquid phase vessel is only 4c.c.

7.2.4 Circulating pump

Preliminary calculations showed that the approximate requirements for the pump where that it should circulate the gas phase in the system at the rate of 40 to 80c.c per minute, against a pressure head of 7cms. of mercury.

As in the case of the stirrer, high pressure gland packings are avoided by actuating the pump with a permanent magnet, the actual construction is shown in Fig. 7.6.

A pump housing fabricated from non magnetic stainless steel, having a bore diameter fo 1/4" and an outside diameter of 3/4", is connected at either end to a double acting ball check valve. Now, when the piston is pulled along the bore by the outer magner, pumping takes place on both forward and backward strokes. In order to reduce friction, the bore of the housing is honed to a high polish (6 micro inches), and the piston is accurately machined from a piece of soft iron to give a clearance of 0.0005 inches throughout its length. The soft iron piston is 1" long, and has soldered to each end of it 1" lengths of brass rod, so that the clearance volume is reduced to a minimum. A further refinement is

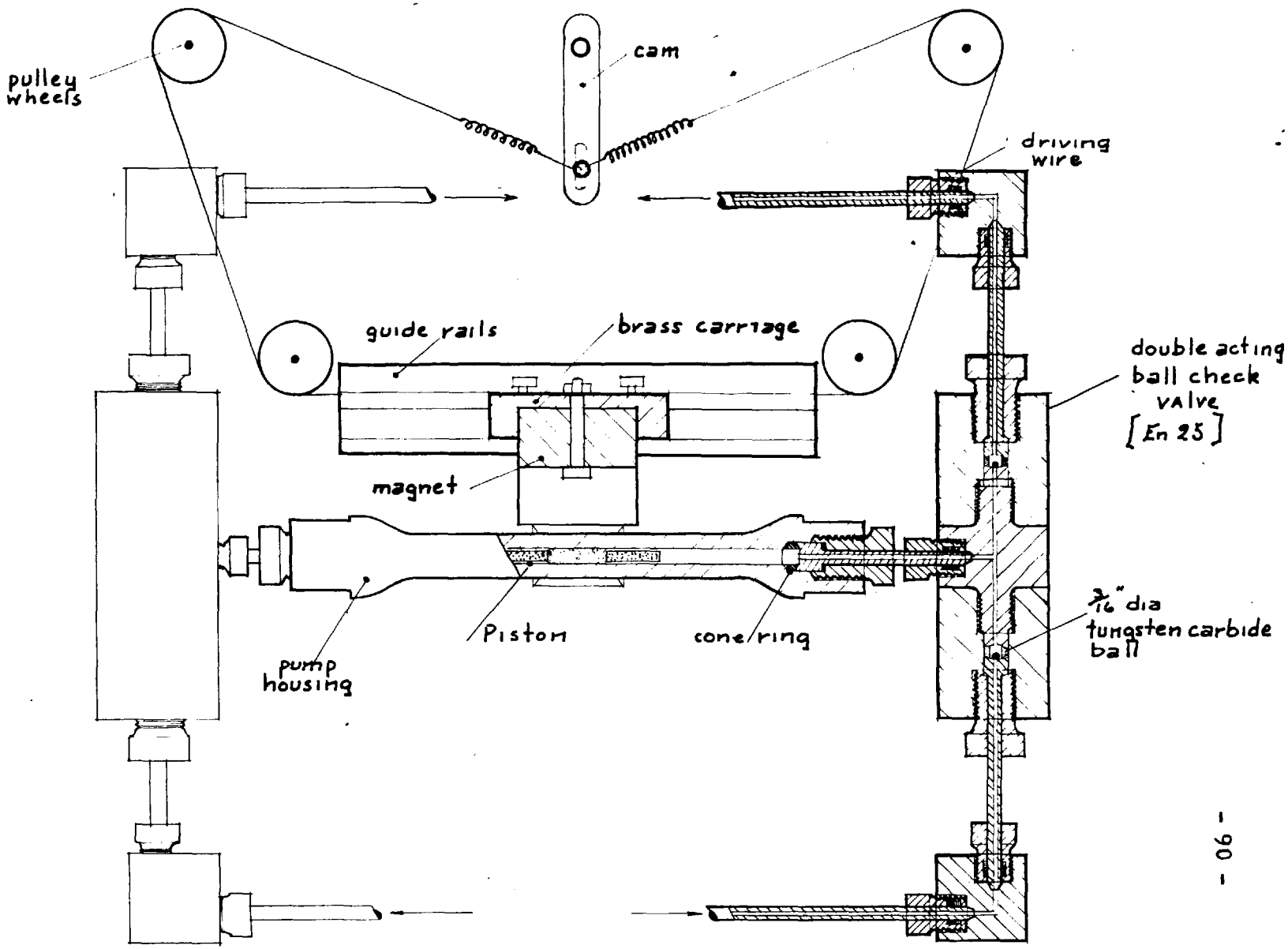

FIG. 7.6. GAS CIRCULATING PUMP

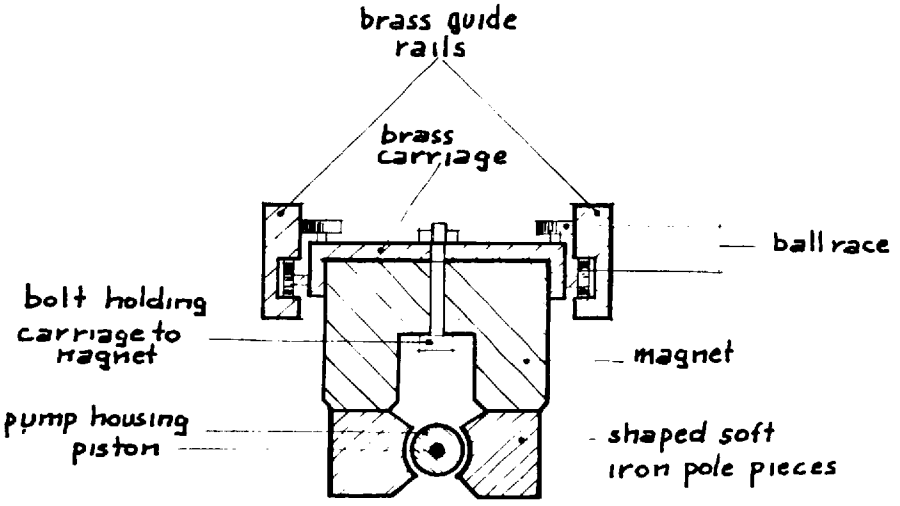

FIG. 7.7. SECTION THROUGH PUMP HOUSING

0 1" 2" 3"
Scale

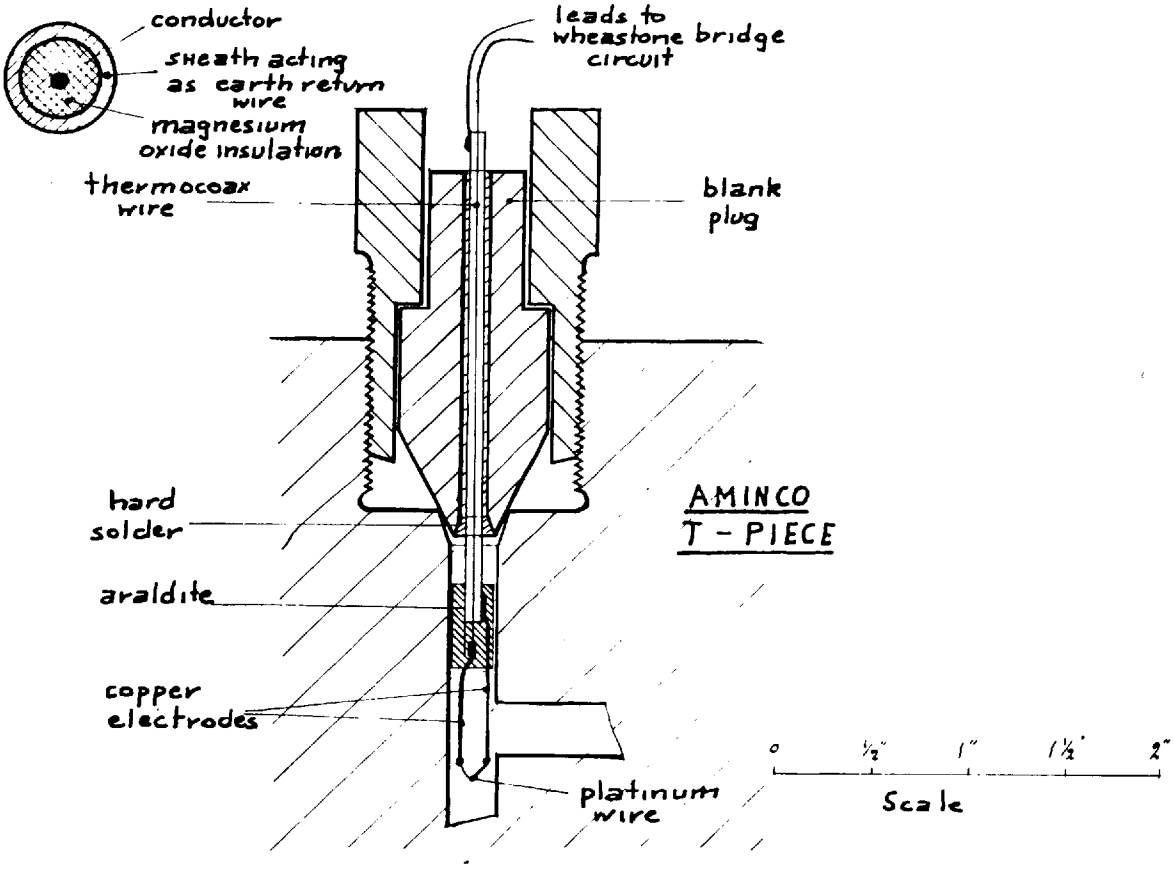

FIG 7.8. HOT WIRE ANEMOMETER

the shaping of the magnet pole pieces to the outside of the pump housing; this has the effect of concentrating the magnetic flux through the soft iron piston.

To facilitate the reciprocation of the magnet, it is attached to a brass carriage which will move easily along guide rails as depicted in Fig. 7.7. The carriage is driven by a flexible wire passing over pulleys, and connected to a cam wheel rotated by a small D.C. motor. The length of stroke can be varied by adjusting the diameter of the cam wheel, and the speed of the motor may be varied with a small resistance.

Before the pump was put into service it was subjected to a number of preliminary experiments with air under normal atmospheric conditions. These showed that different sizes and materials for the balls in the check valves produced marked changes in the operating characteristics of the pump. The balls which gave the best results and which were finally used, were 3/16" in diameter, and were fabricated from tungsten carbide. At its maximum speed of 24 r.p.m. the pump delivered 116c.c of air per minute against a head of 7cms. of mercury, the volumetric efficiency being approximately 65%. At lower speeds however, the volumetric efficiency decreased quite quickly, and was about 45% at 15 r.p.m.

At atmospheric pressure the limitation of the pump is governed by the relatively large clearance volume on each stroke, however, at

higher pressures the gas becomes more incompressible, and the force developed by the permanent magnet becomes the limiting factor. It is calculated that for argon at 3000 atm. the maximum head which the pump could deliver is 9.2cms. of mercury.

7.2.5 Hot wire anemometer

This device, shown in Fig. 7.8, consists of a piece of platinum wire 1/8" long, and 0.005" in diameter, soldered to 2 copper electrodes and contained in a standard Aminco tee piece. The Platinum wire is heated with an eletric current so that the energy dissapated is of the order of 0.5 watt, and the gas flow is then detected by the fall in resistance which occurs when the wire is cooled by forced connection. The actual flow indicator is a galvanometer in a Wheatstone bridge circuit.

An interesting feature of the design is the type of pressure seal used for the electrodes. A piece of stainless steel sheathed wire (obtained from Research and Control Instruments Ltd.,) 1.5m.m outside diameter is pushed through a hole in a blank plug, the diameter of the hole being 0.003" greater than that of the wire. In an atmosphere of nitrogen the wire is then hard soldered into the plug, so that solder is present over the total length of the seal. Seapage of the gas through the magnesium oxide packing is prevented by covering the end exposed to the high pressure with a layer of araldite. This seal was only pressure tested to 5000 atm., but Cornish & Ruoff [11] have found that it will withstand pressures up to 30,000 atm.

7.2.6 General arrangement of equipment

The whole apparatus is mounted on a box shaped frame work of Handy - Angle 2'2" by 1'4½" and3'6" high (see Plate II). An important feature of this arrangement is that all the valves are clamped to one side of the framework so that they may be operated easily from one position. Since under normal working conditions the apparatus is immersed in an oil tank, this means that the valves have to be actuated by short spindle extensions passing through the front face of the tank.

The oil tank, which acts as the thermostating bath is constructed from a 1/4" steel plate and has a detachable lid, the insulation being provided by covering the outside with a 1" thick layer of rigid asbestos felt. Inside the tank the oil used as the thermostating liquid is Shell Telus 23; it has a relatively low viscosity at 25°C and yet only fumes to a limited degree at 100°C. The oil is circulated by a 3" diameter propeller rotating centrally 8" from the bottom of the tank, and driven at 960 r.p.m. by a 1/4 h.p. electric motor. In order to increase the circulation baffles 4" high are welded to the base of the tank along the diagonals as recommended by B.R.Reavell [76]. The effectiveness of the circulation was checked by measuring the temperature variations at six points in the tank with thermocouples, and except for the extreme corners the variation was not greater that 1/5°C.

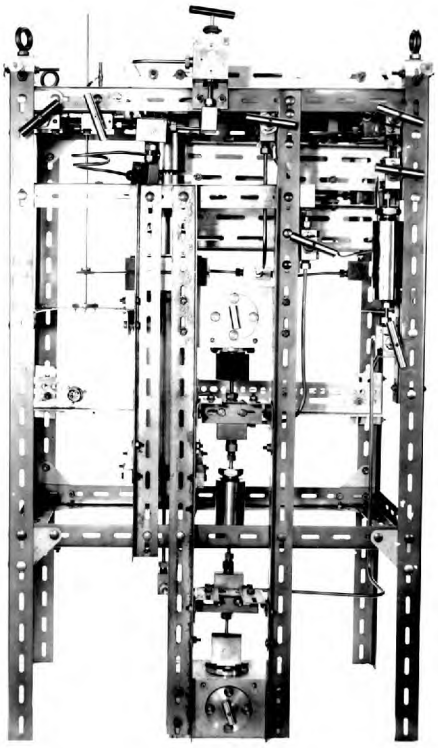

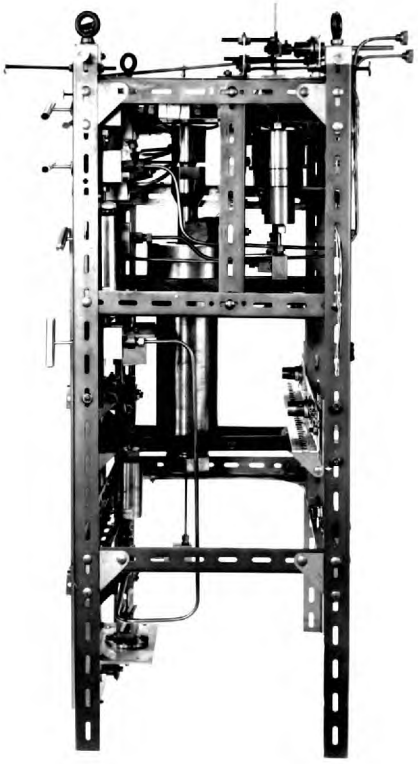

PLATE II

Equilibrium Section of Apparatus

Heat is supplied to the oil by two immersion heaters each having a maximum power dissipation of 2 kilo watts, which may be reduced through a three - way series parallel switch. The heaters are controlled using a Sunvic electronic relay, actuated by a mercury xylene thermoregulator such that the temperature variation with time is better than $1/10^{\circ}C$. The actual temperature is measured with a calibrated mercury in glass thermometer, engraved in $1/10^{\circ}C$.

7.3 Detailed design of gas compressor

7.3.1 Ist. Stage

The two vessels which constitute the first stage are 1000c.c Hoffer gas cylinders-; they each have an internal diameter of 2.1/8", an outer diameter of 5", and are suitable for a maximum working pressure of 1000 atm. The closure used for the top of the vessel is shown in Fig. 7.9. It may be noticed that the leads to the stainless steel probes are obturated in a manner similar to that used in the construction of the hot wire anemometer (see Fig 7.8).

7.3.2 2nd Stage

It has been the experience both in this , and other high pressure laboratories, that at pressures above 1500 atm. mercury will attack steel and cause the vessel to rupture at a pressure well below its normal working pressure. Bridgman [8] suggested that a rupture of this type

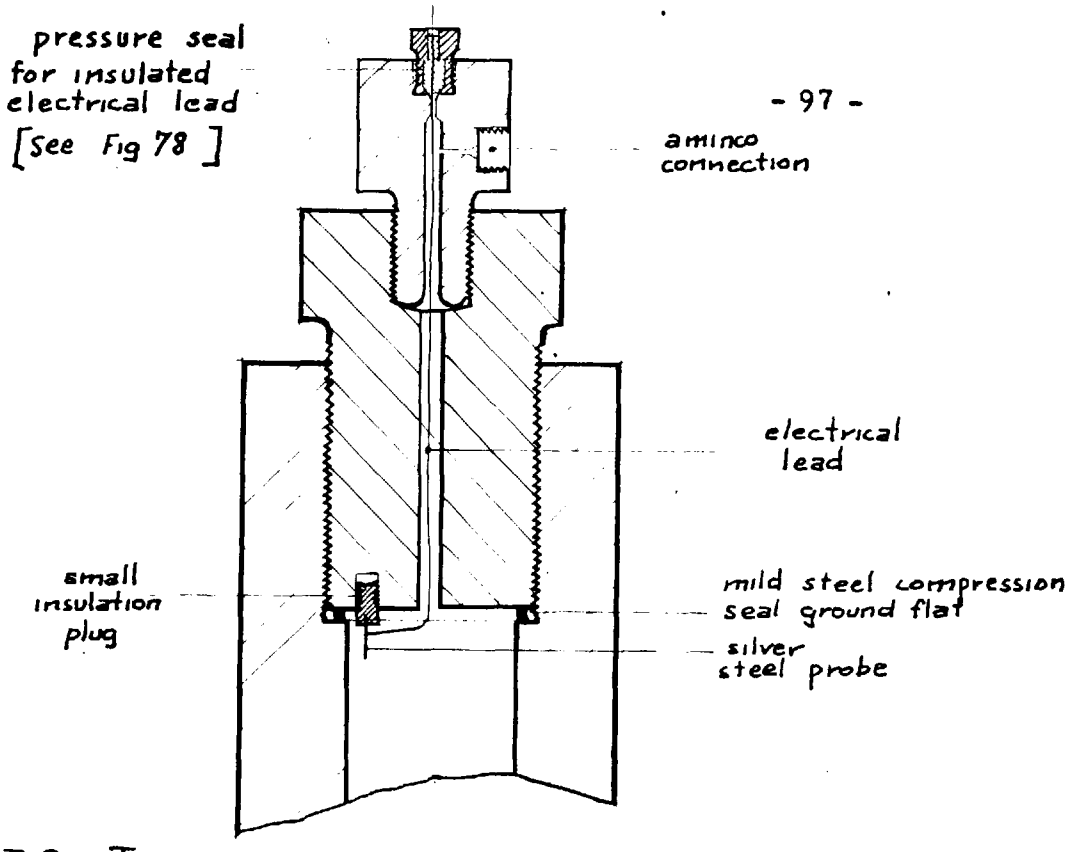

FIG 7.9. TYPE OF END CLOSURE USED FOR VESSELS A & B

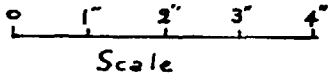

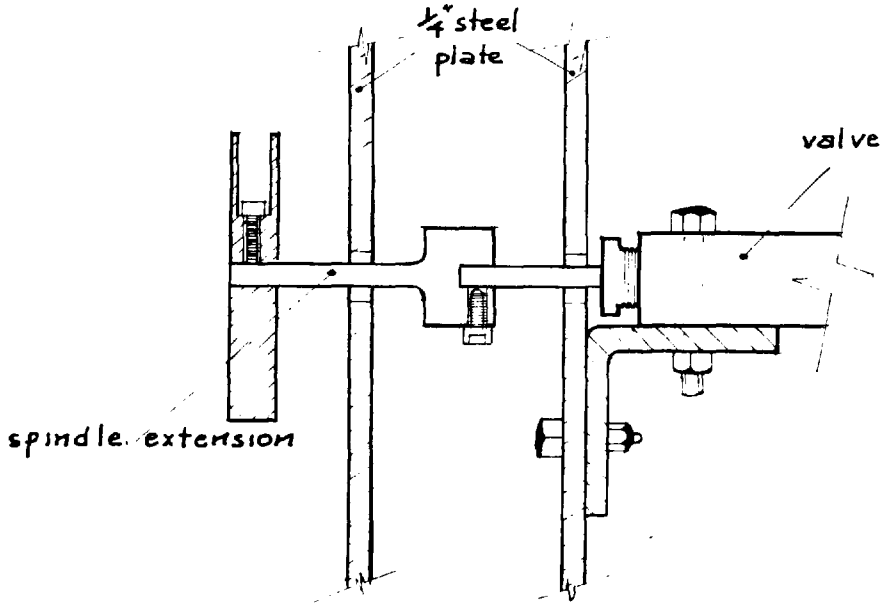

FIG 7.10. PROTECTION FOR VALVE SPINDLES OF COMPRESSOR

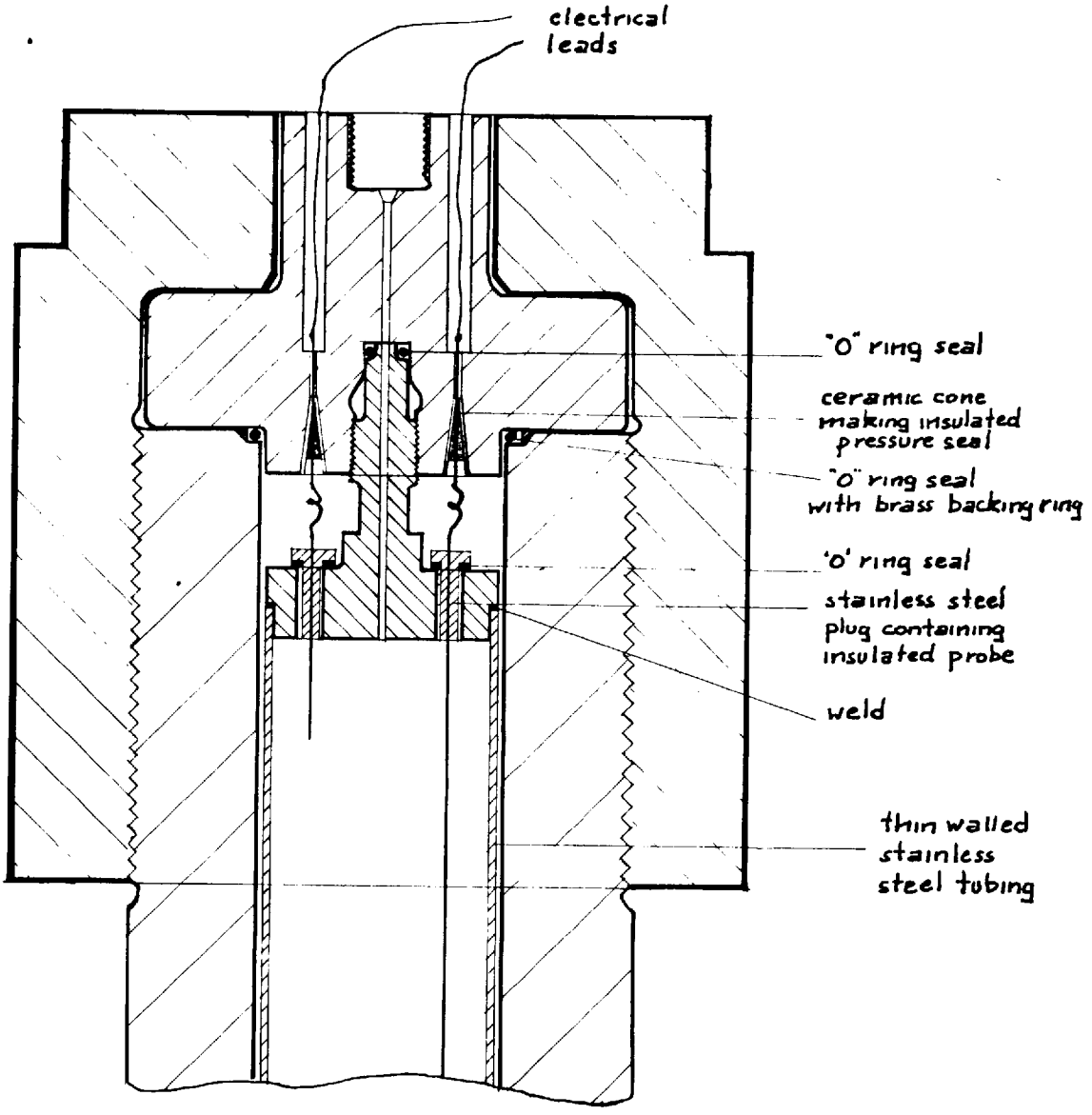

FIG 7. 11. UPPER CLOSURE OF PRESSURE VESSEL C.

occurs when the metal is subjected to such large strains that the mercury is forced into microscopic cracks where it amalgamates with the steel, and so produces rapid deterioration in its strength. As a consequence the second stage of the compressor is designed so that the mercury lute is always contained in a vessel which is exposed to only a small pressure differential, and in these conditions there is no possibility of mercury attack. The actual form of construction may be observed in Fig. 6.3.

The inner cylinders C_1 and C_2 containing the mercury, are made up from thin walled stainless steel tubing which is a close fit inside the pressure vessel C . It is important to arrange for the capacity of C_2 to be somewhat greater than C_1 , and for there to be sufficient mercury present so that a condition can never occur where oil rises through the mercury. This consideration limits the maximum permissable swept gas volume to approimately 270c.c

The pressure vessel C is fabricated from a length of pressure tubing 3' long 1.34" internal diameter and 2.75" outside diameter. It has a measured bursting pressure of 8000 atm., and therefore the safety factor is reduced to 2.7 for a working pressure of 3000 atm. The closure at both ends of the tube is made with a neoprene 'O' ring in conjunction with a brass backing ring as shown in Fig. 7.11. The backing ring acts as an anti - extrusion device, and is made triangular

in shape, so that with increasing pressure it tends to move upwards and close the gap between the mating surfaces. A further point of interest shown in Fig. 7.11, is the method by which the pressure seals are made at the points where the electrical leads enter the vessel. It is a similar technique to that employed by Newitt [68] and by Bridgman [8] for pressures up to 3000 atm., but in this case the insulating cone is fabricated from Hylumina (made by K. L. G. Sparking Plugs Ltd.,) having a compressive strength of 141 tons per square inch; so that it may be used at pressures up to 10,000 atm.

7.3.3 Arrangement of equipment

The entire compressor except for the hydraulic hand pump is housed in a 1/4" thick steel protective cabinet 6' 8" by 2' square. The cabinet is open at the top, and the front face acts as a door so that easy access may be obtained for maintainance purposes.

Plate III shows the general arrangement inside the cabinet. The main pressure vessels A, B and C are securely anchored to the walls by 2" steel angle, and the valves are all bolted to a steel plate $13\frac{1}{2}$" x 22" rigidly held just inside of the front face of the cabinet. In order to operate the valves without entering the cabinet a rectangular hole $12\frac{1}{2}$" x 16" is cut in the door to allow the valve spindles to protrude as shown in Fig. 7.10.

The hydraulic hand pump is anchored to the outside of the

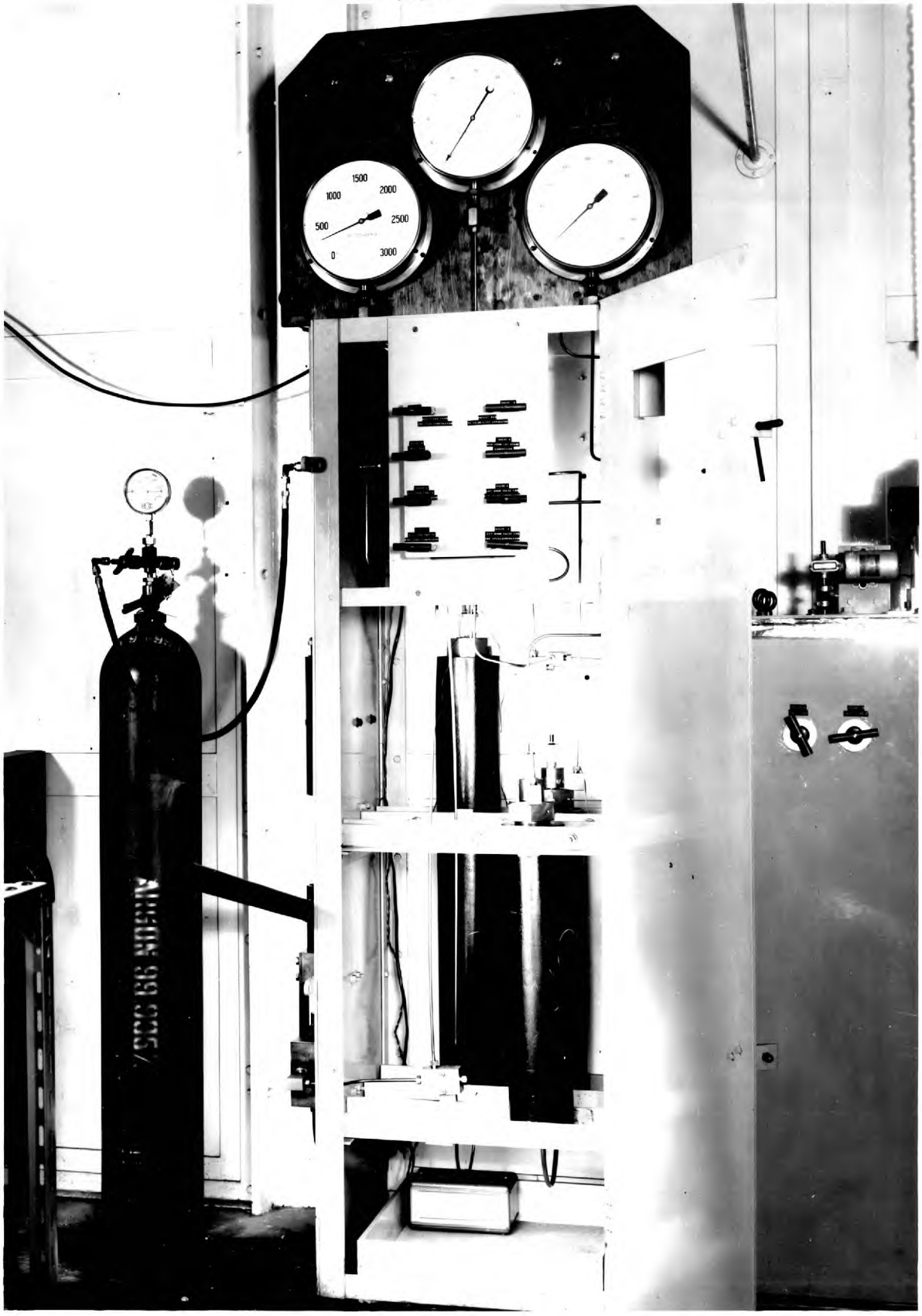

PLATE III Gas Compressor

cabinet and is fed with oil by a gravity feed from a large reservoir. Attached to the top of the reservoir is a constant head sight glass to prevent any mercury which may inadvertantly come over from the compressor, entering the pump. Hydraulic brake fluid (D. T. D. 585) was chosen as the pressure transmiting fluid because, its freezing pressure at room temperature is well above 3000 atm.

The two pressure gauges for the compressor and the one for the equilibrium apparatus are held on a wooden board attached to the top of the cabinet. Also mounted on the board are the warning lights indicating the limiting positions of the mercury levels.

7.4 Safety aspects of design

High pressure gas constitutes a great potential hazard because of the large amount of stored available energy and therefore great importance has been attached to this aspect of the design. All the vessels have been designed with adequate safety factors, and each piece of the quipment has been tested to $1\frac{1}{2}$ times the maximum working pressure.

The equilibrium apparatus is entirely surrounded by the oil tank, and calculations have shown that any fragments of steel caused by rupture of a vessel will be contained by the 1/4" steel plate used in the construction of the tank. In addition there is an exhaust vent 4" high by 2' 6" long, at the rear of the tank, which is designed to allow the gas

and oil to escape freely and harmlessly to atmosphere in the event of a pressure vessel failing. Connections to the compressor and pressure gauge are made through the vent and only a small length of pressure tubing is unprotected.

In the case of the compressor this is housed in a protective cabinet, and since the second stage is thought to involve the greatest hazard, this is further surrounded by a mild steel tube $5\frac{1}{2}$" in diameter and $\frac{1}{2}$" thick. Instances have been reported [62] of the valve spindles being blown out of the body of valves, and therefore to afford protection against this contingency they are operated through a mild steel plate by spindle extensions, as shown in Fig. 7.10. It may be noted that similar protection is provided in the case of the equilibrium apparatus. There is a danger that valve 4 may be opened when the 2nd stage of the compressor is at 3000 atm.; to prevent this causing any major failure a non return valve is placed in the line between valve 4 and vessel B, and also a bursting disc set to rupture at 1200 atm. is incorporated in the oil line between vessel A and valve 6. A further bursting disc is placed between the gas cylinders and valve 3, to avoid high pressure gas entering the gas cylinder due to the accidental opening of valve 3.

7.5 Limitation of the apparatus

The apparatus is designed to operate up to a pressure of 3000 atm.

however, two factors prevent this maximum being attained at the present time. Firstly, the pressure gauges in use have a maximum reading of 2000 atm. , and secondly, the hydraulic hand pump can only develop a pressure of 1500 atm. In order to use the apparatus over its full pressure range , two 4000 atm. gauges are required, together with a means of generating a pressure of 3000 atm.

One difficulty found with the Mercury Lute type compressor, is that the oil transmitting fluid tends to seap past the moving mercury piston and create an oil - gas interface, with the result that the compressed gas becomes contaminated with small quantities of oil. This effect is caused by the mercury not wetting the walls of the vessel, and may be overcome by coating the bore with a layer of Platinum. Such a procedure is expensive and was therefore not used. Instead the mercury surface is periodically observed and any oil removed.

CHAPTER 8

EXPERIMENTAL PROCEDURE

8.1 Operation of the gas compressor

Initially the mercury levels in B and C , see Fig. 6.3, are at their lowest positions, so that contact is just being made with the probes 'a' and 'd', as shown by the lighting of the indicator bulbs. Then, with valves 3, 4, and 1 open, (all other valves closed) the gas under consideration, which in this case is argon, is introduced into the vessels B and C at a pressure of between 100 and 150 atm.

After closing valve 3, valve 5 is opened and oil pumped into vessel A to compress the gas to a pressure of around 1000 atm., as recorded by the Bourdon tube pressure - gauge; the 1st. stage of the compressor is then isolated by closing valves 4 and 5.

To boost the gas pressure above 1000 atm., valve 7 is opened and oil is pumped in to the bottom of pressure vessel C , so that mercury is displaced from container C_2 to C_1. At the desired pressure valve 7 is closed, and argon is allowed to pass directly into the equilibrium apparatus by opening valve 2.

When the upper position of the mercury surface is reached, as detected by the silver steel probes 'b' and 'c', further high pressure gas

can only be produced by re-loading the compressor. In order to do this the let down valves 6 and 8 are opened slowly; this causes the mercury levels to be forced down by the high pressure gas remaining in B and C , and also displaces the oil into the reservoir. Care is taken during the operation to keep the oil flow rate, as observed through the sight glass, to about 30 to 50c.c per minute, in order to ensure that no mercury is pulled over. When the mercury levels are again at their lowest positions, valves 6 and 8 are closed and B and C refilled with gas at 100 atm.

8.2 Attainment of equilibrium between gas and liquid phases under pressure

The equilibrium apparatus as shown schematically in Fig. 6.1, is evacuated to a vacuum of 10^{-1} m.m. of mercury, and filled with argon at atmospheric pressure. With valves 9 and 13 closed (all other valves open) 110c.c of pure solvent is introduced slowly into the apparatus from a graduated burette via valve 10. The position of valve 10 is such that the solvent falls by gravity into vessel E, the equivalent volume of argon being displaced through valves 11 and 16. The small quantity of air that is dissolved in the solvent (approximately 0.0004c.c per gram of solvent) is removed by repeatedly saturating with argon and venting to atmosphere.

After introducing the solvent into the vessel, valves 10, 11 and 16 are closed, and argon from the compressor is allowed to enter the apparatus slowly through valve 9, until the required pressure is reached. The oil bath is now brought to the desired temperature which is measured on the mercury-in-glass thermometer.

When the temperature of the oil bath has been constant for several hours the magnetic stirrer is switched on, and the pressure in the apparatus is seen to fall as the gas dissolves in the solvent. The fall in pressure indicates that the stirrer is working satisfactorily. The magnetic pump is then also switched on and the gas phase circulated around the apparatus. To check that the pump is operating correctly, the hot wire anemometer is periodically turned on, and the deflection of the galvanometer connected to the Wheatstone Bridge circuit - [illegible] is measured. The hot wire anemometer is not kept on permanently, since although its heat input is very small, it will affect the isothermal conditions of the system over a prolonged period.

An indication of when the system has reached equilibrium is given by the pressure becoming constant, this generally occurs after 15 to 20 minutes of mixing. However, in order to make sure that both phases are completely saturated, the operation of the stirrer and circulating pump is continued for at least 1 hour. After equilibrium has been attained, a further 30 minutes is then allowed for any gas

bubbles to rise from the liquid phase, and for the gas and liquid phases to separate completely. This waiting period is expecially important at conditions near the critical point when the densities of the two phases are very similar.

Before samples of each phase are taken, the pressure of the system as registered by the Bourdon tube gauge is noted; in order to eliminate any effect of backlash in the mechanism, the gauge is always tapped prior to a reading being taken.

The liquid phase sample is obtained by opening valve 13, and allowing the liquid to flow by gravity into vessel L and also into the tubing between valves 12 and 13. Thus, when valves 13, 12 and 14 are closed, the sample is isolated in L. Similarly, a sample of the gas phase is isolated in G by closing valves 15 and 17.

At 1500 atm. the closing of valves 13, 12, 14, 15 and 17 causes an increase in pressure of as much as 7 atm. However, it is safe to assume that this makes no difference to the composition of the samples, since both the vessel L and G are well away from the gas - liquid interface.

8.3 Analysis of the gas and liquid samples

To facilitate the description of this part of the experimental procedure reference is made to Figs. 6.1 and 6.2.

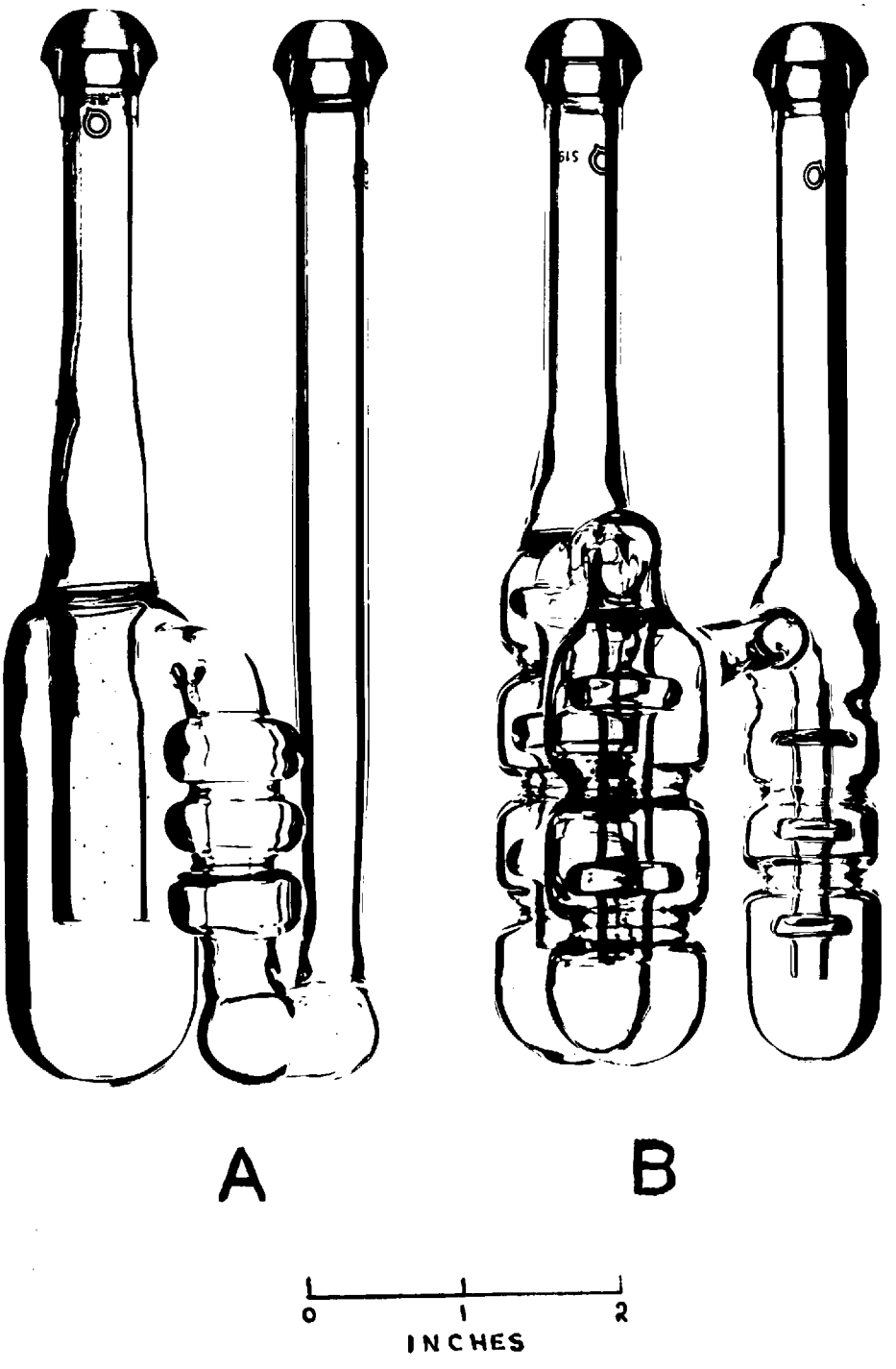

PLATE IV The two types of Freezing Trap employed

Liquid Sample:- Valve 11 is slowly opened to atmosphere and the line between valves 13 and 14, and taps 7 and 8 is evacuated to 10^{-1} m. m. of mercury, as indicated by the vacustat. At this stage it is important to see that the vacuum is maintained, since air entering the system will cause an error in the final gas volume. If the system is leaktight, valve 12 is then very carefully cracked open, and the sample allowed to expand through the freezing trap into the gas measuring system, at such a rate that practically all the solvent is caught in the trap. An occasional check is also made of the quantity of solvent vapour that does in fact pass through the trap, by analysing a gas sample from the measuring system with a Vapour Phase Chromatography unit. Using this technique, it is found that provided the gas flow rate is not greater than 60c. c per minute, then the loss of solvent vapour does not exceed 10^{-8} gm. moles/ c. c. Two types of freezing trap are used in the experiments; type A see Plate IV is employed when the quantity of solvent is large, and type B, when it is relatively small i. e. less than 0. 5 gms.

The technique used for measuring the gas volume varies according to the quantity of argon in the sample. For volumes over 500c. c, the argon is passed directly into an evacuated flask or flasks having a volume slightly less than that expected, and then when the pressure is equalised the remaining gas is transferred via the Toepler Pump to

the gas burettes. However, for gas volumes under 500c.c there is no necessity to make use of the calibrated flasks, and the argon is transferred directly via the Toepler Pump. All the volumes are measured at ambient temperature and pressure, as recorded respectively on a mercury-in-glass thermometer and a Fortin barometer, and then corrected to N. T. P. condition.

After the line between valves 13 and 14, and taps 7 and 8 has been evacuated by the Toepler Pump, the solvent in the trap is melted to enable any trapped gas to escape, then frozen once more, and the space above it re-evacated. Valve 11 is now closed, and the solvent trap disconnected, stoppered and warmed up to room temperature. With the solvent under its own vapour pressure, the trap is then accurately weighed to determine the weight of solvent in the sample.

Gas Sample:- With tap 1 closed and tap 2 open, the line between valve 16 and taps 7 and 8 is evacuated as before. Valve 16 is then cracked open slowly, and the experimental procedure repeated as for the liquid sample.

To re-establish equilibrium at another pressure, either argon is introduced from the gas compressor or valve 11 is opened, depending on whether measurements are required at a higher or lower pressure. The experimental procedure is then repeated as described in sections 8.2 and 8.3. In this way it is possible to take measurements at

increasing and decreasing pressure., and so determine whether saturation or supersaturation of the phases is taking place. Since the apparatus is charged originally with 110c.c of solvent, as many as 10 samples from each phase may be taken, and this is found to be sufficient to describe a complete P - x isotherm.

CHAPTER 9

EXPERIMENTAL RESULTS

The pressure - composition loops for the system argon - heptane and argon - carbon tetrachloride were determined at 30, 50 and 100°C. Results were also obtained for the system nitrogen - benzene at 25, 75 and 100°C but in this case the complete loop is only completed for the 100°C isotherm. The measurements recorded in the experiments are set out in Tables 1 to 9 of Appendix 2, together with the calculated values of the mole fraction and density. Also in the Appendix (Appendix 3) is a brief discussion in the purity of the materials used in the experiments.

9.1 Presentation of results

The results have been presented in Figs. 9.1 to 9.6 in the form of isotherms of pressure vs. mole fraction and pressure vs. density. The mole fraction and density of each phase are calculated from the recorded measurements in the following manner:-

For the liquid phase;

Mole fraction of gas present x_2 = $\dfrac{V_L/V_0}{V_L/V_0 + W_L/M_1}$ ...(9.1)

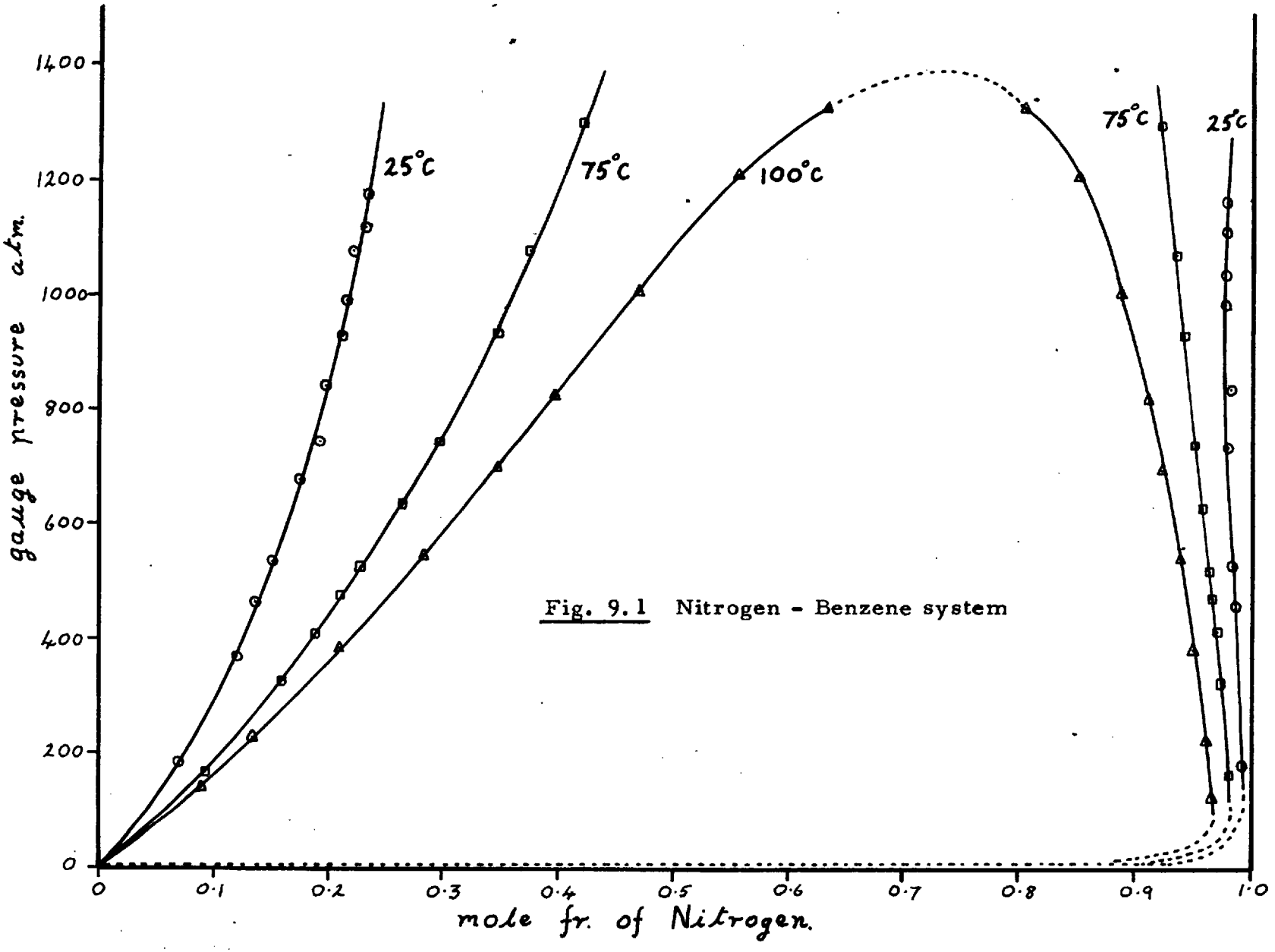

Fig. 9.1 Nitrogen - Benzene system

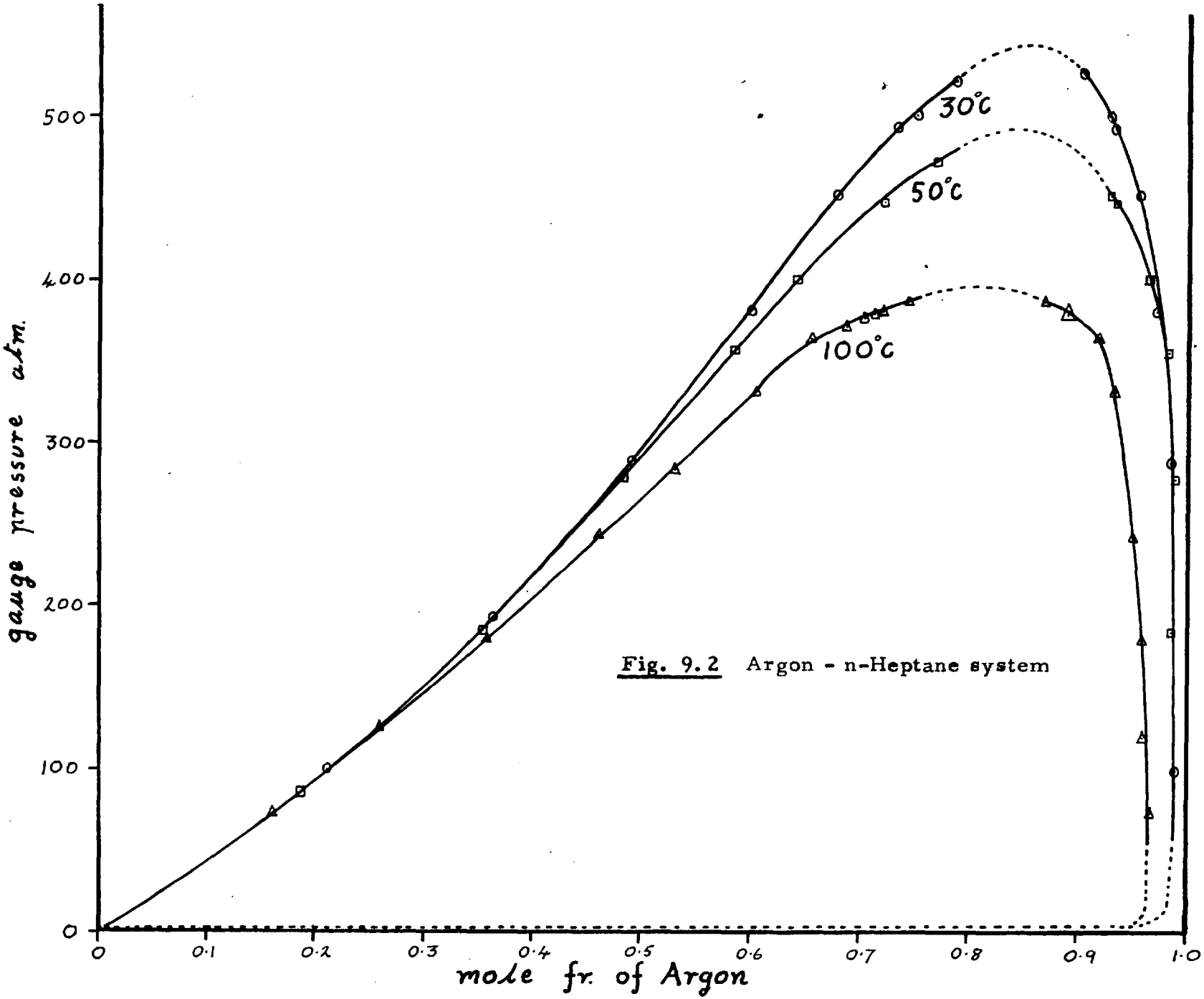

Fig. 9.2 Argon - n-Heptane system

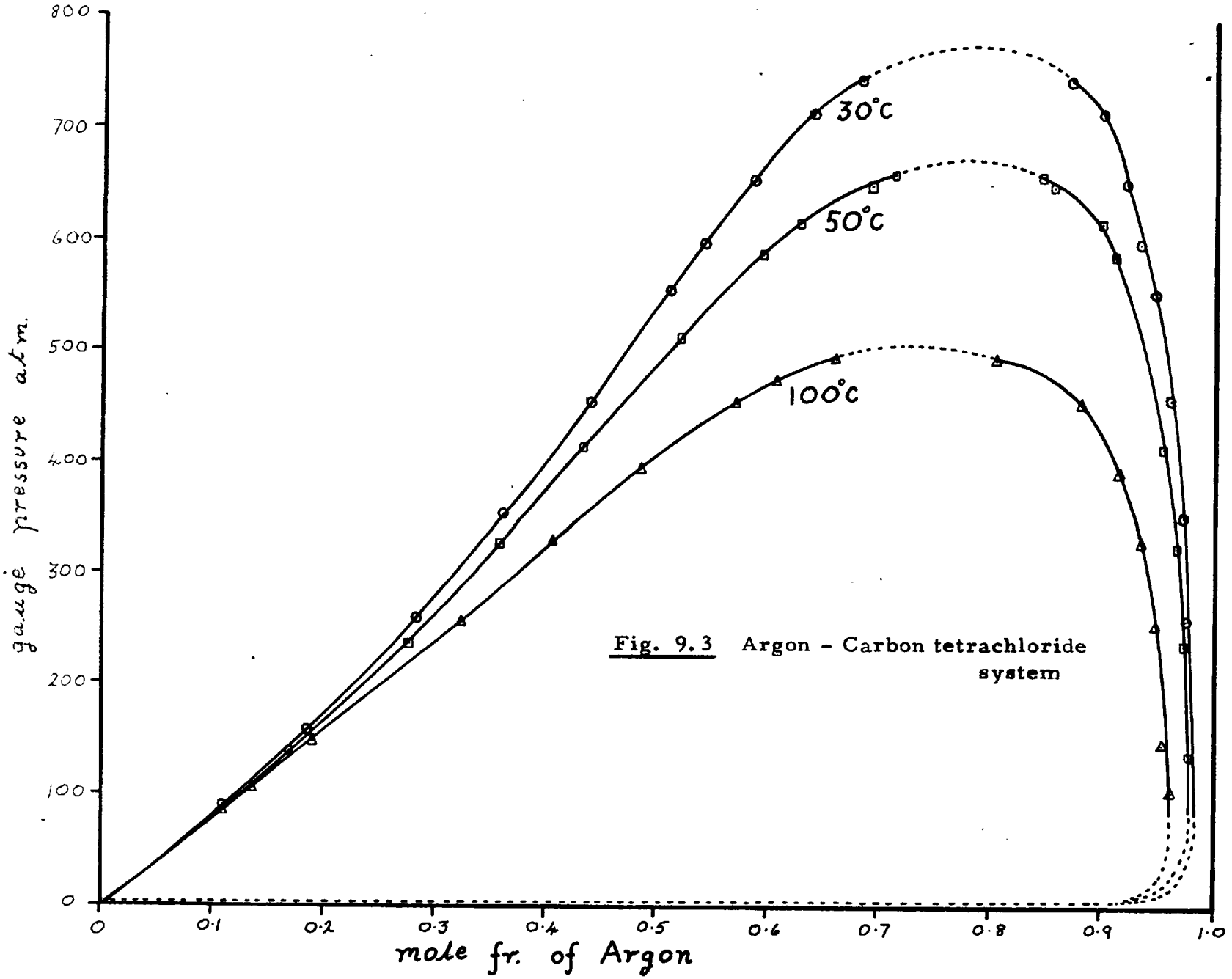

Fig. 9.3 Argon - Carbon tetrachloride system

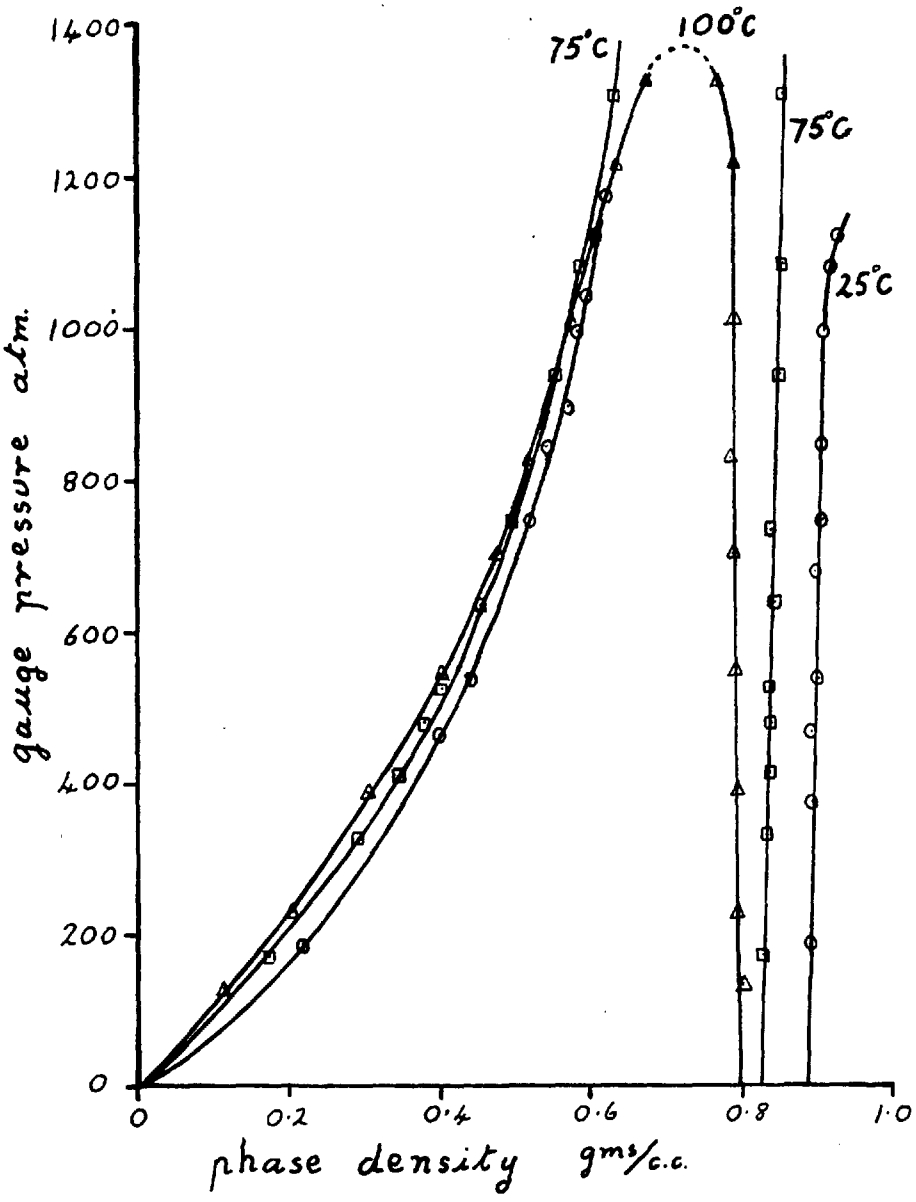

Fig. 9.4 Nitrogen - Benzene system

Fig. 9.5 Argon - n-Heptane system

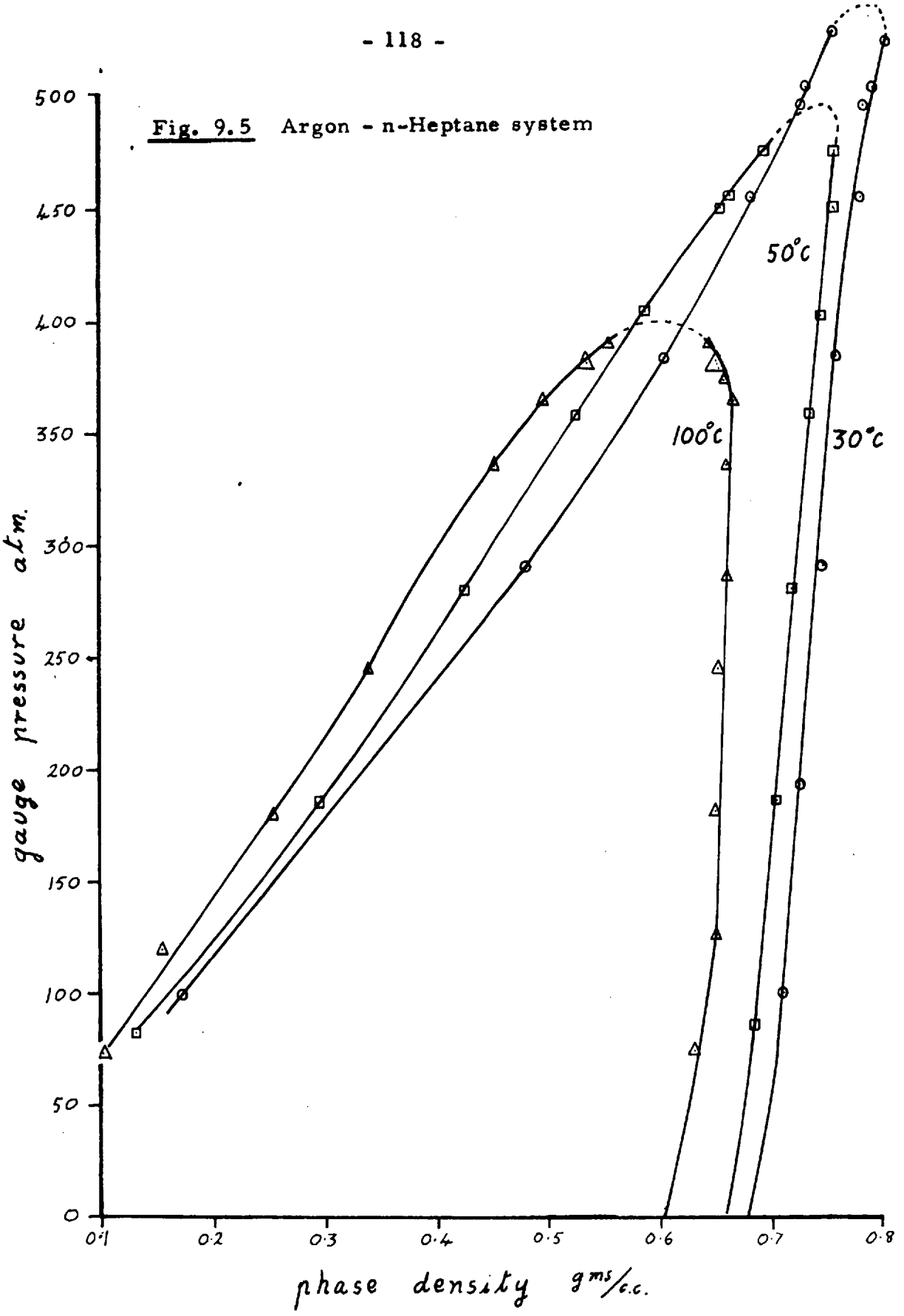

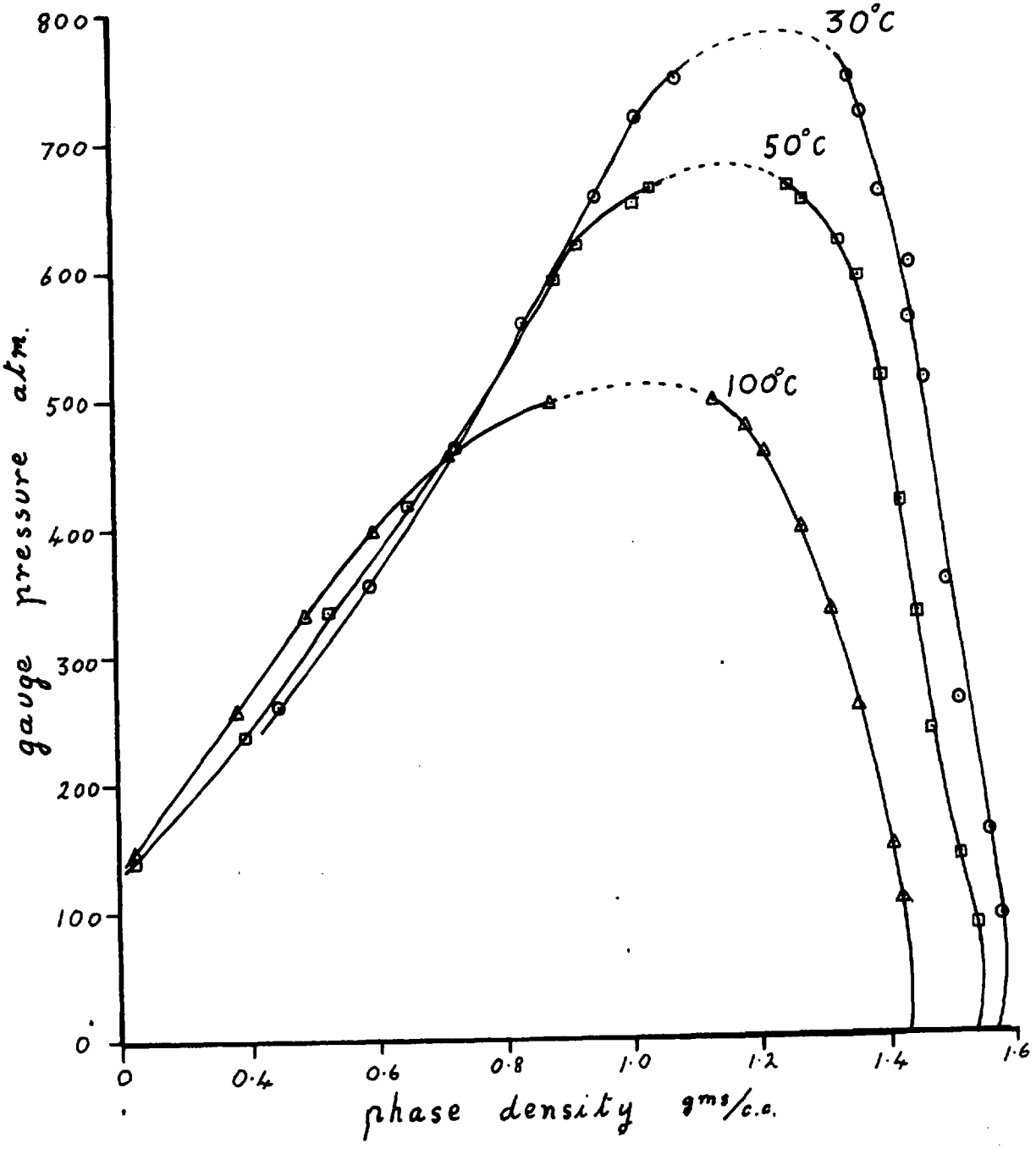

Fig. 9.6 Argon - Carbon tetrachloride system

$$\text{Density } \rho_L = \frac{V_L \rho_0 + W_L}{V_s'} \quad \ldots(9.2)$$

For the gas phase;

$$\text{Mole fraction of solvent present } y_1 = \frac{W_G/M_1}{V_G/V_0 + W_G/M_1} \quad \ldots(9.3)$$

$$\text{Density } \rho_G = \frac{V_G \rho_0 + W_G}{V_s''} \quad \ldots(9.4)$$

where

V_L & V_G = volume of gas present at N. T. P. in the liquid and gas phase samples respectively

W_L & W_G = weight of solvent present in the liquid and gas phase samples respectively

V_0 = molecular volume of the pure gas at N. T. P.

M_1 = molecular weight of solvent

ρ_0 = density of gas at N. T. P.

V_s' & V_s'' = the volume of the liquid and gas sampling vessels respectively

The physical constants that have been used in these calculations are given in Appendix 5.

The volume of the sampling vessels can not be measured directly with any great accuracy and hence they must be calibrated. This is carried out by introducing into each vessel, Argon at a known temperature and pressure, and measuring the volume of the gas at N.T.P. Knowing the P.V.T. data for Argon [16], it is then a simple calculation to determine the volumes of each sampling vessel. The average calculated volumes are:-

Liquid Sampling Vessel V's 4.47c.c (+0.09, - 0.14c.c)

Gas Sampling Vessel V"'s 10.07c.c (+0.16, - 0.25c.c)

The actual measurements recorded are given in Table 10 Appendix 2.

9.2 Accuracy of measurements

During each run the following six measurements are recorded; the equilibrium pressure and temperature, the weight of solvent and volume of gas in the sample, and finally the ambient temperature and pressure at which the gas volume is measured.

9.2.1 Equilibrium pressure

Since pressure readings are taken from 80 to 1400 atm. sufficient accuracy cannot be obtained with one Bourdon tube gauge over the entire range. Therefore, for pressures between 75 and 400 atm. a gauge is used having a range of 0 - 500 atm. and from 400 to 1400 atm. one of range 0 - 2000 atm. This means that the accuracy with which the

equilibrium pressure is measured varies with the pressure.

From 75 to 400 atm. the pressure is measured to ± 0.5 atm.

From 400 to 1400 atm. the pressure is measured to ± 1.0 atm. Both gauges are calibrated periodically against a dead weight tester to ensure that an accurate measurement is being obtained and that no systematic error is being introduced..

9.2.2 Equilibrium temperature

Temperatures are recorded to $\pm 0.05^{\circ}C$ in the range 25 to $100^{\circ}C$ on a mercury in glass thermometer, the scale of which is divided into $0.1^{\circ}C$. Calibration of the thermometer was carried out against a standard Platinum resistance thermometer which was accurate to $0.01^{\circ}C$.

A greater source of error is that caused by temperature variations in the oil thermostating bath, which were measured to be as much as $0.2^{\circ}C$. Therefore, since the average temperature of the bath is the one recorded the error introduced on this account is $\pm 0.1^{\circ}C$. If the two errors are combined, then the accuracy with which the equilibrium temperature is known is $\pm 0.15^{\circ}C$.

9.2.3 Weight of solvent

This is measured accurately to ± 0.001 gms on a sensitive analytical balance.

9.2.4 Measured volume of gas

The accuracy with which this volume is determined is dependent

upon the accuracy of calibration of the gas measuring system. Over a range of volumes from 100 to 5000c.c the calibration is always better than ±0.1%, and hence it may be assumed that the actual gas volumes are also known to this figure.

9.2.5 Ambient temperature

The ambient temperature at which the gas volumes are measured varies from about 19 to 25°C, and is read to an accuracy of ±0.1°C on a calibrated mercury on glass thermometer.

9.2.6 Barometric pressure

This measurement is determined to within ±0.1mm Hg. on a Fortin Barometer.

9.3 Accuracy of the Results

The results are subject to three kinds of error:-

(1) A random error which may be estimated fairly accurately knowing the sensitivity of the measuring apparatus

(2) An indeterminate and occasional error which might occur due to some failure in the experimental procedure. It is estimated comparing the precision of the results with the total random error.

(3) A systematic error observed by comparing the results with those of other workers. (this is discussed in Chapter 10).

9.3.1 Random errors

If one considers first the mole fraction of the gas in the liquid phase then from equation 9.1.

$$x_2 = \frac{1}{1 + \frac{W_L}{M_1} \cdot \frac{V_0}{V_L}} \quad \ldots\ldots (9.5)$$

The maximum error in x_2 due to errors δW_L and δV_L in W_L and V_L respectively is given by:-

$$\delta x_2 = \frac{\delta x_2}{\delta W_L} \delta W_L + \frac{\delta x_2}{\delta V_L} \delta V_L \ldots\ldots (9.6)$$

[The error in V_L due to errors in ambient temperature and pressure measurements is negligible and may be neglected.]

However, since the errors in δW_L and δV_L vary between + and - limits the most probable error δx_2 is better expressed:-

$$(\delta x_2)^2 = \left(\frac{\delta x_2}{\delta W_L} \cdot \delta W_L\right)^2 + \left(\frac{\delta x_2}{\delta V_L} \cdot \delta V_L\right)^2 \ldots (9.7)$$

Substituting for $\delta x_2 / \delta W_L$ and $\delta x_2 / \delta V_L$ by differentiating equation 9.5.

$$(\delta x_2)^2 = \left[\frac{-V_0 \delta W_L}{M_1 V_L \left(1 + \frac{V_0 \cdot W_L}{M_1 V_L}\right)^2}\right] + \left[\frac{V_0 W_L \delta V_L}{M_1 V_L^2 \left(1 + \frac{V_0 \cdot W_L}{M_1 V_L}\right)^2}\right]$$

$\ldots\ldots (9.8)$

Consider the argon - carbon tetrachloride system at 100°C and

Substituting values for M_1 and V_0 and rearranging:-

$$\left(\delta x_2\right)^2 = \frac{2.12 \times 10^4}{V_L^2 \left(1 + \frac{145.6\, W_L}{V_L}\right)^4} \left[\frac{W_L\, \delta V_L}{V_L} - \delta W_L\right] \quad \ldots (9.9)$$

In addition to errors in W_L and V_L there are also errors in the equilibrium temperature and pressure which if added to equation 9.9 give the total error in x_2 in the following form:-

$$\delta x_2 = \sqrt{\left[\, A + B + C \,\right]} \quad \ldots\ldots\ldots (9.10)$$

where A $= \dfrac{2.12 \times 10^4}{V_L \left(1 + \frac{145.6\, W_L}{V_L}\right)^4} \left[\dfrac{W_L\, \delta V_L}{V_L} - \delta W_L\right]$

$$B = \left(\frac{\delta x_2}{\delta P} \cdot \delta P\right)^2 \quad \text{and} \quad C = \left(\frac{\delta x_2}{\delta T} \cdot \delta T\right)^2$$

The error in y_1 (i.e. δy_1) may be expressed in the same form as equation 9.10 but in this case:-

$$A = \frac{V_G \cdot \frac{\delta W_G}{W_G} - \delta V_G}{2.12 \times 10^4\, W_G \left(1 + \frac{V_G}{145.6\, W_G}\right)^4}$$

$$B = \left(\frac{\delta y_1}{\delta P} \cdot \delta P\right)^2 \quad \text{and} \quad C = \left(\frac{\delta y_1}{\delta T} \cdot \delta T\right)^2$$

If the errors in the density results are calculated in the same way as δx_1 and δy_1, then the expression for $\delta \rho_L$ may be written:-

$$\delta \rho_L \qquad \sqrt{\left[D + E + F \right]} \qquad \ldots\ldots\ldots (9.11)$$

where $D = \dfrac{\rho_o^2 \delta V_L^2 + \delta W_G^2}{(V_s')^2}$

$E = \left(\dfrac{\delta \rho_L}{\delta P} \cdot \delta P \right)^2$ and $F = \left(\dfrac{\delta \rho_L}{\delta T} \delta T \right)^2$

In the case of $\delta \rho_G$ the values of E, D and F in expression 9.11 are:-

$$D = \frac{\rho_o^2 \delta V_G^2 + \delta W_G^2}{(V_s'')^2}$$

$$E = \left(\frac{\delta \rho_G}{\delta P} \cdot \delta P \right)^2 \text{ and } F = \left(\frac{\delta \rho_G}{\delta T} \delta T \right)^2$$

In order to give some indication of the relative sizes of the random errors involved in the experiments, equations 9.10 to 9.13 have been analysed for a complete P - x isotherm in Tables 9.1 to 9.4. It will be observed that except at a pressure of 495 atm. the percentage error in the results is extremly small and never greater than 0.35%. The larger error at 495 atm. is due to the increase in the rate of

TABLES 9.1 to 9.4 GIVE THE CALCULATED RANDOM ERRORS FOR THE ARGON - TETRACHLORIDE ISOTHERM AT 100°C.

Table 9.1 Errors in mole fraction x_2 as calculated from equation 9.10.

Errors in x_2	Pressure Atms			
	147	256	395	495
Due to errors in W_L and V_L (term A) x 10^8	1.64	3.18	3.93	2.36
Due to errors in pressure (term B) x 10^8	41.8	39.0	37.5	1850.0
Due to errors in temperature (term C) x 10^8	0.2	0.9	3.6	16.4
Total Error dx_2 x 10^4	6.6	6.5	6.7	43.2
% Error $\frac{dx_2}{x_2}$ x 100	0.35	0.20	0.14	0.65

Table 9.2 Errors in mole fraction y_1 as calculated from equation 9.10

Errors in y_1	Pressure Atms			
	147	256	395	495
Due to errors in W_G and V_G (term A) x 10^8	0.65	0.068	0.084	1.58
Due to errors in pressure (term B) x 10^8	0.062	0.25	5.06	1300.0
Due to errors in temperature (term C) x 10^8	0.18	0.29	1.39	11.0
Total Error dy_1 x 10^4	0.95	0.78	2.2	36.0
% Error $\frac{dy_1}{y_1}$ x 100	0.20	0.16	0.26	1.83

Table 9.3 Errors in density ρ_L as calculated from equation 9.11

Errors in ρ_L	Pressure Atms.			
	147	256	395	495
Due to errors in W_L and V_L (term D) x 10^8	5.7	7.3	11.0	20.0
Due to errors in pressure (term E) x 10^8	7.5	7.5	7.5	1220.0
Due to errors in temperature (term F) x 10^8	10.0	13.0	20.0	50.0
Total Error $d\rho_L$ x 10^4	4.8	5.3	6.2	36.0
% Error $\frac{d\rho_L}{\rho_L}$ x 100	0.034	0.039	0.048	0.31

Table 9.4 Errors in density ρ_G as calculated from equation 9.11.

Errors in ρ_G	Pressure Atms.			
	147	256	395	495
Due to errors in W_G and V_G (term D) x 10^8	45.0	11.0	20.6	21.7
Due to errors in pressure (term E) x 10^8	49.0	49.0	81.0	5190.0
Due to errors in temperature (term F) x 10^8	1.6	2.3	1.1	6.6
Total error $d\rho_G$ x 10^4	9.8	5.1	10.1	72.0
% error $\frac{d\rho_G}{\rho_G}$ x 100	0.44	0.13	0.17	0.82

change of mole fraction and density with pressure near the critical point, and this effect is even more pronounced since the accuracy of the pressure measurement is lowest just above 400 atm. where the higher range pressure gauge is employed.

In estimating the error for the liquid and gas phase density no account is taken of the error that occurs in measuring the volume of the sampling vessels. There is in fact a possible systematic error of $\pm 2.0\%$ and $\pm 1.6\%$ in Vs' and Vs'' respectively and therefore it is important to realise that these errors must be added to the random errors given in Tables 9.3 and 9.4 to give absolute errors in the densities.

9.3.2 Indeterminate errors

Figs. 9.1 to 9.6 show that in general all the results lie within the calculated random error and therefore only in a few cases do the indeterminate errors have any significant effect.

The most probable causes of any indeterminate errors that do occur are, failure to bring the system to equilibrium, an unrepresentative sample of either phase being taken and finally small quantities of solvent passing through the freezing trap. The latter will introduce a significant error in the gas phase results for very dilute solution of the liquid in the gas at high pressures. For example in the nitrogen -

benzene system at 25°C and 1045 atm. the error introduced in y_1 becomes approximately 1.2% if it is assumed that the concentration of solvent in the gas passing through the freezing trap is the maximum permissable of 10^{-8} gm moles/c.c. It is extremely difficult to make a correction for this since the concentration of solvent vapour passing through the trap varies more than ten fold for differing experiments, and is only measured for one or two runs in each isotherm.

9.3.3 Conclusion

The results for the mole fractions x_1 and y_1 have in nearly all cases an accuracy of better than + or - 1%. The errors may become slightly greater than 1% either when the critical point occurs where the pressure measurement is most inaccurate i.e. between 400 and 600 atm. or for very dilute solutions of the liquid in the gas when the amount of solvent not condensed in the freezing trap becomes significant.

For the density results a further error is introduced due to the inaccuracy with which the volumes of the sampling vessels are measured. Thus the absolute accuracy of the liquid phase densities, may only be quoted as better than + or - 3% and the gas phase densities as better than + or - 2.7%.

CHAPTER 10

DISCUSSION OF RESULTS

Since it is impossible to investigate experimentally the phase behaviour of all binary systems under varying conditions of temperature and pressure, it is important to be able to predict their behaviour from a knowledge of the properties of the pure components. If the two components have similar molecular characteristics, as, for example, in the systems methane - propane and oxygen - nitrogen, the behaviour of the mixture will not vary appreciable from that of the pure substances. But if, on the other hand, the components are dissimilar, as for example with hydrogen - heptane or nitrogen - benzene, the phase behaviour of the mixture will differ widely from that of the pure substances. In the latter case the effect of interactions between unlike molecules is a significant factor, and since at the present time very little is known about these effects, the phase behaviour can be predicted only empirically. Most of the previous experimental investigations have been made on systems containing components of like characteristics, and very little data is available on the phase behaviour of a mixture of two dissimilar molecules. In this work the three systems studied, nitrogen - benzene ($N_2 - C_6H_6$), argon - n-heptane ($Ar - C_7H_{16}$), and argon - carbon tetrachloride ($Ar - CCl_4$) are all representative of a mixture of two

dissimilar molecules.

The system N_2 — C_6H_6 has been studied by a number of workers [45, 53, 66] over a limited pressure and temperature range, and the results obtained have been used to check the accuracy of the experimental technique. The $Ar - C_7H_{16}$ and $Ar - CCl_4$ systems were chosen, firstly because the critical points at temperatures between 25 and 100°C would be attained well within the pressure range of the equipment, and secondly, to enable a comparison to be made of the behaviour of a system containing symetrical carbon tetrachloride molecules, with one containing long chain n-heptane molecules.

The results have been presented in two ways; firstly, Figs. 9.1 to 9.3 represent pressure vs. mole fraction (P - x) diagrams, and secondly, Figs. 9.4 to 9.6 represent pressure vs. phase density ($P - \rho$) diagrams. The shape of the P - x curves are all of the same form and are discussed for each system in sections 10.1, 10.2 and 10.3. The $P - \rho$ curves have been included since the data will be of value in any rigerous thermodynamic analysis of the results which might be carried out in the future and also since they were found to be useful in checking the consistency of the solubility measurements.

It may be observed that no measurements have been recorded very near the critical point. This is because of a limitation in the apparatus [illegible], whereby it is impossible to [illegible] liquid

phase sample when the densities of the two phases approach one another closely. The position of the critical point was determined by extrapolation of the liquid and gas phase curves using the approximation of rectalinear diameters, so that the critical pressure is known only to ±5 atm. A more accurate measurement of the critical point could be made if the equilibrium vessel were fitted with a visual cell through which the mixture could be observed.

One of the main objects of this investigation is to determine how accurately the theoretical expressions discussed in Chapter 3 fit experimental data. Prausnitz [74] has derived a number of equations, 3,63 to 3.65, which in theory enable any point on the (P - x) isotherm to be predicted if the critical point for that temperature is known. In practice however, the solving of these equations is a tedious process, since the fugacity coefficients must be determined from an equation of state, itself dependent on the shape of the (P - x) curve.

Prausnitz applied his theories to the methane - nitrogen system, in which the critical temperature are similar, and his agreement with the experimental was good. Nevertheless, it is doubtful whether they may be applied with equal success when the two molecules are of different molecular size and energy, since he assumes that the activity coefficient composition curve, can be described from a knowledge of only Henry's

Law Constant, and the composition at the critical point. No attempt has been made at the present time to apply these equations, although it is hoped that in the continuation of this work, such calculations will be made.

The results have been used to test the applicability of the Krichevski equation 3.16 and 3.40 for the liquid phase, and Rowlinson's equation 3.58 for the gas phase, Although neither of these equations is rigerous,because of the assumptions that have been made in their derivation, it is of importance to determine the conditions under which they may be applied and to correlate the data for the systems investigated.

10.1 Nitrogen - Benzene System

10.1.1 Liquid phase results

The results are compared in Fig. 10.1 with the measurements recorded by Krichevski and Efremova [45] at 25°C for pressures up to 750 atm. and those of Miller and Dodge [66] at 75 and 100°C for pressures up to 300 atm. Krichevski & Efremova used a similar experimental technique to that employed in this work, and give the accuracy of their results as ±0.5%. Fig. 10.1 shows that the agreement with Krichevski's measurements is very good over the whole pressure range, and well within the experimental accuracy of the measurements. On the other hand slight disagreement is observed with the data of Miller & Dodge.

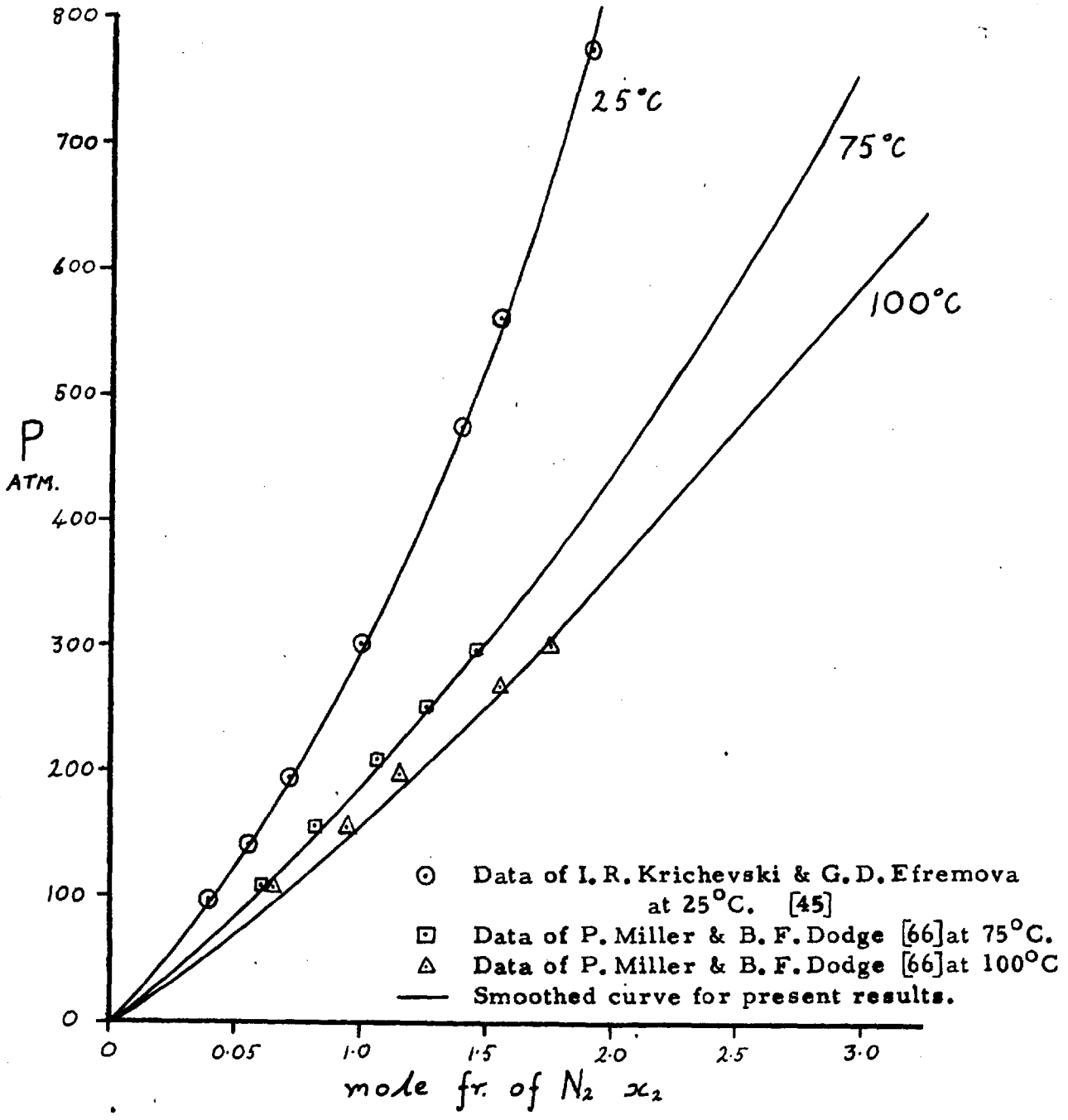

Fig. 10, 1 Comparison of liquid phase results for Nitrogen - Benzene system with previous published data.

At the lowest pressure at which solubility measurements have been taken, i.e. 137 atm at 75°C and 165 atm. at 100°C, the difference in the results between the present work and that of Miller & Dodge is 3 & 5% respectively. The disagreement becomes much less as the pressure is increased, and at 300 atm. it is less than 1%. Since Miller & Dodge estimate the accuracy of their results to be within ±1%, the deviations at low pressure cannot be due solely to the combined inaccuracy i.e. ±2% of the two experimental methods. Errors in the results of Miller & Dodge might be incurred by not being able to judge if and when equilibrium was attained using the 'flow method'. It is also noteworthy that Miller & Dodge found that their experimental procedure did not give consistant results at a temperature above 125°C, and that under these conditions the values of the solubilities were low. This is consistant with the discrepency found when a comparison is made with the present work at 75 and 100°C, since the difference between the results increases at the higher temperatures. The only source of error in the present work at low pressure that could give a high reading for the solubility, would be supersaturation of the liquid phase. No indication was found of this when measurements were taken at increasing and decreasing pressure.

Over the temperature range 30 to 125°C Miller & Dodge found that the solubility of nitrogen in benzene increased significantly with

an increase in temperature. This effect is confirmed by the results of this study shown in Fig. 9.1. Even at the relatively low pressures e.g. 100 atm. the temperature dependency is appreciable, but at the higher pressures the effect is even more pronounced, so that at 1300 atm. an increase of temperature from 25 to 100°C increases the solubility of nitrogen by two and half. This very large increase in solubility with rise in temperature enabled the P - x loop to be completed at 1400 atm for the 100°C isotherm. The results of Horiuti [35] shows that a similar increase of solubility with temperature also occurs at atmospheric pressure, where at 20°C $x_1 = 0.000412$ and at 25°C $x_1 = 0.000422$.

At 25°C no indication was found of the mixture freezing even at 1100 atm; although the freezing pressure of pure benzene at this temperature is reported [113] to be 700 atm. The presence of 24% of argon has therefore increased the freezing pressure of benzene by over 400 atm. It would thus appear that small quantities of a permanent gas have quite large effects on the freezing pressure of a solvent.

Finally a feature shown clearly on the P -ρ diagram Fig. 9.4, is that over a large pressure range no variation in the liquid phase density occurs, and therefore the molecular volume remains constant.

10.1.2. Gas phase results

A comparison is made in Fig. 10.2 of the results of this work

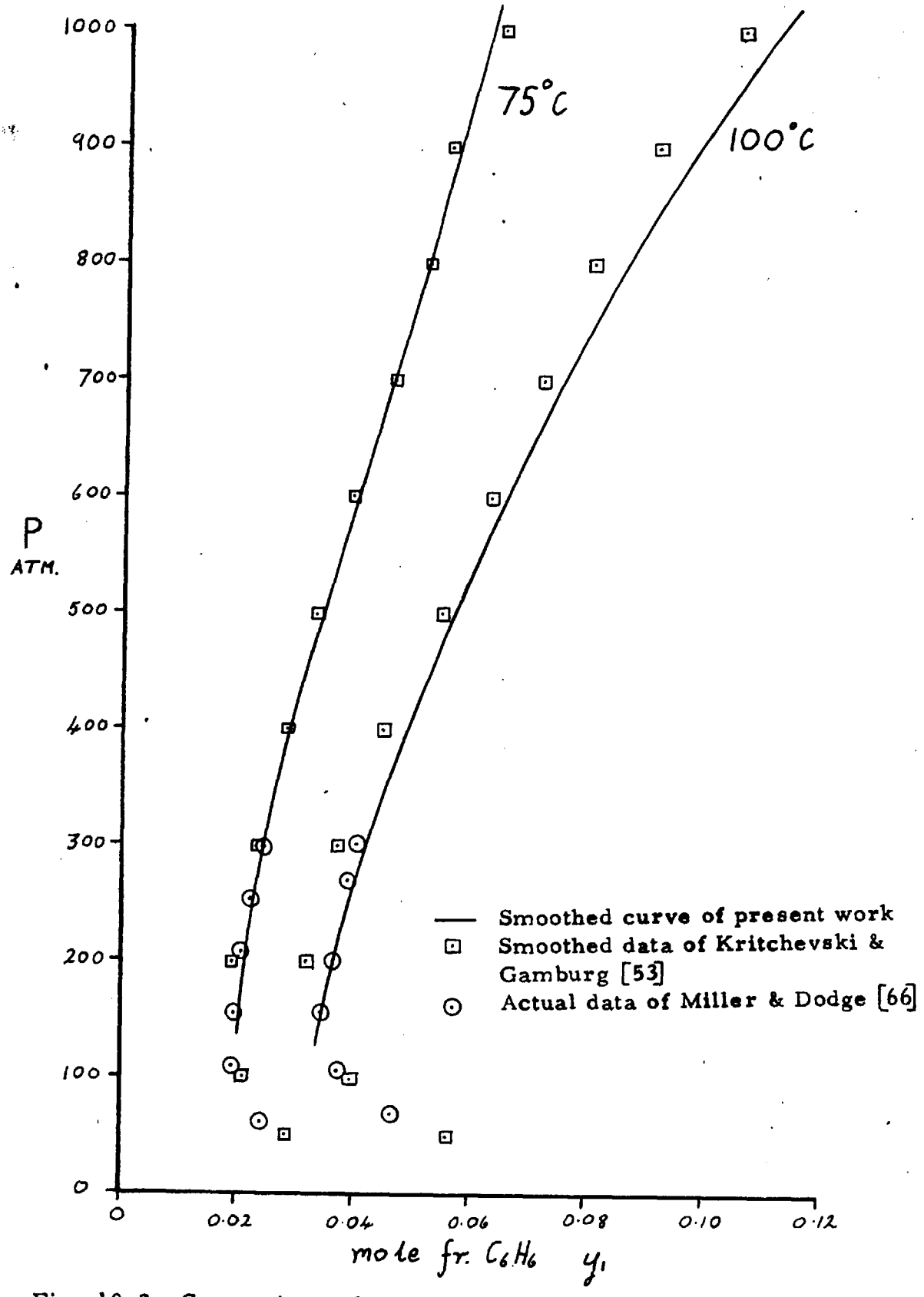

Fig. 10.2 Comparison of gas phase results for Nitrogen - Benzene system with previous published data

with the previous investigations of Krichevski & Gamburg [53] and Miller & Dodge [66] . In both these investigations the phases were brought to equilibrium using the 'flow method', and Krichevski & Gamburg calculated their results to be accurate to ± 3% whilst Miller & Dodge quoted a value of ± 1%.

At 75°C all the results agree within the accuracy of the experiments over the pressure range 160 to 1000 atm., but at 100°C the values obtained by Krichevski & Gamburg are somewhat lower than those obtained in this work. Over most of the pressure range the differences in the mole fractions are less than 5 or 6%, but at 200 atm. the variation is as much as 10%. Very much better agreement at 100°C is found with the results of Miller & Dodge; between 150 and 300 atm. the differences are never greater than the combined experimental error of 2%.

The greatest source of systematic error in the present investigation is the possible failure to remove all the solvent in the freezing trap. Such an error cannot account for the difference since it would lead to a low value for the solubility, and so increase the discrepency between the present results and those obtained by Krichevski & Gamburg. The most likely reasons for errors in Krichevski & Gamburg's experiments are firstly due to equilibrium not being maintained throughout the one or two hours duration of the

experiments and secondly failure to keep the pressure constant.

The results of Krichevski & Gamburg and Miller & Dodge both indicate that the solubility passes through a minimum with increasing pressure, and that the pressure at which this minimum occurs increases with temperature. This phenomenon was not observed in the present work because readings were not taken at pressures below 125 atm. Nevertheless, the existence of such a minimum in the gas phase curve is to be expected, since the composition will always approach 100% benzene at zero pressure, as shown by the dotted lines in Fig. 9.1. Above the minimum solubility the effect of temperature is to increase the solubility and as for the liquid phase the effect is more pronounced at higher pressures.

10.2 Argon - n-Heptane System

The P - x loop was completed at 30, 50 and 100°C and the critical pressure was found to fall as the temperature increased. This tendency coincided with a decrease in the mole fraction of argon in the critical mixture. The values of the critical pressures and compositions given in Table 10.1 were interpolated from Fig. 9.2. From Fig. 9.2 it may be observed that the effect of temperature on the shape of the (P - x) loop is only significant near the critical point, and at lower pressures very little variation occurs. Thus, even at

250 atm. it is not possible to separate the 30 and 50°C isotherm for either the liquid or gas phase curves.

Table 10.1 The Critical Pressures & Compositions for the argon - n-heptane system

Temperature °C	Critical Pressure atm.	Mol. Fr. of Ar in critical mixture
30	540	0.860
50	495	0.845
100	400	0.815

For the 30°C isotherm the critical point was reached at 546 atm, and it is interesting to note that at about this pressure the densities of pure argon and pure n-heptane become identical. In the region of the critical point one might therefore expect the gas phase to sink through the liquid phase, and the system to exhibit the phenomenon of 'barometric condensation', first found for the system nitrogen - ammonia by Krichevski [50]. However, the density of the liquid phase increases slightly with pressure - see Fig. 9.5, due to the density of the argon in solution being greater than that of pure heptane, and this is sufficient to prevent the phenomenon occuring. If the (P - x) loop were to be completed for the 0°C isotherm, the critical point would then probably occur at about 650 atm, and at this pressure 'barometric condensation' would almost certainly take place.

10.3 Argon - Carbon tetrachloride System

The critical pressures and compositions for the 30, 50 and 100°C isotherms interpolated from Fig. 9.3, are given in Table 10.2

Table 10.2 The Critical Pressures & Compositions for the argon - carbon tetrachloride system

Temperature °C	Critical Pressure atm.	Mol. Fr. of Ar in critical mixture
30	775	7.85
50	672	7.85
100	505	7.40

At all three temperatures the critical pressure is higher and the mole fraction of argon in the critical mixture lower than that for the argon - n-heptane system. A simple explanation for this fact is that it is easier for the argon molecules to penetrate a liquid consisting of large long chain n-heptane molecules, than one composed of the smaller symetrical carbon tetrachloride molecules.

Above 100 atm. the effect of temperature on the liquid phase composition is to increase the solubility of the argon, and as in the previous two systems the effect is greater near the critical point. Below 100 atm. the shape of the isotherms show a tendency for this effect to be reversed; the greater solubility of argon being observed at lower temperatures. The pressure at which this reversal of the

temperature dependency takes place was found to be about 70 atm., although this could not be determined accurately since no measurements were taken below 80 atm. Such a change in the effect of temperature with pressure is to be expected since Reeves & Hildebrand [77] found that at atmospheric pressure a temperature decrease caused an increase in the solubility of argon in carbon tetrachloride.

The results for this system may be compared with the earlier work of Graham [27] shown in Fig. 4.5. He found that over the pressure range 50 to 275 atm. lower solubilities were always obtained at the higher temperatures, and that the isotherms did not cross at pressures as high as 275 atm. These results are difficult to reconcile with the fact that the critical pressure is always lower at higher temperatures, and that the critical pressure at 100°C is only 506 atm. One must therefore assume that Graham's results are in error especially at the high temperatures.

10.4 General phase behaviour.

One of the objects of this work was to determine how the general phase behaviour of a binary system varies with the molecular characteristics of its components. As a result of this work it is possible to make a number of observations concerning the systems studied.

For the N_2 — C_6H_6 system the critical pressure was only attained for the 100°C isotherm. At the two lower temperatures the results suggests that a maximum occurs for the solubility in both the gas and liquid phases; this was especially evident for the 25°C isotherm. It is therefore doubtful whether the (P - x)loop can be completed even at three or four thousand atmospheres, at temperatures much below 100°C. At 25°C the shape of the curve suggests that the loop would never be completed even if the benzene did not freeze, which is in fact likely to occur. This suggestion is substantiated by the (P -ρ) plot shown in Fig. 9.4. Phase behaviour of this type conforms to that found for the nitrogen - ammonia system, in which at temperatures below 87°C Tsiklis [97] was not able to complete the (P - x) loop even at pressures as high as 17,000atm. However, for the nitrogen - benzene system this result is important, since it provides the first experimental evidence that this type of phase behaviour can occur with a system containing non - polar substances.

The phase behaviour of the systems is better shown by plotting the locus of the critical points, on a critical temperature - critical pressure graph such as that shown in Fig. 10.3. With a mixture of two similar molecules the locus will always join the critical points of the two pure components C_1 & C_2, but it may be seen from Fig. 10.3, that it is unlikely that the curves will return to the critical point of the more volatile component. It is impossible to confirm this experimentally,

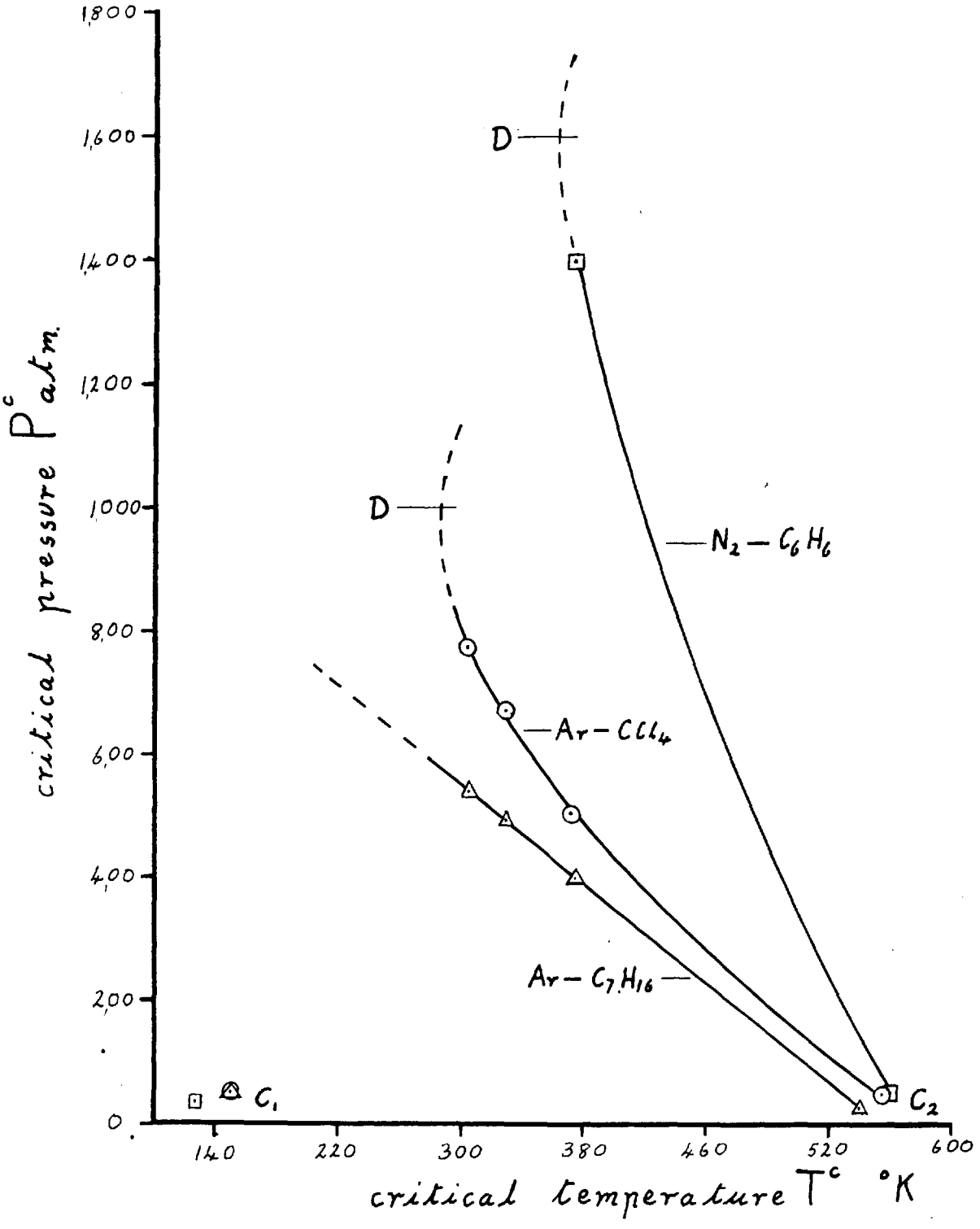

Fig. 10.3 Critical pressure vs. critical temperature for systems N_2 - C_6H_6 , Ar - C_7H_{16} and Ar - CCl_4

since measurements at C_1 are impossible because of the formation of a solid phase. For $N_2 - C_6H_6$ and $Ar - CCl_4$ the shape of the curves are such that they will certainly become vertical (i.e. $dT^c/dP^c = 0$), at some higher pressure, and if the pressure is increased still further the curves will most probably move towards higher temperatures, in which case the slope dP^c/dT^c will be positive. The dotted lines in Fig. 10.3 suggest the shape the curves might take with increasing pressure; the point D, at which $dT^c/dP^c = 0$, is estimated to be 1600 atm & 360°K for $N_2 - C_6H_6$, and 1000 atm & 284°K for $Ar - CCl_4$. If the (P^c — T^c) graph does have the form shown, then at temperatures above D the mixture will have both an upper and lower critical pressure.

Until recently it was thought that the pattern of behaviour exhibited in Fig. 10.3 was abnormal, since it had only been observed for the polar systems, nitrogen - ammonia [50,62], methane - ammonia [101] and carbon dioxide - water [96]. The results of this work suggest tha this is not the case, and that for two components of very different intermolecular energies and sizes, it is in fact the normal behaviour. This confirms the view held by Rowlinson, who in a recent publication [87] predicted that the shape of the (P^c - T^c) curves would change in the manner shown in Fig. 10.4, for different binary systems of increasing intermolecular disparity. Curves 'a' and 'b' represent a simple binary mixture for which the critical locus curve passes through

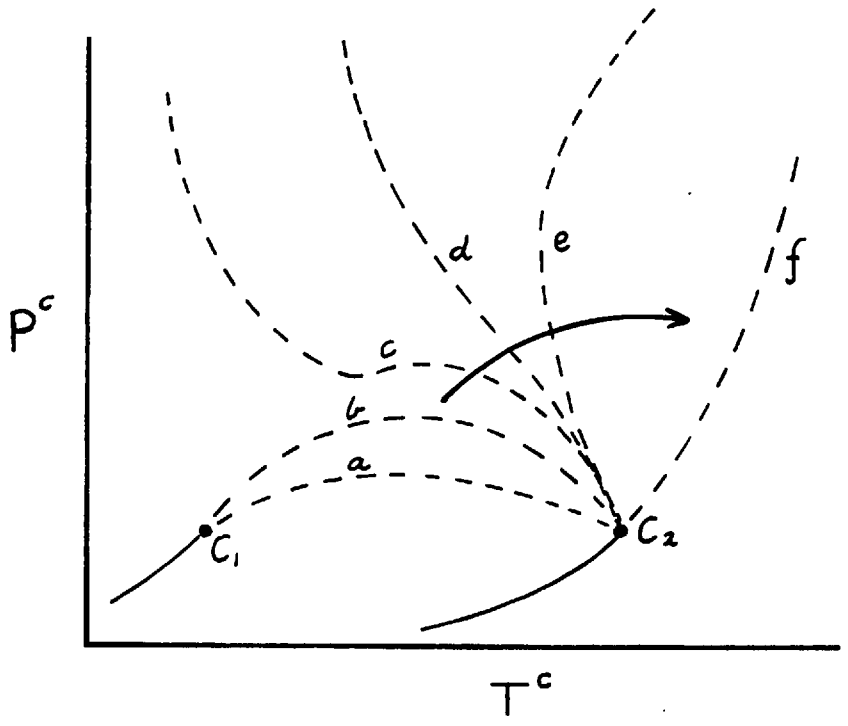

Fig. 10.4 Shows the way in which Rowlinson [87] envisages the critical locus curve of a binary mixture will change, as the disparity between the molecular properties of the two components increases.

a maximum, whilst 'c' shows a system where the disparity between the molecules is just sufficient to cause immiscibility. In the latter case, although the critical locus still has a maximum, the pressure rises indefinitely at lower temperatures. As the differences between the molecules of the two components increase further, then the fluid - fluid critical line moves towards 'f', so that the entire curve is located in a region above the critical temperatures of both components; this is the region of so called gas - gas immiscibility described in Chapter 2. The systems that have been studied in this work therefore conform to this pattern, in that the results for the $Ar - C_7H_{16}$ system, probably correspond to curve 'c' while those for the system $N_2 - C_6H_6$ correspond to 'd'.

King [41], using the theory of corresponding states, found that he was able to predict the shape of the critical locus curve from the critical constants of the pure components. Although this correlation only applies to simple mixtures which exhibit the type of behaviour represented by curve 'a' & 'b' in Fig. 10.4, it suggests that the shape of all (P^c - T^c) curves could be determined in a similar way. A first attempt at such a correlation is to see how the shape of the curves change with the difference between the critical temperatures of the two components, - since this is a measure of the disparity between the molecules. Unfortunately, very few experimental measurements are

available, but it will be seen from Table 10.3 that the difference in critical temperatures, is related in some way to the shape of the critical curves.

Table 10.3 Shows the variation in the critical locus curve for binary mixtures, with the difference in critical temperatures.

Systems	Difference in Critical Temp. $^{o}K.$	Approximate shape of $P^c - T^c$ curve.
$CH_4 - C_2H_6$ [93]	114.6	a
$CH_4 - C_4H_{10}$ [90]	236.0	b
$Ar - C_7H_{16}$	289.1	c
$CH_4 - C_6H_{14}$ [39]	317.3	c
$Ar - CCl_4$	405.4	d
$N_2 - C_6H_6$	435.6	d

In Table 10.3 a number of the methane - normal hydrocarbon systems have been included. It would therefore be of interest to examine further the shape of the critical locus curve for such systems up to say $CH_4 - C_{15}H_{32}$, where the difference in critical temperatures is 519.5$^{o}K.$ It would then be possible to obtain a clearer picture of the variations in the phase behaviour of a series of systems, with gradually changing intermolecular enrgy and molecular size. Davenport & Rowlinson [14] have carried out experiments near the critical temperature of methane, and found that methane is insoluble in hydrocarbons above

C_6. This means that unless solidification of the less volatile component occurs, the curves should show the trend illustrated in Fig. 10.4. If this is in fact the case, then it will disprove the generally accepted belief quoted in Comings[10], that the critical locus curve for all the systems belonging to the methane - normal hydrocarbon series, join to the critical points.

10.5 Prediction of the liquid phase composition curve

10.5.1 Henry's Law

The liquid phase isotherm is usually roughly sigmoidal, beginning as a straight line, curving towards the pressure axis, and then reversing its curvature to end at the critical point. It is to be expected therefore that the simple Henry's Law relationship, which predicts a linear increase in solubility with pressure, will be applicable over only a limited range of pressure at low concentrations. When the total pressure is plotted against mole fraction, as in Figs. 9.1 to 9.3, then significant deviations from Henry's Law occur below 100 atm. The extent of these deviations varies with temperature and from system to system, being greatest for the N_2 - C_6H_6 isotherm at 25°C, and smallest for the Ar - CCl_4 isotherm at 100°C.

If an allowance is now made for the composition of the solvent vapour in the gas phase, by plotting the partial pressure of the gas rather than the total pressure, then somewhat better agreement with

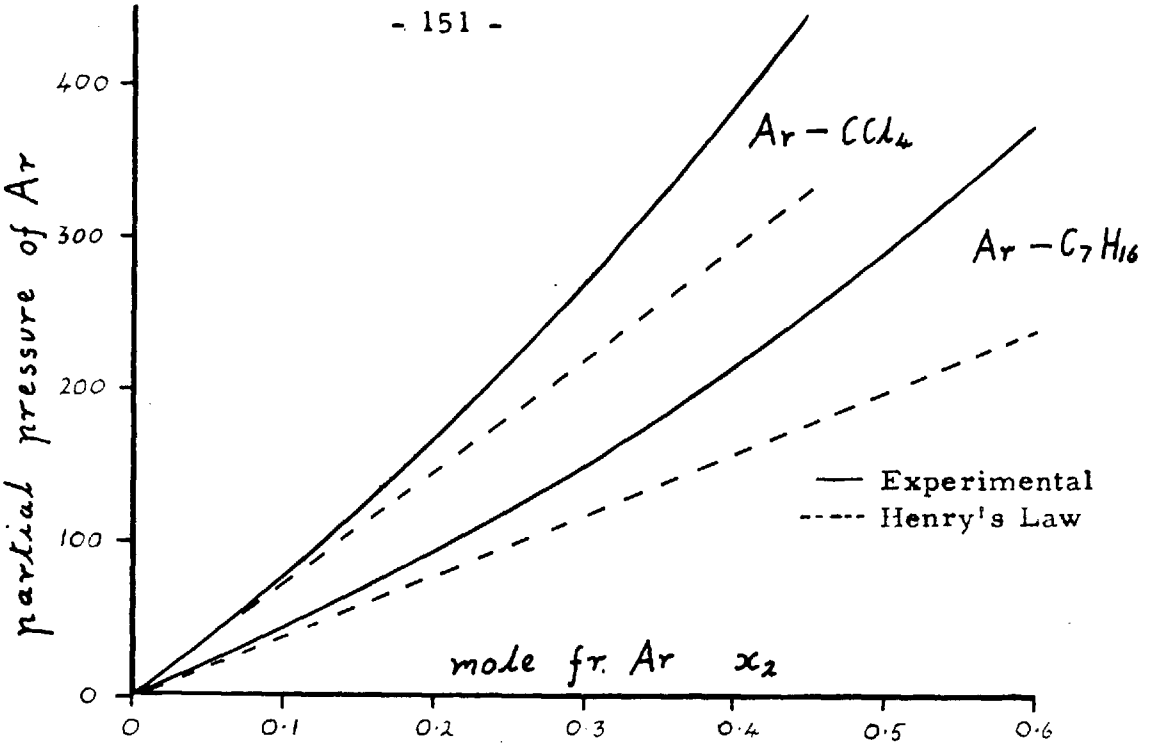

Fig. 10.5 Comparison of Henry's Law with the experimental solubilities for the systems Ar - CCl_4 & Ar - C_7H_{16} at 30^0C.

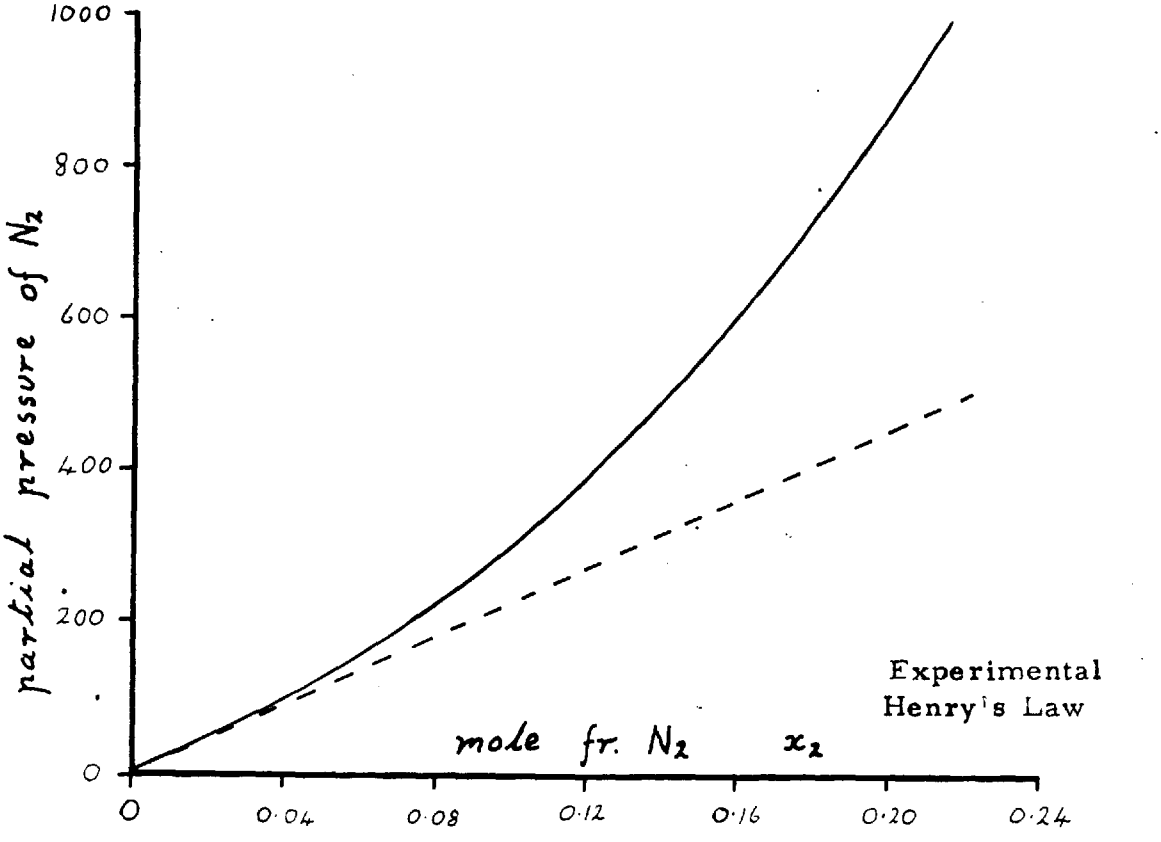

Fig. 10.6 Comparison of Henry's Law with the experimental lubilities for the system N_2 - C_6H_6 at 25°C.

Henry's Law is obtained. This is illustrated in Figs. 10.5 and 10.6 , in which the partial pressure has been plotted against the mole fraction for one isotherm of each system, and comparison made with the Henry's Law equation calculated from experimental solubility data at 1 atm. [9, 23, 24, 35] . In each case the actual solubility is less than that predicted by Henry's Law, and for the N_2 - C_6H_6 system at 25°C the actual percentage error in the solubility is 60 at a pressure of 600 atm. For the other two systems, i.e. Ar - CCl_4 & Ar - C_7H_8 at 30°C, much better agreement is obtained, and at the same mole fraction the errors are only 8 & 12.5% respectively. As the solubility increases, these errors become much greater due to the curvature of the isotherms towards the pressure axis, and it is apparent that Henry's Law is a valid approximation only at low pressures, say $<$100 atm, or low concentrations, say $x_2 < 0.2$.

10.5.2 The Krichevski equation

The poor agreement of Henry's Law for the system N_2 - C_6H_6 at 25°C, is due to the erroneous assumption made in its derivation, that the pressure of the solvent remains constant as the pressure rises and hence throughout the integration of the Gibbs - Duhem equation - see Chapter 3. A better equation at high pressures is 3.40, first presented by Krichevski.

In Fig. 10.7 the experimental data has been plotted over the

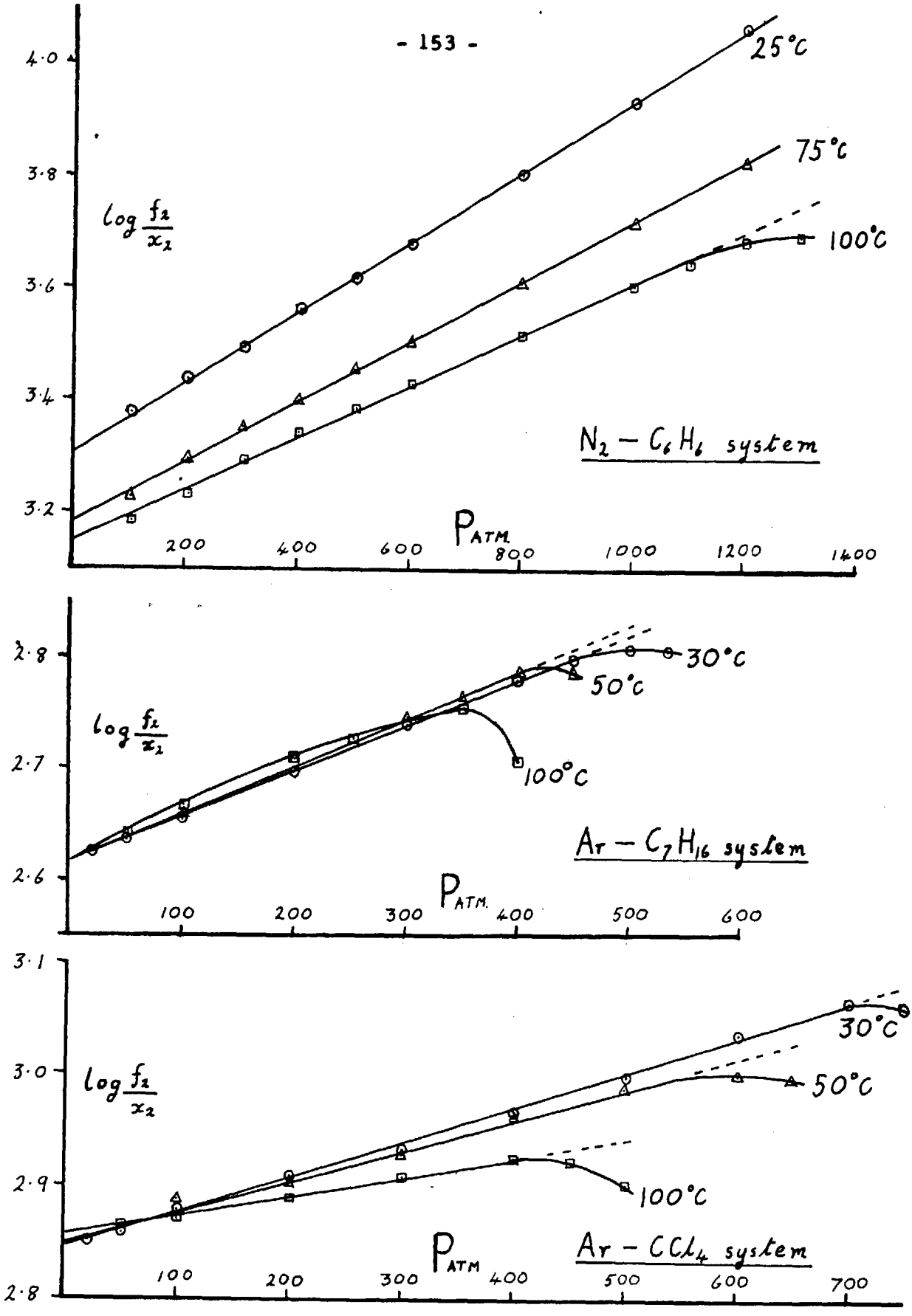

Fig. 10.7 The Krichevski equation applied to the gas solubility results

complete pressure range for all the systems investigated using the following form of Krichevski's equation;

$$\log \frac{f_2}{x_2} = \log K + \frac{\bar{v}_2}{2.3RT}(P_2 - 1) \quad \ldots\ldots\ldots (3.40)$$

For nitrogen the fugacity was obtained from the data of Demming & **Shupe** [15], and in the case of argon it was calculated by solving the following equation graphically.

$$\log f = \log P - \frac{1}{RT}\int_0^P \alpha \, dP \quad \ldots\ldots\ldots (10.1)$$

where $\alpha = V(ideal) - V(actual)$

The compressibility data for argon was taken from Din [16].

All the experimental results except those for Ar - C_7H_{16} at 100°C can be accurately predicted with the Krichevski equation, and as may be seen from Fig. 10.7, plots of log f_2/x_2 vs. (P - 1) are straight lines until the critical point of the mixture is approached. This very good agreement with the experimental data is somewhat surprising, since in the derivation of the Krichevski equation from the exact thermodynamic expression --- see Chapter 3, four assumptions must be made. Briefly these are:-

(1) the mole fraction of gas in the gas phase is equal to unity

(2) the partial molar volume of the gas in the gas phase is equal to the molar volume of the pure gas under the same conditions of temperature and pressure.

(3) the molar volume of the liquid phase increases linearly with concentration of gas up to the saturation value.

(4) the partial molar volume of the gas in the liquid $\bar{v}_2$ is independent of pressure.

Therefore in the case of Ar - C_7H_{16} at 100°C the deviation from the straight line in the region of the critical point, is probably due to the quantity of solvent in the vapour becoming so large as to invalidate assumptions (1) & (2). It is noteworthy that assumptions (3) & (4) apparently hold over the whole range of concentration.

From the intercept and slope of the graphs it is possible to determine the solubility of the gas at atmospheric pressure, and the partial molar volume of the gas in the liquid $\bar{v}_2$, respectively.

In Table 10.4 the values of the gas solubility at 1 atmosphere determined from 3.40 are presented for the systems investigated, and compared wherever possible with the experimental values. In all cases the agreement is better than 10%.

The values of the partial molar volume $\bar{v}_2$, determined from the slopes of the curves are given in Table 10.5, where they are compared with values calculated from the equation 10.2

$$\bar{v}_2 = x_1 \left(\frac{\delta v}{\delta x_1} \right)_{p,T} + v \qquad \ldots\ldots\ldots (10.2)$$

Table 10.4 Comparison of solubilities at 1 atm. as determined experimentally and calculated from the Krichevski equation

System	Temp °C	x_2 at 1 atm.	
		Actual Value	Extrapolation from high pressure equ^{n}. 3.40.
N_2 - C_6H_6	25	4.42×10^{-4} [24,35]	4.96×10^{-4}
	75		6.57×10^{-4}
	100		7.11×10^{-4}
Ar - C_7H_{16}	30	2.48×10^{-3} [9]	2.36×10^{-3}
	50		2.36×10^{-3}
	100		2.36×10^{-3}
Ar - CCl_4	30	1.34×10^{-3} [23]	1.43×10^{-3}
	50		1.42×10^{-3}
	100		1.39×10^{-3}

Table 10.5 Values of the partial molar volume of the gas in the liquid

System	Temp °C	$\bar{V}_2$ c.c's moles^{-1}	
		Cal^{d} by equ^{n} 10.2 for x = 0.1	Cal^{d} by Krichevski equ^{n}. 3.40
N_2 - C_6H_6	25	34.1	34.7
	75	43.2	35.3
	100	47.7	52.5
Ar - CCl_4	30	32.4	18.3
	50	32.2	17.4
	100	42.0	12.0
Ar - C_7H_{16}	30	17.0	23.3
	50	22.0	26.1
	100	51.0	-

where V = molar volume of liquid phase mixture.

Since $\delta V/\delta x_1$ at constant pressure and temperature is not known for the systems which have been studied, it was necessary to assume that the molar volume increased linearly with concentration, and to evaluate $\delta V/\delta x_1$ at the saturation point of the mixture. (a specimen calculation is given in Appendix 4). The assumption that the molar volume increases linearly with concentration could introduce a significant error, and may account for the large difference in values for the Ar - CCl_4 system. Nevertheless, since this assumption is made in the derivation of Krichevski's equation and in the calculation of from equation 10.2, it is surprising that the discrepency between the two values is so large. This suggests that the fourth assumption made in the Krichevski equation, (i.e. $\bar{V}_2$ independent of pressure) does not apply over the whole pressure range.

If the values of $\bar{V}_2$ determined from equation 10.2 are used to calculate the mole fraction x_2, it is found that comparitively small errors in the calculated solubility are introduced. For Ar - CCl_4 at 100°C, where the discrepency in $\bar{V}_2$ is over 250%, the error in x_2 at 300 atm. is only 25%. Therefore, since the Krichevski equation is relatively insensitive to large variations in $\bar{V}_2$, it may be used to estimate the value of x_2, even when $\bar{V}_2$ is not known very accurately.

10.6 Prediction of the gas phase composition curve

10.6.1 Poynting relationship

The Poynting equation only takes into account the increased solubility at high pressures due to the rise in vapour pressure of the liquid; and does not allow for the increased interaction between the molecules on compression. It is to be expected therefore that the Poynting equation will always give a low value for the solubility of the solvent in the gas phase. This is found to be so in Figs. 10.8 to 10.10, in which $ln.\ y_1/y_1^\circ$ is plotted against total pressure P for the various systems studied. The Poynting effect has been calculated in terms of from the equation,

$$ln\ \frac{y}{y_1^\circ} = \frac{(P - p_1^\circ)\, v_l}{RT} \qquad \ldots\ldots (10.3)$$

where the molar volume of the liquid V_l is assumed to be independent of pressure.

If the experimental gas phase composition curve is compared with that predicted by equation 10.3, it is possible to gain some insight into the interaction that occurs between the molecules under pressure. For the systems Ar - CCl_4 and Ar - C_7H_{16}, the molecular interaction increases the gas solubility enormously over the whole pressure range, and as one would expect, the attractive forces between the different molecules become greater as the gas is compressed, and are greatest

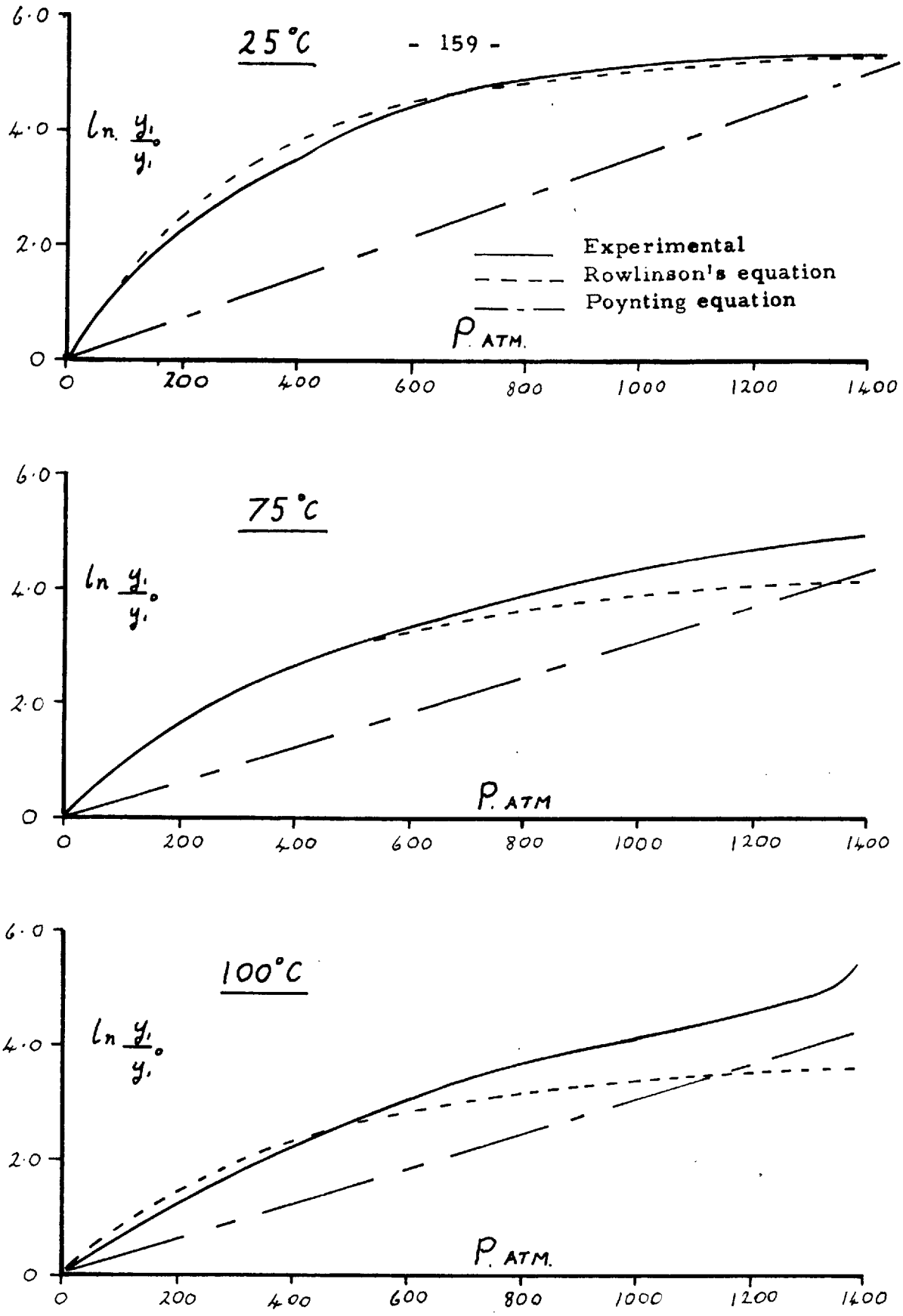

Fig. 10.8 Shows applicability of Rowlinson's equation and the Poynting relationship to N_2 - C_6H_6 system

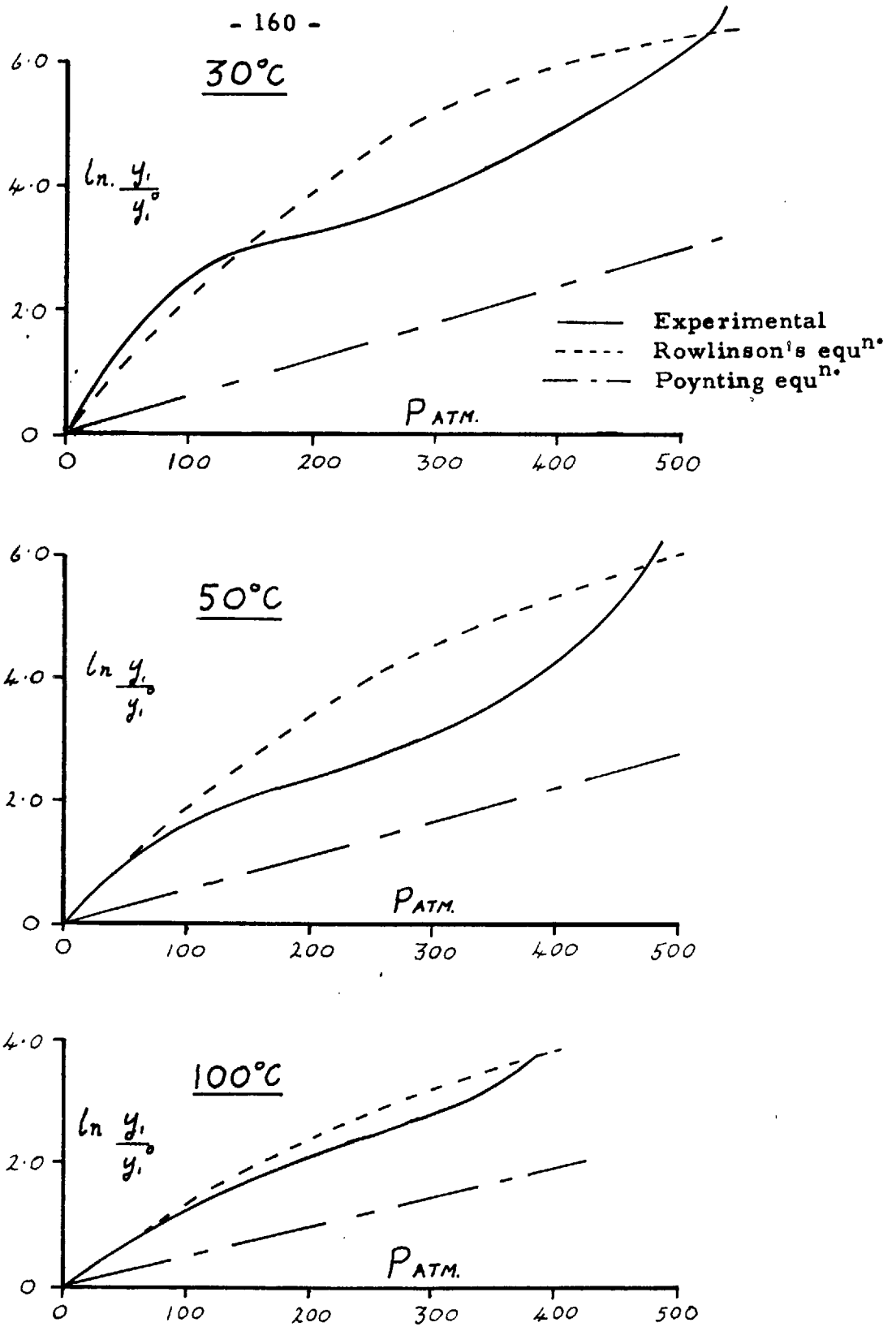

Fig. 10.9 Shows applicability of Rowlinson's equation and the Poynting relationship to Ar - C_7H_{16} system

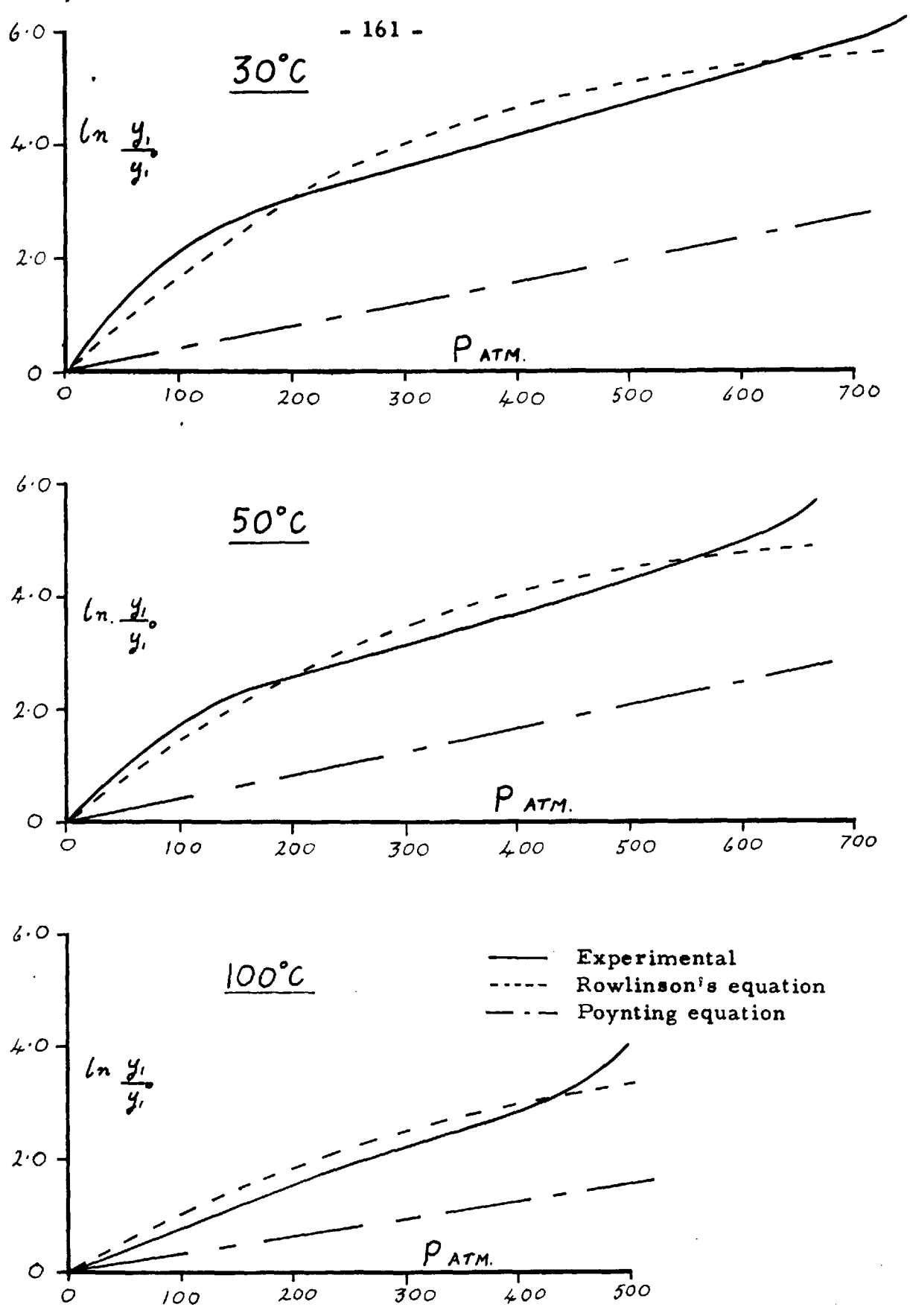

Fig. 10.10. Shows applicability of Rowlinson's equation and the Poynting relationship to Ar - CCl_4 system

at the critical point. On the other hand, Fig. 10.8 for the N_2- C_6H_6 system, shows that, the molecular interaction has most effect at pressures well below the critical point, and at 25°C the curves cross in the region of 1400 atm. This suggests that at high pressures the repulsive forces between the molecules become more significant than the attractive forces, and that the nitrogen molecules are tending to force the benzene molecules out of solution.

10.6.2 Rowlinson's equation

It is obvious from the discussion of the Poynting relationship, that if an accurate prediction of the gas phase composition is required, then some assessment has to be made of the intermolecular forces. Robin & Vodar [79] and Rowlinson et al [86] have both expressed this interaction in terms of a virial expansion, in which the successive coefficients represent the clustering of single gas molecules, pairs of gas molecules etc, around a single solvent molecule. The Robin & Vodar equation 3.54 only uses terms up to the second virial coefficient, and it is found to be inaccurate at high pressure. Rowlinson's equation 3.58, on the other hand, includes the third term in the virial expansion, and is therefore more applicable to the present results.

Since the coefficient D_{111} cannot be determined, the actual expression used in the calculation has been limited to the first two terms

of 3.58.

$$\text{i.e.} \qquad \frac{y_1}{y_1^0} = \frac{V_1 - 2B_{12}}{V} + \frac{V_1 B_{11} - 3/2\, C_{112}}{V^2} \qquad \ldots.(10.4)$$

The virial coefficients in equation 10.4 have been computed from the properties of the pure components by making two basic assumptions. Firstly, that all the intermolecular potentials are of the form which lead to the principal of corresponding states, and secondly, that interactions between pairs of unlike molecules can be related to those between pairs of like molecules by defining a characteristic critical temperature T^c, and volume V^c, by the following equations:-

$$(T^c_{11\ldots\ldots 2}) = (T^c_1)^{n-1/n} \cdot (T^c_2)^{1/n} \qquad \ldots.(10.5)$$

$$(V^c_{11\ldots\ldots 2}) = (n - 1/n)(V_1^c)^{1/3} + (1/n)(V_2^c)^{1/3} \qquad \ldots.(10.6)$$

From a knowledge of T^c & V^c all the coefficients have been calculated for the Lennard - Jones 12, 6 potential, by relating the critical constants to the intermolecular energy ϵ, and collision diameter σ with the aid of equations 10.7 and 10.8.

$$kT^c = 1{\cdot}28\,\epsilon \qquad \ldots.(10.7)$$

$$V^c = 1{\cdot}46\,(2/3\,\pi N\sigma^3) \qquad \ldots.(10.8)$$

The molar volume of the pure gas [16] has been used in equation 10.4 in place of the molar volume of the mixture.

This assumption was found to introduce only a very small error over most of the pressure range, and it enables the composition of the gas phase to be calculated without any previous knowledge of the P. V. T. properties for the mixture.

The values of y_1/y_1° calculated from 10.4 are compared in Figs. 10.8 to 10.10 with the experimental values. Considering the assumptions that have been made the agreement is reasonably good, and in all cases it is found to be better than the Poynting relation. As is to be expected, the initial slope of the experimental line is well reproduced, but large deviations occur at high pressures. In the region of 200 atm. all the calculated curves show a greater solubility than that found experimentally; this is due to the gas dissolving in the liquid and so reducing the chemical potential of the liquid phase. It is noticeable that the deviation is least for the N_2 - C_6H_6 system, where the smallest gas solubility was recorded. The compressibility of the liquid will also introduce and error in this direction, but its effect was calculated to be very small at 200 atm.

In all the systems it may be observed that the curves cross near the critical point, so that deviations from the experimental are in the direction of lower solubility. This is undoubtedly due to the increased importance of the fourth and fifth terms in the virial expansion at high pressures, where interactions betweeen one liquid molecule and clusters

of four and five gas molecules become prevalent. From these results it would therefore appear that the third term in equation 10.4 is positive at high pressures.

CHAPTER 11.

CONCLUSIONS

In this chapter conclusions are drawn from the experimental results for the three binary systems investigated, and in the light of these conclusions suggestions are made as to future work.

11.1 Conclusions from the present investigations

11.1.1 Form of the P - x isotherms

The P - x isotherms form a regular set of loops, having a maximum pressure when the liquid phase composition curve meets the gas phase composition curve, which is, the critical pressure.

At high pressures an increase in temperature increases the solubility of the gas in the liquid phase, the effect being more significant at the higher pressures. For a system which shows a negative temperature dependence of solubility at atmospheric pressure, for example argon - tetrachloride, the isotherms cross over at low pressure. This effect of temperature on the solubility of the systems studied at high pressure, is independent of that observed at atmospheric pressure.

At low pressures the gas phase composition curve always shows a minimum solubility of the liquid near 100% gas. Above this pressure a rise in temperature produces small increases in the solubility of the

liquid in the compressed gas, the effect being greatest near the critical point.

11.1.2 Predictions of the P - x curve for the liquid phase

At pressures below 100 atm., and for concentrations of gas in the liquid below 0.2 mole fractions, Henry's Law gives reasonable agreement with experimental data. Above these limits the deviations become large, and the Krichevski equation,

$$\log \frac{f_2}{x_2} = \log K + \frac{\bar{v}_2}{2.3\,RT}(P_2 - 1)$$

must be used.

The Krichevski equation may be successfully applied at pressures up to very near the critical point of the mixture, where the percentage of liquid dissolved in the gas phase becomes execessive. However, its use is restricted owing to the uncertainty in the value of the partial molar volume of the gas in the liquid $\bar{v}_2$, even though the equation is not sensitive to small changes in $\bar{v}_2$.

11.1.3 Prediction of the P - x curve for the gas phase

The solubility of the liquid in the compressed gas is much greater than can be accounted for by the rise in vapour pressure of the liquid at high pressure, i.e. the Poynting effect. The greater solubility is due to the increased interaction that occurs between the unlike molecules as the system is compressed.

Rowlinson's equation [86] expresses the intermolecular interaction in terms of a virial expansion, and agreement with experimental solubility measurements is far better than for the Poynting expression alone, although above 200 atm. discrepencies of over 30% may occur.

The errors involved in Rowlinson's equation arise firstly, because no allowance is made for the gas dissolving in the liquid phase, and secondly, because terms in the virial expansion are limited to C_{111}.

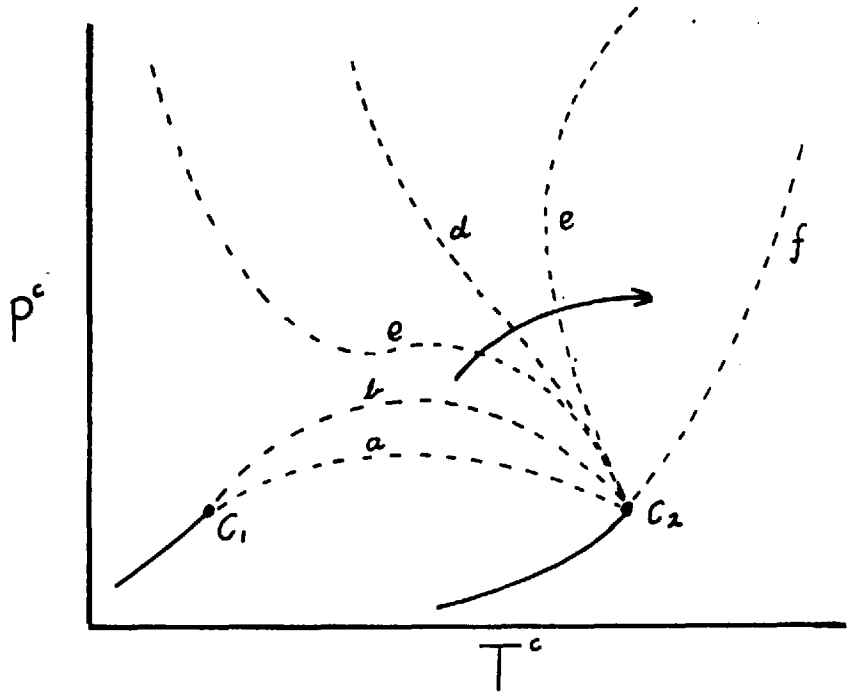

fig. 11.1

11.1.4 Critical Phenomena

For non - polar binary systems the shape of the critical locus curve changes from curve 'a', (shown in Fig. 11.1), to curve 'f', as the difference between molecular energies and sizes of the two pure components increases. From the results for the three systems studied, it seems probable that a correlation exists between the shape of the critical curves and the difference in the critical temperatures. The actual form of the correlation could not be determined due to the limited experimental data that was available.

11.2 Suggestions for further work

This investigation has revealed that the shape of the critical locus curve for non-polar systems varies, in the manner shown in Fig. 11.1, as the difference between the critical temperatures C_1 and C_2 increases; the curve does not always join C_1 and C_2 as was previously thought to be the case .

It would be of interest to determine the shapes of the critical locus curves for a series of systems, such as those formed by methane and the straight chain hydrocarbons, where the difference in critical temperature varies from 114°K for CH_4 - C_2H_6 to 519°K for CH_4 - $C_{15}H_{32}$.

From the results of such experiments, it might be possible to determine some quantitative correlation whereby the critical point for

a non-polar mixture could be calculated from the properties of the pure components. If such a correlation exists, then it might further be possible to calculate the shape of the complete P - x loop, using a method similar to that suggested by Prausnitz [74] .

In order to carry out this programme of work, the following modifications would have to be made to the existing apparatus. Firstly, the pressure gauges and hydraulic pump must be replaced by instruments capable of the maximum working pressure of the apparatus, that is 3000 atm. Secondly, a visual cell should be added to the equilibrium vessel, so that the critical pressure may be determined quickly and accurately. Finally, the temperature range of the equipment must be extended down to at least $-50^{\circ}C$, by including a refrigerating unit in the constant temperature bath.

APPENDICES

I. Vapour - liquid equilibrium data for systems of permanent gases and non polar liquids.

II. Tabulated Experimental Results.

III. Purity of Materials.

IV. Specimen Calculation of the Partial Molar Volume of the gas in the liquid .

V. Physical Constants.

APPENDIX 1

Vapour - liquid equilibrium data for systems of permanent gases and non polar liquids

TABLE 1 Systems containing hydrogen

Ref.	Year.	Solvent	Temperature range °C	Pressure range atm. or kg/cm
20	1931	liq. methane	-182.5	17 to 205
104	1931	liq. carbon monoxide	-185 to -205	17 to 225
104	1931	liq. nitrogen	- 185 to -210	1 to 225
21	1931	propane	25	up to 140
21	1931	pentane	25	up to 140
36	1935	benzene	25 to 300	50 to 300
36	1935	toluene	-65 to 300	50 to 300
36	1935	n - zylene	25 to 240	50 to 300
36	1935	cyclohexane	25 to 240	45 to 300
36	1935	methycyclohexane	25	45 to 300
42	1939	liq. nitrogen	-164 to -194	up to 180
59	1939	liq. ethene	- 85 to -105	up to 80
25	1939	liq. methane	-146 to -183	up to 230
94	1940	n - hexane	35.2	50 to 150
94	1940	cyclohexane	35.2	50
94	1940	m - zylene	35.2	50
94	1940	benzene	35.2 to 72.6	50 to 150
67	1943	butane	23.9 to 115.6	22 to 100
13	1946	iso butane	35 to 121	34 to 200
13	1946	iso octane	35 to 150	12 to 340
13	1946	isomeric dodecanes	93 to 150	34 to 340
45	1948	benzene	25	50 to 500
37	1948	benzene	25 to 150	250 to 3000
91	1953	propane	5 to 88	34 to 545
40	1954	liq. ethylene	- 17 to -157	17 to 550
40	1954	liq. ethane	10 to -170	17 to 550
40	1954	liq. propylene	24 to -157	17 to 550
40	1954	liq. propane	24 to -184	17 to 550
57	1955	n - heptane	25 to 50	100 to 300
57	1955	D in n-heptane	25 to 50	100 to 300

TABLE I - continued.

Ref.	Year	Solvent	Temperature range °C	Pressure range atm. or kg/cm
69	1957	n-hexane	0 to 240	up to 680
47	1958	cyclohexane	20 to 60	up to 700
71	1960	n-heptane	150 to 230	1 to 1000
71	1960	iso - octane	150 to 230	1 to 1000
71	1960	methylcyclohexane	150 to 230	1 to 1000

TABLE II - Systems containing Nitrogen

Ref.	Year	Solvent	Temperature range °C	Pressure range atm. or kg/cm
21	1931	propane	25	up to 140
21	1931	propane	25	up to 140
7	1938	n-heptane	25 to 115	100
66	1940	benzene	30 to 125	60 to 300
53	1942	benzene	16 to 125	50 to1100
45	1948	benzene	25	50 to 775
46	1951	methane	25	250 to 750
85	1953	liq. methane	-100 to -155	0 to 30.6
5	1953		-110 to -155	0 to 47
1	1954	n-heptane	32 to 182	68 to 680
1	1954	n-butane	38 to 150	35 to 287
27,111	1957	iso-octane	50 to 100	50 to 300
27,111	1957	n-octane	50 to 100	50 to 300
78	1961	n-butane	38 to 138	16 to 213
55	1962	carbon dioxide	15 to 30	50 to 100

TABLE III - Systems containing Argon

Ref.	Year	Solvent	Temperature range °C	Pressure range atm. or kg/cm
27,111	1957	iso-octane	50 to 100	50 to 300
27,111	1957	n-octane	50 to 100	50 to 300
27,111	1957	carbon tetrachloride	50 to 100	50 to 300
27,111	1957	perfluromethylcyclo-hexane	50	50 to 300

APPENDIX II

Tabulated experimental results

In Tables 1 to 9 the experimental measurements are recorded with the calculated valves of mole fractions x_2 and y_1 and phase densities ρ_L and ρ_G. Table 10 gives the results obtained for the calibration of the liquid and gas sampling vessels.

For convenience the following nomenclature is used:-

V_L = volume of gas present in the liquid phase sample at N.T.P. - c.c's

V_G = volume of gas present in the gas phase sample at N.T.P. -c.c's.

W_L = weight of solvent in the liquid phase sample - gms.

W_G = weight of solvent in the gas phase sample - gms.

ρ_L = density of liquid phase - gms/c.c

ρ_G = density of gas phase - gms/c.c

x_2 = mole fraction of gas in liquid phase

y_1 = mole fraction of solvent in gas phase

V_s' = volume of liquid phase sampling vessel - c.c's

V_s'' = volume of gas phase sampling vessel - c.c's

TABLE I

Nitrogen - Benzene System at 25°C

Gauge Pressure Atm.	Liquid Phase				Gas Phase			
	W_L gms	V_L cc's	ρ_L gms/c.c.	x_2	W_G gms	V_G cc's	ρ_G gms/c.c.	y_1
182	3.8842	82.0	0.892	0.0687	0.0410	1713.8	0.217	0.00677
370	3.8128	146.9	0.894	0.118				
462	3.7745	169.0	0.892	0.135	0.1264	3102.0	0.398	0.0114
535	3.7886	190.4	0.901	0.149	0.2036	3398.3	0.442	0.0169
675	3.7460	225.8	0.901	0.173				
742	3.7406	260.9	0.909	0.192	0.2726	3972.2	0.520	0.0193
842	3.7360	260.6	0.909	0.195	0.2487	4196.6	0.546	0.0167
992	3.7232	289.0	0.913	0.213				
993	3.7239	283.1	0.912	0.209	0.3346	4334.0	0.571	0.0216
1045					0.3360	4535.4	0.596	0.0208
1080	3.7586	303.1	0.925	0.219				
1120	3.7624	320.7	0.931	0.229	0.3471	4632.7	0.609	0.0210
1173	3.7214	321.3	0.922	0.231	0.3552	4724.8	0.622	0.0211

TABLF II

Nitrogen - Benzene System at 75°C

Gauge Pressure Atm.	Liquid Phase				Gas Phase			
	W_L gms	V_L cc's	ρ_L gm/c.c.	x_1	W_G gms	V_G c.c's	ρ_G gm/c.c.	y_1
168	3.5512	100.2	0.823	0.0914	0.088	1266.5	0.166	0.0196
328	3.4908	186.9	0.833	0.157	0.2017	2159.0	0.288	0.0261
410	3.4531	227.2	0.836	0.187	0.2574	2578.9	0.346	0.0278
477	3.4297	261.2	0.840	0.209	0.3246	2761.6	0.375	0.0326
522	3.3973	282.2	0.838	0.225	0.3744	2908.5	0.398	0.0356
635	3.3372	340.7	0.842	0.262	0.4938	3255.9	0.453	0.0417
745	3.2654	390.6	0.839	0.294	0.6214	3472.4	0.493	0.0488
938	3.1554	475.1	0.838	0.344	0.8232	3773.6	0.550	0.0589
1080	3.1484	534.4	0.854	0.372	0.9680	3957.0	0.587	0.0656
1303	3.0504	631.1	0.859	0.418	1.2320	4115.5	0.633	0.0791

TABLE III

Nitrogen - Benzene System at 100°C

Gauge Pressure Atm.	Liquid Phase				Gas Phase			
	W_L gms	V_L c.c's	ρ_L gms/cc	x_2	W_G gms	V_G c.c's	ρ_G gms/cc	y_1
125					0.1008	833.1	0.113	0.0335
137	3.4694	98.1	0.804	0.0897				
227	3.3555	148.1	0.792	0.133	0.1923	1484.1	0.203	0.0358
385	3.2429	245.9	0.794	0.209	0.4010	2188.9	0.302	0.0499
545	3.0939	351.3	0.790	0.283	0.6112	2730.3	0.399	0.0604
700	2.9760	453.0	0.792	0.347	0.8910	3099.9	0.473	0.0762
827	2.8547	539.5	0.789	0.397	0.1000	3300.1	0.519	0.0873
1010	2.6918	680.3	0.792	0.468,	0.5167	3441.6	0.578	0.112
1213	2.4458	872.9	0.791	0.555	2.0948	3433.3	0.634	0.149
1323	2.1346	1050.1	0.771	0.632	2.7612	3242.3	0.677	0.196

TABLF V

Argon - Heptane System at 50°C

Gauge Pressure Atm.	Liquid Phase				Gas Phase			
	W_L gms	V_L c.c's	ρ_L gms/c.c.	x_2	W_G gms	V_G c.c's	ρ_G gms/c.c.	y_1
85.5	2.8062	141.7	0.684	0.184				
184.5	2.5823	314.8	0.703	0.353	0.0886	1608.2	0.294	0.0122
280	2.3488	488.2	0.720	0.482	0.1097	2328.8	0.423	0.0104
358	2.1154	660.5	0.737	0.583	0.2050	2840.6	0.523	0.0158
402	1.9528	776.0	0.746	0.640				
403					0.4746	3041.8	0.586	0.0337
450	1.6783	976.5	0.763	0.721	0.9505	3157.9	0.654	0.0630
455	1.6542	973.3	0.758	0.721	1.0570	3152.1	0.663	0.0698
475	1.4586	1087.9	0.760	0.769	1.4282	3087.4	0.694	0.084

TABLE VI

Argon - Heptane System at 100°C

Gauge Pressure Atm.	Liquid Phase				Gas Phase			
	W_L gms	V_L cc's	ρ_L gms/c.c.	x_2	W_G gms	V_G c.c's	ρ_G gms/c.c	y_1
73.5	2.6273	112.3	0.632	0.160	0.0828	529.0	0.102	0.0337
119.5					0.1482	781.2	0.153	0.0407
124.5	2.5562	198.7	0.651	0.258				
180	2.3777	296.8	0.650	0.358	0.2482	1285.0	0.252	0.0414
244	2.1843	415.7	0.655	0.460	0.3848	1691.4	0.338	0.0482
285	2.0426	514.7	0.662	0.530				
335	1.8392	625.7	0.661	0.604	0.6800	2193.2	0.456	0.0648
364	1.7138	712.5	0.668	0.656	0.8962	2305.7	0.497	0.0799
373	1.5774	772.1	0.661	0.686				
378	1.5112	797.6	0.656	0. 703				
381	1.4654	816.0	0.653	0.713	1.2822	2306.7	0.536	0.110
383	1.4376	827.9	0.652	0.720	1.2939	2309.4	0.537	0.111
390	1.3360	870.0	0.646	0.744	1.5200	2282.3	0.555	0.130

TABLE VIII

Argon - Carbon tetrachloride System at 50°C

Gauge Pressure Atm.	Liquid Phase				Gas Phase			
	W_L gms	V_L c.c's	ρ_L gms/c.c.	x_2	W_G gms	V_G c.c's	ρ_G gms/c.c.	y_1
84.5	6.6808	116.7	1.541	0.107				
138.5	6.4125	189.9	1.510	0.169	0.1841	1191.9	0.229	0.022
237	5.9982	332.3	1.474	0.275	0.3929	2014.0	0.395	0.0276
327	5.6919	460.8	1.457	0.357	0.6054	2637.8	0.527	0.0323
415	5.3624	594.1	1.436	0.432	1.0207	3108.5	0.652	0.0456
513	4.9024	769.0	1.403	0.519				
590	4.4128	945.4	1.364	0.595	2.4757	3616.3	0.886	0.0905
618	4.1732	1022.4	1.341	0.627	2.8218	3626.4	0.922	0.102
650	3.6430	1180.8	1.286	0.690	4.0411	3475.5	1.016	0.145
662	3.4253	1235.9	1.259	0.712	4.3450	3434.9	1.039	0.155

TABLE VII

Nitrogen - Carbon tetrachloride System at 30°C

Gauge Pressure Atm.	Liquid Phase				Gas Phase			
	W_L gms	V_L cc's	ρ_L gms/c.c.	x_2	W_G gms	V_G c.c's	ρ_G gms/c.c	y_1
90.0	6.8421	124.4	1.580	0.111				
157	6.5879	217.5	1.560	0.185				
260	6.1644	351.9	1.519	0.282	0.3825	2366.3	0.457	0.0230
353	5.8628	481.1	1.503	0.360	0.5711	3042.0	0.595	0.0266
460	5.4671	626.3	1.473	0.440	1.0030	3565.1	0.731	0.0394
557	5.0879	771.9	1.446	0.510	1.4818	3911.3	0.839	0.0521
600	4.9684	855.3	1.453	0.542	1.9556	3976.6	0.898	0.0667
655	4.5600	961.2	1.403	0.585	2.4229	4053.4	0.958	0.0800
717	4.2702	1059.1	1.378	0.639	3.1359	4026.8	1.024	0.102
745	3.9004	1221.2	1.359	0.682	3.9730	3906.6	1.086	0.129

TABLE IX

Argon - Carbon tetrachloride System at 100°C

Gauge Pressure Atm.	Liquid Phase				Gas Phase			
	W_L gms	V_L cc's	ρ_L gms/c.c.	x_2	W_G gms	V_G cc's	ρ_G gms/cc	y_1
104	6.1154	139.4	1.42	0.135	0.2038	735.6	0.150	0.0388
147	5.9514	203.8	1.413	0.190	0.3578	1049.3	0.221	0.0473
256	5.4062	375.8	1.359	0.323	0.6458	1785.4	0.380	0.0499
330	5.0116	500.6	1.321	0.407	1.0439	2198.2	0.493	0.0647
395	4.5934	627.4	1.278	0.484	1.5919	2492.5	0.599	0.0850
455	4.0511	785.9	1.219	0.571	2.4746	2674.4	0.719	0.119
475	3.8048	851.3	1.191	0.606				
495	3.3602	971.6	1.139	0.659	4.3017	2561.4	0.881	0.196

TABLF X Measurements and calculations for determining the volumes of the sampling vessels.

Temperature 30°C.

Pressure Atms.	Volume of Ar. under given temperature and pressure. c.c's/gm.mole	Liquid sampling vessel		Gas sampling vessel	
		Vol. of Ar. in vessel at N.T.P. c.c's	Volume V's c.c's	Vol. of Ar. in vessel at N.T.P. c.c's	Volume V''s c.c's
54	456	212.4	$\frac{212.4}{22390} \times 456 = 4.33$	482	$\frac{482}{22390} \times 456 = 9.82$
50	485	207.5	$\frac{207.5}{22390} \times 485 = 4.51$	468	$\frac{468}{22390} \times 485 = 10.15$
70	343	296.8	$\frac{296.8}{22390} \times 343 = 4.56$	668	$\frac{668}{22390} \times 343 = 10.23$
			MEAN VALUE 4.47		

% Error in V's = 2.0

% Error in V''s = 1.6

APPENDIX III

Purity of Materials

Benzene:-

This was purchased from Hopkin & Williams Ltd., as "Benzene for Molecular Weight Determination" and had the following properties:-

Distillation range	between 79.7 and 80.2°C.
Refraction Index at 20°C	1.5011
Water Content	0.03%
Aromatic Content	99.5%

This was further purified by a series of five fractional crystalisations and finally dried over sodium. The resulting pure benzene was checked for impurities by Vapour Phase Chromatography (non were evident), and also the refraction index n_D was measured to be 1.50596 at 12.5°C. Using a value of $\frac{dn_D}{dt}$ of 0.00055 then this value gives n_D at 15°C equal to 1.50439 which compares favourably with 1.50439 as given in the literature [112].

Heptane:-

This was kindly given by the Shell organisation and was quoted as that used for knock rating having a purity of better than 99.5%. No impurities were shown on Vapour Phase Chromatography and the

refraction index n_D at 8.75°C was 1.39333. Using a value of $\frac{dn_D}{dt}$ = 0.00046 this gives n_D at 15°C equal to 1.39045 compared with n_D at 15°C in literature [112] 1.39002.

Carbon tetrachloride:-

This was purchased from Hopkin & Williams Ltd., as "Micro Analytical Standard". It had the following limits of impurity:-

Density	1.593 gms/c.c
Refraction Index at 20°C	1.4610
Water Content	0.016%
Non valuable matter	none

No further purification of this material was attempted but the refraction index was checked against the value given in Timmermans [112] i.e. n_D at 15°C = 1.46305. The measured refraction index was 1.46675 at 9.25°C. which is equivalent to 1.46459 at 15°C for $\frac{dn_D}{dt}$ = 0.00055.

Nitrogen and Argon:-

Both gases were purchased from British Oxygen Gases Ltd., and were quoted as having the following composition:-

	Nitrogen	Argon
Pressure Supplied	120 ats	143 ats.
Purity	not less than 99.9%	99.995%
Impurities		
N_2	-	500 p.p.m.

	Nitrogen	Argon
Ar	5 p.p.m.	-
O_2	less than 10 p.p.m.	5 p.p.m.
H_2	" " 20 p.p.m.	0.5 p.p.m.
CO_2	" " 5 p.p.m.	5 p.p.m.

APPENDIX IV

Calculation of the partial molar volume of the gas in the liquid

The partial molar volume may be calculated from the equation given below which has been derived by Young & Vogel [114].

$$\bar{V}_2 = x_1 \left(\frac{\delta V}{\delta x_1} \right)_{P,T} + V \quad \ldots\ldots (10.1)$$

For the systems studied V is only known for the pure liquid and the saturated mixture, and hence to obtain the value of $\left(\delta V / \delta x_1\right)_{P,T}$, one must assume that the molar volume increases linearly with concentration.

Consider the N_2 - C_6H_6 system at 25°C. From Fig. 9.1

$x_2 = 0.1$ P = 300 atm.

Density of C_6H_6 at 25°C and 300 atm [8] = 0.896 gms/c.c.

Molal Volume of C_6H_6 at 25°C and 300 atm = 87.1 c.c.

Now from the experimental data the no. of moles present in the liquid sampling vessel at saturation = 0.0546

Molal Volume at saturation = 81.8 c.c.

$$\left(\frac{\delta V}{\delta x_1} \right)_{P,T} = \frac{81.8 - 87.1}{0.1} = -53$$

Substituting values into equation 10.1 at saturation:-

$$\bar{V}_2 = -0.1 \times 53 + 81.8 = 34.1 \text{ c.c.}$$

Property.	Ar.	N_2	CCl_4	C_7H_{16}	C_6H_6
Molecular Weight	39.94	28.02	153.84	100.20	78.11
Density gms/c.c	0.001784 at N.T.P.	0.00125 at N.T.P.	1.595 at N.T.P.	0.6837 at N.T.P.	0.879
Boiling Point °C	- 185.7	- 195.7	76.8	98.43	80.10
Melting Point			- 22.8	- 90.5	5.50
Refracture index			1.46305 at 15°C	1.38764 at 20°C	1.50112 at 20°C
Molecular Volume at N.T.P. c.c's	22390	22403			
Critical Temperature °K	150.7	125.9	556.1	539.1	561.5
Critical Pressure atm.	48	33.5	45	26.8	47.7
Critical Density gms/c.c	0.531	0.311	0.558	0.234	0.304

LIST OF SYMBOLS

(Note: Minor symbols which occur at only one isolated place in the text are not listed).

B, C	Virial coefficients
G	Gibbs Free energy
K	Henry's Law Constant
K_ε	Equilibrium Constant
L	Ostwald coefficient
M	Molecular weight
N	Avogadro's number, 6.02×10 molecules/mole also - with subscript means number of moles of that component.
P	Pressure
R	Gas constant per mole
S	Entropy
T	Temperature
V	Volume
W	Weight of solvent in liquid and gas phase samples
a	activity
f	fugacity
k	Boltzmans constant, or in design of high pressure vessels - the ratio of the outside diameter to inside diameter.

p	vapour pressure, partial pressure
v	molal volume
x	mole fraction (liquid phase)
y	mole fraction (gas phase)
γ	activity coefficient
δ	solubility parameter
ϵ	energy parameter in intermolecular pair potential energy function.
θ	surface tension
μ	chemical potential
ρ	density
σ	collision diameter, distance parameter in intermolecular pair potential energy function. - or in Chapter 7 ultimate tensile strength
Φ	volume fraction
ϕ	fugacity coefficient

Superscripts.

^{o}	pure component or reference state
^{c}	critical conditions
^{g}	gas phase
^{l}	liquid phase
^{s}	saturation conditions

Subscripts

$1,2$	components 1 and 2
G	gas phase
L	liquid phase

REFERENCES

1. Akers W.W, Atwell L.L, Robinson J.A; Industr. Engng Chem. 46 2536 (1954)

2. Allen P.C, "Plastics", February 1945.

3. Basset J., Dode M; Acad. Sci. Paris 203 775 (1936)

4. Benham A.L, Katz D.L, Williams R.B; Amer. Inst. Chem. Eng. J. 3 236 (1957)

5. Bloomer O.T, Parent J.D; Chemical Engineering Progress p. 11. vol. 49, Symposium Series N . 6 (1953)

6. B.S. 1797 Pub. 1952. also - Notes on Applied Science No. 6 (Volumetric Glassware)

7. Bommer E.H. et al.; Canad. J. Res. 16B 319 (1938)

8. Bridgeman P.W.; "The Physics of High Pressures" (G. Bell & Sons Ltd., London 1958)

9. Clever L.H, Battino R, Sayler J.H, Cross P.M. J. Phys. Chem 61 1078 (1957)

10. Comings E.W., "High Pressure Technology" (McGraw - Hill Book Co., 1956. New York)

11. Cornish R.H, Ruoff A.L; Rev. Sci. Instrum 32 639 (1961)

12. Culbertson O.L, J.J. McKetta; J. Petr. Techn. 3, 223, (1951)

13. Davenport A.J, Rowlinson J.S; Trans. Faraday Soc. 59 (1963)

14. Dean M.R; Tooke T.W; Industr. Engng. Chem. 38 389, (1946)

15. Demming, Shupe; Phys. Rev. 37 638, (1931)

16. Din F; "The Thermodynamic Functions of Gases." (Butterworths London 1956)

17. Dodge B. F; "Chemical Engineering Thermodynamics", equations IV - 18 & 19 (McGraw Hill Book Co. Inc. 1944)

18. Dodge B. F, Dunbar A. K; J. Amer. Chem. Soc. 49, 591, (1927)

19. Euken, Bressler; Z, physich Chem 134, 230, (1928)

20. Freeth F. A, Verschagle J. J. A; Proc. roy. Soc. A130, 453, (1931)

21. Frolich P. K, Tauch E. J, Hogen J. T, Peer A. A, Industr. Engng. Chem. 23, 548, (1931)

22. Gamburg D. Y; Zhur. Fiz. Khim. 24, 272, (1950)

23. Gjaldbach J. C; Acta. Chem. Second. 6, 623, (1952)

24. Gjaldbach J. C. Hildebrand J. H; J. Amer. Chem. Soc. 71, 3147 (1949)

25. Gonckberg M. G., Fastovski; Zhur. Fiz. Khim. 14, 427, (1940)

26. Gonckberg M. G; J. Phys. Chem. USSR 14, 582, (1940)

27. Graham E. B; Ph. D. Thesis, Univeristy of London 1958.

28. Henry W.; Phil. Trans. 93, 24, 274, 1803

29. Hildebrand H. J; J. Amer. chem. Soc. 51, 66, (1929)

30. Hildebrand. J. H; J. Phys. Chem 15, 225, (1947)

31. Hildebrand J. H, Scott R. L; "The Solubility of Non-Electrolytes". (3rd. Ed. Rheinhold, New York 1950)

32. Hildebrand J. H, Scott R. L; "Regular Solutions". (Prentice Hall, New Jersey 1962)

33. Hirschfelder J. O, Rosveave; J. Physic. Chem 15, 43, (1939)

34. Hirschfelder J. O; Curtiss, Bird; "Molecular Theory of Gases and liquids." (John Wiley, New York 1954)

35. Horiati J. ; Sci Papers, Inst. Phys. Chem. Res, Tokyo 17, No, 341 125, 1931.

36. Ipatiev V. V, Levina M. I; Zhur. Fiz. Khim. 6, 632, (1935)

37. Ipatiev V. V, Teoderavich V. P, Brestkin A. P, Artemavich V. S; Zhur. Fiz. Khim. 22, 833, (1948

38. Jepson W. B, Richardson M. J, Rowlinson J. S, Trans. Faraday Soc. 53, 1586 (1957)

39. Joosup Shim, Kohn J. P; Journal of Chemical & Engineering Data 7, No. 1. 3 (1962)

40. Katz D. L, Williams R. B; Industr. Engng. Chem 46, 2512 (1954)

41. King M. B; Trans. Faraday Soc 54, 149 (1958)

42. Krichevski I. R, Zhavoronkov N. M, Tsiklis D. S Zhur. Fiz. Khim. 9, 317 (1937)

43. Krichevski I. R, Il'inskaya A. A; Zhur. Fiz. Khim 19, 621 (1945)

44. Krichevski I. R, Tsiklis D. S; Zhur. Fiz. Khim 17, 126 (1943)

45. Krichevski I. R, Efremova G. D, Zhur. Fiz. Khim 22, 1116, (1948)

46. Krichevski I. R, Efremova G. D, Zhur. Fiz. Khim 25, 577, (1951)

47. Krichevski I. R, Sarina G. A; Zhur. Fiz. Khim 32, 2080 (1958)

48. Krichevski I. R, Kasarnovski J. S; J. Amer. Chem. Soc. 57, 2168, (1935)

49. Krichevski I. R; J. Amer. chem. Soc. 59, 596, (1937)

50. Krichevski I. R; Acta phys. - chim. URSS 12, 480, (1940)

51. Krichevski I. R, Bolshakov P. E; Acta phys -chim URSS 14, 353, (1941)

52. Krichevski I. R, Tsiklis D. S; Acta phys -chim URSS 18, 264, (1943)

53. Krichevski I. R, Gamburg D. Y; Acta Physicochimica 16, 362, (1942)

54. Krichevski I. R, Khazanova N. E, Lesnevskaya L. S, Sandulara L. Yu. Khim. Prom 169 (1962.)

55. Kuene J. P, Z. phys. chem. 11, 38 (1893)

56. Lachowocz S. K, Journal Imperial College, Chem Eng. Soc. 8, 51 (1954)

57. Lachowicz S. K, Weale K. E, Trans, Faraday Soc 51, 1198 (1955)

58. Lachowicz S. K, Ph. D. Thesis, University of London 1954.

59. Levitskaya E, Pryannikov K; Zhur. Tekh. fiz 9, 1949, (1939)

60. Lewis Chinsum Yen, McKetta Jr. J. J. Amer. Inst. Chem. Eng. J. 8, 501, (1962)

61. Lewis, Luke, Industr. Engng. Chem 25, 725, (1933)

62. Lindroos A. E, Dodge B. F; Chemical Engineering Progress p. 10. Vol. 48, Symposium Series No. 3. (1952)

63. Manning W. R. D, "High Pressure Engineering". (Bulleid Memorial Lectures 1963, University of Nottingham)

64. Michels A, Gerver J, Bijl A; Physica Grav. 3, 797 (1936)

65. Michels A, W de Graff, J. van der Somme.; J. Appl. Sci. Res. Hague. 4A, 105, (1943)

66. Miller P, Dodge B. F; Industr. Engng. Chem. 32, 434 (1940)

67. Nelson E. F, Bonnell W. S; Industr. Engng. Chem. 35, 204, (1943)

68. Newitt D. B, "High Pressure Plant & Fluid at High Pressure". (Clavendon Press 1940)

69. Nichols W. B, Reamer H. H, Sage B. H,; Amer. Inst. Chem. Eng. J. 3, 262, (1957)

70. Onnes H. K, Keesom W. H; Commun. phys. Lab., Univ.. Leiden. Suppl. No. 15. 1907.

71. Peter. S, Reinhartz K.; Zeitschrift fuer Physikalische Chemie Neue Folge 24 1/2 (1960)

72. Pierotti R.A; J. Phys. Chem. 67 1840 (1963)

73. Prausnitz J.M, Bensen P.R;Amer.Inst. Chem.Eng.J. 5, 161, (1959)

74. Prausnitz J.M,;Chemical Engineering Science.

75. Prausnitz J.M, Shaw F.H;Amer.Inst. Chem. Eng. J. 7, 682,(1961)

76. Reavell B.N; Trans.Instn.Chem.Engrs. 29, 3 (1951)

77. Reeves L.W, Hildebrand J.H;J. Amer. chem. Soc. 79, 1313 (1957)

78. Roberts L.R, McKetta Jr. J.J;Amer.Inst. Chem. Eng. J. 7, 173 (1961)

79. Robin S, Vodar B; Disc. Faraday Soc. 15, 233, (1953)

80. Robin S, Vodar B, ; C.R. Acad. Sci, Paris 230, 1840 (1950)

81. Robin S, Vodar B; J. Phys. Radium 13, 264, (1952)

82. Robin S, Vodar B, Bergson; Compt. rend. 232 , 2189 (1951)

83. Robin S.; J. Chim. Phys. 48, 501, (1951)

84. Rott L.A.; Russian Journal of Physical Chemistry 1205, (1962)

85. Rowland C.H, Hogan R.J, Roach J.T, Cines M.R,; Chemical Engineering Progress p.1. Vol 49, Symp. Series. No. 6. (1953).

86. Rowlinson J.S, Ewald A.H, Jepsen W.B, Disc. Faraday Soc. 15, 238, (1953)

87. Rowlinson J.S, "The Physics & Chemistry of High Pressures". Papers read at the Symposium in London 1962. (Soc. of Chem Ind. 1963

88. Rowlinson J.S, "Liquids and Liquid Mixtures". (Butterworths 1959)

89. Saddington A.W, Krase N.W; J. Amer. chem. Soc. 56, 353, (1934)

90. Sage B.H, Hicks, Lacey W.N.;Industr.Engng.Chem. 32, 1085,(1940)

91. Sage B.H, Burriss W.L, Hsu N.T, Reamer H.H., Industr. Engng. Chem, 45, 210, (1953)

92. Sage B.H, Lacey W.N.; Industr. Engng. Chem. 26, 103, (1934)

93. Sage B.H, Lacey .W.N; "Some Properties of Hydrocarbons", (Am. Petr. Institute, New York 1955)

94. Sattler H.; Z. tech Phys. 21, 410,(1940)

95. Shanbhag,; Ph.D. Thesis, Univ. of London, 1954)

96. Todheide K, Franck E.U., Zeitschrift fuer Physikalische Chemie Neue Folge 37, 5/6 1963.

97. Tsiklis D.S.; Dokl. Akad. Nauk. USSR. 86, 993, (1952)

98. Tsiklis D.S.; Dokl. Akad. Nauk. USSR. 101, 129 (1955)

99. Tsiklis D.S.; Dokl. Akad. Nauk. USSR. 91, 1361 (1953)

100. Tsiklis D.S.; Dokl. Akad. Nauk. USSR 86, 1159 (1952)

101, Tsiklis D.S.; Zhur. Fiz. Khim 21, 349, (1947)
" " " 17, 126, (1943)

102. Uhlig H.H.; J. Phys. Chem 41, 1215, (1937)

103. Van der Waals J.D.; Verslag. Zittingen Wis- Eq. Natuurk Adfeel Koninkt. Akad Wetenschap. Amsterdam p. 133. Nov. 1894.

104. Verschoyle T.T.A.; Phil. Trans. Roy.Soc. A 230, 189, (1931)

105. Wiebe R, Trmearne J.H.; J.A.C.Soc. 55, 975, (1933)

106. Wiebe R, Tremearne J.H.; J.Amer.chem.Soc. 57, 2601 (1935)

107. Wiebe R, Gaddy V.L, Heins C.;J.Amer.chem.Soc. 55, 947, (1933)

108. Wiebe R, Gaddy V.L, Heins C.; Industr.Engng.Chem 24, 823,(1932)

109. Wiebe R, Gaddy V.L,; J.Amer.chem.Soc. 63, 475, (1941)

110. Wan Shen - Wu, Dodge B. F; Indust. Engng. Chem. 32, 95, (1940)

111. Weale K. E, Graham E. B.; "Progress in International Research in Thermodynamics & Transport Properties". (Academic Press 153, 1962, New York)

112. Timmermans,; " Physico - Chemical Constants". (Elsevier 1950)

113. Deffet L.; Bull. Soc. chim Belg 44, 41, 1935
and Bull. " " " 51, 237, 1942

114. Young J. F., Vogel O. G.; J. Amer. chem Soc. 54, 3025, (1932)